2012

Entanglement Entropy in Ordered and Quantum Critical Systems

Wenxin Ding

THE FLORIDA STATE UNIVERSITY

COLLEGE OF ARTS AND SCIENCES

ENTANGLEMENT ENTROPY IN ORDERED AND QUANTUM CRITICAL SYSTEMS

By

WENXIN DING

A Dissertation submitted to the
Department of Physics
in partial fulfillment of the
requirements for the degree of
Doctor of Philosophy

Degree Awarded:
Summer Semester, 2012

Wenxin Ding defended this dissertation on May 11, 2012.

The members of the supervisory committee were:

Kun Yang
Professor Directing Dissertation

Phillip Bowers
University Representative

Nicholas Bonesteel
Committee Member

Jorge Piekarewicz
Committee Member

Peng Xiong
Committee Member

The Graduate School has verified and approved the above-named committee members, and certifies that the dissertation has been approved in accordance with the university requirements.

To my beloved father,
my wife,
and my little angel.

ACKNOWLEDGMENTS

I would like to express my gratitude to my advisor Professor Kun Yang for his support and guidance during my graduate studies. I have learned and benefited so much from his remarkable insights in physics, without which this work can never be finished, as well as his rigorous scholarship. I am truly grateful for his patience and advice through. I also wish to thank Professors Nicholas E. Bonesteel and Alexander Seidel, with whom I am fortunately to collaborate. The inspiring discussions I had with both of them also play a key role in this work. My many thanks also go to Professors Nicholas E. Bonesteel again, Peng Xiong, Phillip Bowers, and Jorge Piekarewicz, who served in my dissertation committee, for their time and effort.

TABLE OF CONTENTS

LIST OF FIGURES

ABSTRACT

This dissertation investigates the entanglement properties of extended quantum systems which exhibit either long-range order or quantum criticality. While we mainly focus on the von Neumann entanglement entropy, the mutual information is also studied for certain systems when a mixed state is of concern. For extended quantum systems, all the gapped local Hamiltonians, as well as a large number gapless systems, are known to follow the so called "area law", which states that the entanglement entropy is proportional to the surface area of the subsystem. However, violations of the area law, usually in a logarithmic fashion, do exist in various different systems. They are found to be associated with quantum criticality in certain one dimensional systems. For free fermions in higher dimensions, it is found that the area law is enhanced by a logarithmic factor. Besides, such logarithmic terms also appears as subleading corrections to the area law. The central goal of this dissertation is, by studying specific solvable models, to explore and discuss the connections of such logarithmic divergence of entanglement entropy to quantum criticality and long-range order, and the intrinsic relations among such terms in different dimensions, and seek generalization to interacting systems.

In the first part, we study two different systems that both exhibit long-range order, namely magnetically ordered Heisenberg spin systems and Bose-Einstein condensate systems, and reveal that this logarithmic divergence (violating the area law) is not particular to quantum criticality. They are present in those long-range ordered systems as well. Therefore, caution must be taken when people try to use such divergence to detect and characterize quantum criticality.

In second part, we explore the relation between logarithmic divergence in one-dimensional fermionic systems and that of free fermions in higher dimensions. We show that both logarithmic factors share the same origin - the singularity at the Fermi points or Fermi surface

- via a toy model. Based on the intuition from our toy model, we make use of the tool of multi-dimensional bosonization to rigorously re-derive the entanglement entropy of free fermions in high dimensions in a simpler way. Then by the convenience of the bosonization technique, we take into account the Fermi liquid interactions, and obtain the leading scaling behavior of the entanglement entropy of Fermi liquids.

CHAPTER 1

INTRODUCTION

The quantum description of our world differs in many ways from the classical theory. For example, it prohibits us from measuring two canonically conjugate observables simultaneously with arbitrary precision, which results from a fundamental uncertainty principle. It also correctly predicts many phenomena that disagree with classical theory, like interference of particles or material waves, quantization of energy levels, etc.. However, it is entanglement, a term which was coined by Schrödinger[1] in 1935, that ultimately distinguishes the quantum theory from the classical ones. It was also one of the earliest aspects of quantum mechanics to be studied and discussed[1, 2]. In short words, entanglement implies that the measurement on one party or a subsystem could affect *instantaneously* the possible outcome of a seperate/independent measurement on the other party/subsystem of the system, even if the two parties are well-separated in space. While in a classical system, the effect of one measurement on the outcome of another is strictly limited by the speed of propagation of signals. Such contradiction of quantum theory with the classical theory is know as the Einstein-Podolsky-Rosen (EPR) paradox[2]. A decisive breakthrough on the subject was achieved by Sir Bell in his 1964 seminal work[3], in which he showed that the correlations predicted by quantum mechanics cannot be described by any set of local (hidden) classical parameters. Bell derived a set of inequalities known as the Bell's inequalities which can be tested experimentally but was realized only many years later[4, 5, 6, 7] (see [8] for a review).

The quantum entanglement not only rules out the possibility of any underlying classical explanation or interpretation, like hidden variable theory, of the quantum theory, but is also

the resource for quantum computation. It is by this elusive nature of quantum mechanics that Shor's algorithm[9] can beat its classical competitors with much higher efficiency, and that quantum teleportation[10] is made possible. Despite being an old topic, in recent years, there is reviving interest in the study of entanglement, originating from very different fields, and comes together in a very unexpected way. It has led to and continues to lead to important progress and applications in these fields of modern physics such as quantum information[11], condensed matter physics[12, 13, 14], etc.. Particularly for condensed matter, it has lead to better understanding of density matrix renormalization group (DMRG)[15, 16, 17]; it has also been proposed to be a tool for the characterization of certain topological phases[18, 19, 20] and an indicator of quantum phase transitions in various systems.

However, besides the qualitative study, crucial advance of the study of entanglement must come from the quantitative study. Conceptually we want to answer, not just whether a state is entangled or not, but also which state is more entangled than other states and to what extent. Practically, entanglement is considered a resource for quantum computation, thus it is also important to know how to quantify entanglement. Due to its importance, there are huge efforts dedicated to it, and many measures have been proposed and found applications in different situations (For a review, see [21, 22] and references therein). Among various ways of quantifying entanglement, in condensed matter or many-body physics efforts have mainly focused on the (bipartite block) *entanglement entropy* (von Neumann entropy), which is sometimes also known as *geometric entropy* or *entropy of entanglement* in the context of quantum information science, and its generalizations (Rényi or Tsallis entropy, mutual information and entanglement spectrum).

For the rest of this chapter, we will first introduce the definition of entanglement entropy, and its generalizations. Then we will briefly discuss some important results on entanglement entropy in extended quantum systems, especially the area law. After that, we will discuss several systems that exhibit logarithmic violations of the area law, which is also the main focus of this dissertation. In the end, we will outline the rest of this dissertation and the problems we are going to discuss.

1.1 Entanglement Entropy

Entanglement entropy can be defined equivalently from different perspectives. Taking an arbitrary quantum system in a pure state $|\Psi\rangle$, the density matrix of the state then is $\rho = |\Psi\rangle\langle\Psi|$. Partitioning the system into two parts, A and B, and assuming that the Hilbert space of the whole system can be written as a direct tensor product of those of A and B respectively[1]

$$\mathcal{H} = \mathcal{H}_A \otimes \mathcal{H}_B, \tag{1.1}$$

the entanglement properties of this state is then best captured by its Schmidt decomposition, which states that any pure state $|\Psi\rangle$ can be written as

$$|\Psi\rangle = \sum_j c_j |\psi_j\rangle_A \otimes |\psi_j\rangle_B, \tag{1.2}$$

where $|\psi_j\rangle_{A,B}$ are orthonormal vectors of the local Hilbert space of region A, B respectively (note that there is only one sum here). The state is assumed to be normalized, $\sum_j |c_j|^2 = 1$. The c_js can be chosen to be real and ≥ 0. Then we measure the entanglement between A and B by the entropy defined as

$$S = -\sum_j |c_j|^2 \log |c_j|^2. \tag{1.3}$$

From the above definition, we could see that, if $c_1 = 1$ (so the rest c_js vanish), $|\Psi\rangle$ is a product state, i.e. unentangled.

On the other hand, we can define the entanglement entropy as the von Neumann entropy of the reduced density matrix of either partition, which is equivalent to but more general than the definition through Schmidt decomposition. We first obtain the reduced density matrix by tracing out the degrees of freedom in part B from the density matrix of the whole system (ρ)

$$\rho_A = -\mathrm{Tr}_B \rho. \tag{1.4}$$

[1] Such bipartite property could be absent, and in that case a Schmidt decomposition is not permissible. For example, if we consider a gauge theory like the lattice Z_2 gauge theory constructed in Ref. [23] where there is a global constraint on the overall Hilbert space, such a bipartite condition cannot be satisfied due to the global constraint.

Then the entanglement entropy is defined as

$$S_A = -\mathrm{Tr}_A \rho_A \log \rho_A. \tag{1.5}$$

For ρ of a pure state, $S_A = S_B$ as guaranteed by the Schmidt decomposition. This definition also works for a mixed state, but in such cases, in general $S_A \neq S_B$. Comparing with the Schmidt decomposition, the latter is clearly base independent, which demonstrates the universal nature of the entanglement entropy.

The study of entanglement entropy has various fundamental and practical reasons. Its simple and universal definition not only makes it applicable to all quantum states, but comparable between different class of systems as well. One can compare the scaling behavior of entanglement entropy between completely different systems. It is also simple but versatile to study: one only needs to divide a complete set of compatible observables into subsystems and calculate! But the ways to partition the system is *infinite*. For partitions in real space, one can choose geometries of different shapes, different connectivity, different boundaries (smooth or conical), etc.. Although current studies mostly focus on partition in real space, but it is not restricted to just that. The partition of the Hilbert space can be chosen according to any complete set of observables. To date, it has been shown that, by studying entanglement entropy, many fundamental properties can be extracted: the central charge, the boundary entroy, the total quantum dimension of a topological phase, and so on. It is also susceptible to both analytic and numerical study, especially via the 'replica trick'. Even though it is not suitable for techniques like quantum Monte Carlo, one can study its replica generalization: the Rényi entropy or Tsallis entropy, and still extract important information that is universal.

1.1.1 Rényi, Tsallis Entropy, entanglement spectrum and mutual information

In the following, we shall briefly introduce some alternatives and generalizations of the von Neumann entanglement entropy and their benefits.

Rényi entropy and Tsallis entropy. The Rényi entropy[24] $S_\alpha(\rho_A)$ is defined as

$$S_\alpha(\rho_A) = \frac{1}{1-\alpha}\left[\mathrm{Tr}(\rho_A^\alpha)\right], \tag{1.6}$$

for $\alpha > 0$. The equivalent Tsallis $q-$entropy $T_q(\rho_A)$ is defined as

$$T_q(\rho_A) = \frac{1}{q-1}(1 - \mathrm{Tr}(\rho_A^q)), \tag{1.7}$$

for any $q > 0$ and $q \neq 1$. Both definitions reduce to the von Neumann entropy when taking the limit $\alpha \to 1 (q \to 1)$

$$\lim_{q\to 1} \frac{1}{q-1}(1 - \mathrm{Tr}(\rho_A^q)) = \lim_{\alpha\to 1} \frac{1}{1-\alpha}\left[\mathrm{Tr}(\rho_A^\alpha)\right] = -\mathrm{Tr}_A \rho_A \log \rho_A. \tag{1.8}$$

One of the most important motivations for considering these generalizations is that, for numerical approaches only exact diagonalization and density matrix renormalization group (DMRG) are able to compute the von Neumann entropy. Exact diagonalization can only deal with systems of relatively small size, while DMRG is mostly restricted to one dimension (1D) and its efficiency is reduced for highly entangled states. But it has been shown that Quantum Monte Carlo is able to compute Rényi entropy at integer αs[25]. What is more important is that it is possible to extract the topological entanglement entropy from such calculations[26], and possibly other universal terms.

Mutual information. For a generally mixed density matrix,

$$\rho = \sum_j p_j |\Psi_j\rangle\langle\Psi_j|, \tag{1.9}$$

as we stated previously, the von Neumann entropy is not well-defined in the sense that S_A no longer equals S_B hence lost universality. It is generally difficult to determine whether such a state is separable, i.e. ρ can be written as

$$\rho = \sum_j p_j \rho_{A,j} \otimes \rho_{B,j}, \tag{1.10}$$

where $\rho_{A(B),j}$ are arbitrary (pure) density matrices of the subsystems. Otherwise, ρ is said to be entangled. Albeit it remains generally difficult to determine the separability of a mixed state, in some cases, people use an intuitive generalization of the von Neumann entropy, the quantum mutual information[2]

$$S_M = \frac{1}{2}(S_A + S_B - S_0), \tag{1.11}$$

to measure the entanglement within such a state. Here $S_{A(B)}$ is the von Neumann entropy of subsystem $A(B)$, and S_0 is the entropy of mixed state $S_0 = -\sum_j p_j \log p_j$. This is taking an simple average over S_A and S_B and subtracting the contribution from the system itself. It restores the universality since it is uniquely defined for both parties, and reduces to von Neumann entropy the pure state limit.

Entanglement spectrum. Other than the entropy itself, it was proposed by Li and Haldane[20], that the full spectrum of the reduced density matrix, especially the eigenvalues of the "entanglement Hamiltonian" H_A defined as

$$\rho_A = e^{-H_A}/\mathrm{Tr}(e^{-H_A}), \tag{1.12}$$

should contain more information than that carried by the entanglement entropy alone, which is soon confirmed by later works for both topologically ordered states[29] and quantum critical systems[30].

1.2 The Area Law

The usual entropy we know, the thermal entropy, originates from a lack of knowledge about the microstate of the system. In contrast, the entanglement entropy stems from entanglement and is even present at zero temperature when thermal entropy vanishes. Moreover,

[2]This definition is probably not unique. It is one half of the "mutual information" introduced in Ref. [27, 28], and reduces to Eq. (1.5) when ρ is that of a pure state. The same definition was used by Castelnovo and Chamon [Claudio Castelnovo, and Claudio Chamon, Phys. Rev. B **76**, 174416 (2007)]. The name "mutual information" may be first coined by Adami and Cerf [C. Adami and N.J. Cerf, Phys. Rev. A **56**, 3470 (1997)] and Vedral, Plenio, Rippin and Knight [V. Vedral, M.B. Plenio, M.A. Rippin, and P.L. Knight, Phys. Rev. Lett. **78**, 2275 (1997)], although Stratonovich [R. L. Stratonovich, Izv. Vyssh. Uchebn. Zaved., Radiofiz. **8**, 116 (1965); Probl. Inf. Transm. **2**, 35 (1966)] considered this quantity already in the mid-1960s.

the thermal entropy is always extensive, or in other words, scales as the volume of the region of concern. However, this is not true for the entanglement entropy. For typical ground states, one usually finds an *area law*: the entanglement entropy scales linearly in the *boudary* size of the subregion, which in d-dimensional space can be expressed as

$$S_A \sim \alpha L^{d-1} + O(L^{d-2}), \tag{1.13}$$

where α is a non-universal coefficient and generally depend on geometric details of the subsystem, and the second term indicates higher order corrections.

The first derivation of area law was achieved in the work on geoemtric entropy of the free Klein-Gordon field[31] years ago, then rediscovered in [32]. This is later followed in Ref. [33, 34, 35, 36, 37] on geometric entropy of conformal field theories, partly driven by its possible connection to the Bekenstein-Hawking black hole entropy[38, 39]. But in recent years, the interest in the entanglement entropy revived from a whole new perspective[40, 41, 42, 43]: quantum information theory. It has been proposed to be able to characterize phases[44] and phase transitions[41, 43].

One of the key achievements of the area law is that it improves the understanding of numerical simulation of quantum many-body systems. If there is little entanglement in a ground state, the state can be described by relatively few parameters hence can be simulated effectively. This is exactly the case for 1D systems that satisfy the area law, which states that the entanglement entropy saturates with subsystem size. It explains the power of *density-matrix renormalization group*[15, 45] (DMRG) method for most systems in 1D but fails on some exceptions as well as in higher dimensions. For those failing cases, the entanglement entropy is unbounded as the (sub-)system size grows. For those 1D cases, the entanglement entropy violates the area law; in higher dimensions ($d \leq 2$), the area law already says the entanglement entropy at least grows as $\sim L^{d-1}$. The scaling of entanglement entropy actually specifies how well the ground state can be approximated by the matrix-product state[46, 45] generated by DMRG. This understanding has been made rigorous[47, 48, 49, 50].

The area law for local Hamiltonians is generally valid and can be understood in an intuitive way. Entanglement entropy is supposed to measure the quantum correlations; for

local Hamiltonians the systems interact only over a short distance, hence only correlate quantum mechanically over a short (similar) length scale. Naturally, one expects the total quantum correlations between a large enough subregion (linear size much larger than that length scale) and its exterior, as measured by the entanglement entropy, is proportional to the boundary. This is easier to accept for gapped system where the correlation length is finite. However, the area law even holds for some critical systems where the correlation length diverges.

1.2.1 Corrections to the Area Law

Despite the general validity of the area law in so many different systems, the area scaling behavior does not give us much information about the underlying states or phases. The natural thing is then to turn to the subleading terms.

In some cases, important information about the phase can be revealed by studying the subleading *correction* to the area law[19, 18, 51]. One example is the case for topologically ordered phases[19, 18] in two dimensions (2D) where the subleading correction turns out to be a universal constant:

$$S_A = \alpha L_A - \gamma_{\text{topo}} + O(1/L_A), \tag{1.14}$$

where α is again non-universal, while the subleading constant $\gamma_{\text{topo}} = \log \mathcal{D}$ is universal. Here $\mathcal{D}$ is the *total quantum dimension* of the state

$$\mathcal{D} = \sqrt{\sum_a d_a^2}, \tag{1.15}$$

where a runs over quasi-particle types, and d_a is the *quantum dimension* of a particle of type a. For abelian anyons, $d_a = 1$. For example, for a Laughlin state[52] with filling factor $\nu = 1/q$ where q is an odd integer, $\mathcal{D} = \sqrt{q}$.

A subleading and universal term is also found in the ground-state wavefunctions of quantum Lifshitz fixed points[51, 53] for a subregion with a smooth boundary:

$$S_A = \alpha L_A + \gamma_{\text{QCP}} + O(1/L_A) \tag{1.16}$$

1.3 Logarithmic Divergence in Entanglement Entropy

Despite its general validity, there do exist a few important examples[54, 55, 56, 57, 58, 33, 43, 37, 59, 60, 61, 62] in which the area law is violated, most of which involve quantum crtiticality[33, 37, 43, 59, 63, 61, 62]; the specific manner with which the area law is violated is tied to certain universal properties of the phase or critical point. Similar logarithmic terms have also been founder in states with traditional long-range order [64, 65, 66], although attracting less attentions than the quantum critical cases.

In this dissertation, we focus on a specific type of violations, namely a *logarithmic violations* (as a function the subsystem size), which is also the most widely observed violation, and usually considered to be associated with quantum criticality as found in previous works. In a few known cases, the logarithmic violations in lower dimensions can turn into subleading corrections in higher-dimensions. We shall also discuss such cases.

Thus far there are two important classes of systems that violate the area law: in gapless one dimensional (1D) systems, a logarithmic divergence[33, 43] is found where according to the area law the entanglement entropy should saturate as the size of the subsystem grows; in higher dimensions, for free fermions (or systems with quasi-particle Fermi surfaces) the area law is found to be corrected by a similar logarithmic factor $\log L$[55, 56, 57, 58, 67, 68, 69, 70], where L is the linear dimension of the subsystem.

However, one may ask whether such a logarithmic term in entanglement entropy (if violating the area law) always signals quantum criticality? This is not necessarily the case. As we shall demonstrate in Chapter 2 and Chapter 3 of this dissertation, the presence of traditional long-range order can also give rise to similar logarithmic terms in entanglement entropy. In these cases, logarithmic violations could turn into subleading corrections in higher dimensions.

Another aspect of such logarithmic terms in entanglement entropy we will explore in this dissertation is the connection between that of the one-dimensional fermions and that of fermions in higher dimensions and how the Fermi liquid interactions affect those terms. This is discussed in Chapter 4.

For the remaining of this chapter, we will review some important results of entanglement entropy in extended quantum systems, emphasizing on the logarithmic terms in different systems.

1.4 Examples of Entanglement Entropy

First, we will discuss some widely used techniques for computing the entanglement entropy. There are multiple routes to calculate the entanglement entropy either analytically or numerically. In this dissertation, we mostly rely on the analytic methods but some methods are applicable for both. Then we shall review some important results.

1.4.1 Reduced Density Matrices of Free Systems

The most natural approach to entanglement entropy, is of course, the way that it is defined: the reduced density matrices. However, it turns out to be a difficult task for almost all systems as the partition breaks the translational symmetry, perhaps except for one - the (quasi-) free particles[71]. In this case, one can show that the reduced density matrix of a (quasi-) free system can be fully determined from its two-point correlation function (matrix) within the subsystem.

Following Ref. [71], let us first consider the free fermions for example; for other systems, generalization is straightforward. Take a system with free fermions hopping between lattice sites which can be described by the Hamiltonian:

$$H_0 = -\sum_{n,m} t_{n,m} c_n^\dagger c_m. \tag{1.17}$$

Let $|\Psi\rangle$ be an eigensate of H_0 and

$$\hat{C}_{n,m} = \langle\Psi|c_n^\dagger c_m|\Psi\rangle \tag{1.18}$$

is the two-point correlation function of the state. $\hat{C}_{n,m}$ forms a Hermitian matrix $\hat{C}$. Since $|\Psi\rangle$is a Slater determinant, higher order correlation functions can be factorized as

$$\langle c_n^\dagger c_m^\dagger c_k c_l\rangle = \langle c_n^\dagger c_l\rangle\langle c_m^\dagger c_k\rangle - \langle c_n^\dagger c_k\rangle\langle c_m^\dagger c_l\rangle. \tag{1.19}$$

Now consider the reduced density matrix a subsystem A, which we shall denote as ρ_A. Within A, the two-point correlation functions can be calculated just by ρ_A

$$\hat{C}_{i,j} = \mathrm{Tr}(\rho_A c_i^\dagger c_j), \tag{1.20}$$

and the higher order correlation function is also factorized in the same way. Nothing is changed by the virtual partition. According to Wick's theorem, this factorization property holds if ρ (ρ_A) is the exponential of some free-fermion operator, i.e.

$$\rho_A = \mathcal{K}\exp(-\mathcal{H}_A), \tag{1.21}$$

where $\mathcal{K}$ is a normalization factor and

$$\mathcal{H}_A = \sum_{i,j} h_{i,j} c_i^\dagger c_j = \sum_k \varepsilon_k a_k^\dagger a_k. \tag{1.22}$$

In the second equation, $\mathcal{H}_A$ is diagonalized by imposing a transform $c_i = \sum_k \phi_k(i) a_k$. Then according to Eq. 1.20, we have

$$\hat{C}_{i,j} = \sum_k \phi_k^*(i)\phi_k(j)\frac{1}{e^{\varepsilon_k}+1}, \tag{1.23}$$

while $h_{i,j}$ can written as

$$h_{i,j} = \sum_k \phi_k^*(j)\phi_k(i)\varepsilon_k. \tag{1.24}$$

In matrix form we can write

$$\hat{C} = \hat{\phi}^\dagger \tfrac{1}{e^{[\varepsilon_k]}+1}\hat{\phi}, \tag{1.25}$$

$$\hat{h} = \hat{\phi}[\varepsilon_k]\hat{\phi}^\dagger, \tag{1.26}$$

where $[\varepsilon_k]$ denotes the diagonal matrix with diagonal elements ε_k, and $\hat{\phi}$ indicates the matrix formed by $\phi_k(i)$. From the above two equations, we immediately see that the two matrices $\hat{C}$ and $\hat{h}$ are related as

$$\hat{h} = \{\log[(1 - \hat{C})\hat{C}^{-1}]\}^T. \tag{1.27}$$

Similar argument is also applicable to free bosons, for which the matrices $\hat{h}$ and $\hat{C}$ are related as

$$\hat{h} = \{\log[(1 + \hat{C})\hat{C}^{-1}]\}^T. \tag{1.28}$$

For quadratic or quasi-free systems, we can also apply the same argument if taking the pairing correlators into account $\hat{F}_{i,j} = \langle c_i^\dagger c_j^\dagger \rangle$. But such systems are not of concern in this dissertation.

Although here we started from an eigenstate of H_0, Eq. 1.27 and 1.28 are valid as long as Eq. 1.19 is satisfied, i.e. the state (which can be a mixed one and described only by a density matrix) satisfies Wick's theorem, for example the thermal state $\rho_T \sim \exp(-\beta H_0)$. We also did not specify dimensions here, and the results generally hold for arbitrary dimensions. However, in dimensions higher than one, the matrices $\hat{C}$ and $\hat{h}$ becomes complicated for arbitrary geometries and difficult to handle.

1.4.2 Entanglement Entropy of 1D Free Fermions from Reduced Density Matrices

In this section, we will briefly discuss how to use the reduced density matrix obtained in previous section to compute the entanglement entropy of free fermions in 1D. We emphasize the 1D free fermions for a couple reasons. First, it is the simplest fermionic system [3]. Second, it is also one of the simplest quantum critical system. Besides, several other critical spin systems can be mapped onto it, like the transverse field Ising model, the XX model, etc.. It is also a starting point for our work on entanglement entropy of Fermi liquids in Chapter 4.

[3] We shall discuss free bosons in Chapter 2. At zero temperature it is relatively simple since we can easily write down the Schmidt decomposition from the wavefunction, therefore calculate the entanglement entropy even without the above knowledge of its reduced density matrix.

From Eq. 1.21, we obtain the entanglement entropy formally as

$$S_A = -\mathrm{Tr}(\rho_A \log \rho_A) = \sum_k \log(e^{\varepsilon_k} + 1) + \frac{\varepsilon_k e^{\varepsilon_k}}{e^{\varepsilon_k} + 1}. \tag{1.29}$$

Note that the eigenvalues of $\hat{h}$ matrix can be related those of the $\hat{C}$ matrix which we shall denote as ξ_k

$$\varepsilon_k = \log(\xi_k^{-1} - 1). \tag{1.30}$$

Therefore, we have

$$S_A = \sum_k \Big(\frac{1}{1-\xi_k} - \xi_k\Big) \log \xi_k + \Big(\frac{1}{1-\xi_k} - 1\Big) \log(1-\xi_k). \tag{1.31}$$

According to this equation, to obtain S_A one only needs to obtain the eigenvalues of the (truncated) two-point correlation function matrix. This can be done both numerically and analytically. The latter can be achieved by computing the determinant of $D(\lambda) = \det[\lambda I - \hat{C}] = \prod_k (\lambda - \xi_k)$, then doing a contour integral over the entropy function

$$e(\lambda) = \Big(\frac{1}{1-\lambda} - \lambda\Big) \log \lambda + \Big(\frac{1}{1-\lambda} - 1\Big) \log(1-\lambda),$$

i.e.

$$S_A = \oint d\lambda e(\lambda) \log D(\lambda) \tag{1.32}$$

with a proper contour. For the 1D free fermions, $D(\lambda)$ is a Toeplitz matrix, and its determinant can be computed asymptotically through the Fisher-Hartwig conjecture[72] when the (sub)system size is large. We will not go further into technical details, but simply give the result here

$$S_A \simeq \frac{1}{3} \log L + O(1). \tag{1.33}$$

1.4.3 The Replica Trick

As we have discussed in previous section, even for 1D free fermions, a direct calculation of its entanglement entropy is quite complicated. The difficulties are two fold: (1) the reduced density matrix is not easy to obtain due to the breaking of translational symmetry;

(2) taking logarithm of a matrix is equally, if not more difficult. In order to overcome these difficulties, people often turn to the so called *replica trick* for help. The essence is to make use of the following identity:

$$S_A = -\mathrm{Tr}(\rho_A \log \rho_A) = -\lim_{n\to 1} \frac{\partial}{\partial n} \mathrm{Tr}\, \rho_A^n. \tag{1.34}$$

By using the replica trick, the problem is turned into computing $\mathrm{Tr}\, \rho_A^n$, which is further reduced to computing the free energy of the system on a *replica manifold*. This method successfully avoids the two difficulties mentioned above, and has wide applications to both analytical study and numerical calculations[4]. Before taking the replica limit (the $n \to 1$ limit), it can give us the Rényi entropy.

The remaining of this dissertation is organized as the following. In Chapter 2, we present a study of entanglement properties of systems that exhibit magnetic long-range order. In Chapter 3, we study the entanglement entropy (zero temperature) and mutual information (finite temperature) of a set of free boson models which possess Bose-Einstein condensation. After that, we turn to the quantum critical systems in Chapter 4, and consider the entanglement entropy of the Fermi liquids. In the end, we summarize and discuss future studies and open questions in the field.

[4]For numerical study like quantum Monte Carlo, one cannot take the replica limit, but only computing the Rényi entropy.

CHAPTER 2

ENTANGLEMENT ENTROPY IN STATES WITH TRADITIONAL LONG-RANGE MAGNETIC ORDER

A lot of works have been done on entanglement entropy in various aspects, however, there have been relatively few studies of the behavior of entanglement entropy in states with traditional long-range order[64, 65, 66]. This is perhaps because of the expectation that ordered states can be well described by mean-field theory, and in mean-field theory the states reduce to simple product states that have no entanglement. In particular in the limit of perfect long-range order the mean-field theory becomes "exact", and the entanglement entropy should vanish.

In this chapter, we will summarize our recent work[73] on those states and show that this is *not* the case, and interesting entanglement exists in states with perfect long-range order. We will study two exactly solvable spin-1/2 models: (i) An unfrustrated antiferromagnet with infinite range (or constant) antiferromagnetic (AFM) interaction between spins in opposite sublattices, and ferromagnetic (FM) interaction between spins in the same sublattice; (ii) An ordinary spin-1/2 ferromagnet with arbitrary FM interaction among the spins[74][1]. While the ground states have perfect long-range order for both models, we show that they both have non-zero entanglement entropy that grow logarithmically with the size of the subsystem.

[1]The entanglement property of this model has bee previously studied in Ref.[74]. Here we introduce a different definition of the entanglement entropy that properly takes into account the ground state degeneracy, and can be calculated much more straightforwardly using symmetry consideration. See Sec. 2.3.

2.1 Antiferromagnetic Spin Model and the Ground State

We consider a lattice model composed of two sublattices interpenetrating each other as in Fig. 2.1, with interaction of infinite range, i.e., every spin interacts with all the other spins in the system, with interaction strength independent of the distance between the spins. Within each sublattice, the interaction is ferromagnetic, and between the sublattices the interaction is antiferromagnetic; as a result there is no frustration. The Hamiltonian is written as,

$$H = -J_A \sum_{i,j\in A} \boldsymbol{S}_i \cdot \boldsymbol{S}_j - J_B \sum_{i,j\in B} \boldsymbol{S}_i \cdot \boldsymbol{S}_j + J_0 \sum_{i\in A, j\in B} \boldsymbol{S}_i \cdot \boldsymbol{S}_j, \tag{2.1}$$

with $J_A, J_B, J_0 > 0$. The ground state of (2.1) can be solved in the following manner[75]. Introduction the following notations

$$\boldsymbol{S}_A = \sum_{i\in A} \boldsymbol{S}_i, \quad \boldsymbol{S}_B = \sum_{i\in B} \boldsymbol{S}_i, \quad \boldsymbol{S} = \boldsymbol{S}_A + \boldsymbol{S}_B,$$

then the Hamiltonian can be written as,

$$\begin{aligned} H &= -J_A \boldsymbol{S}_A^2 - J_B \boldsymbol{S}_B^2 + J_0 \boldsymbol{S}_A \cdot \boldsymbol{S}_B \\ &= -J_A \boldsymbol{S}_A^2 - J_B \boldsymbol{S}_B^2 + \frac{J_0}{2}(\boldsymbol{S}^2 - \boldsymbol{S}_A^2 - \boldsymbol{S}_B^2). \end{aligned} \tag{2.2}$$

Then it is not hard to see that the ground state should be:

$$|S_A S_B; S m\rangle = \left|\frac{N_A}{2}, \frac{N_B}{2}; \left|\frac{N_A}{2} - \frac{N_B}{2}\right|, m\right\rangle. \tag{2.3}$$

For simplicity we only consider the simplest case with $N_A = N_B = N$, thus the total system size is $2N$. Then the ground state is reduced to an antiferromagnetic ground state which has zero total spin,

$$|S_A S_B; S m\rangle = |\tfrac{N}{2}\tfrac{N}{2}; 00\rangle. \tag{2.4}$$

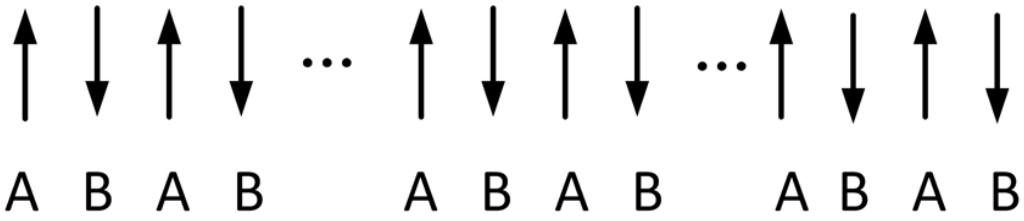

Figure 2.1: Two-sublattice model: two sublattices labeled A and B interpenetrating each other.

This ground state has perfect Neel order, as manifested by the spin-spin correlation function,

$$\begin{aligned} &\langle \boldsymbol{S}_i \cdot \boldsymbol{S}_j \rangle = \frac{1}{4}, \quad i, j \in A \ \text{ or } \ i, j \in B; \\ &\langle \boldsymbol{S}_i \cdot \boldsymbol{S}_j \rangle = -\frac{1}{4} - \frac{1}{4N} \to -\frac{1}{4}, \ \ i \in A \ \text{ and } \ j \in B. \end{aligned} \tag{2.5}$$

2.2 Reduced Density Matrix and Entanglement Entropy

Next, we divide the system spatially into two subsystems which are labeled 1 and 2 respectively and study the ground state entanglement entropy S_E between these two subsystems.

Following is a brief summary about how to solve for the explicit form of the reduced density matrix.

First, we further decompose the system into four parts, $\boldsymbol{S}_{A_1},\ \boldsymbol{S}_{A_2},\ \boldsymbol{S}_{B_1},\ \boldsymbol{S}_{B_2}$, with

$$\begin{cases} \boldsymbol{S}_{A_1} = \sum_{i \in A \wedge i \in 1} \boldsymbol{S}_i, \ \ \boldsymbol{S}_{A_2} = \sum_{i \in A \wedge i \in 2} \boldsymbol{S}_i; \\ \boldsymbol{S}_{B_1} = \sum_{i \in B \wedge i \in 1} \boldsymbol{S}_i, \ \ \boldsymbol{S}_{B_2} = \sum_{i \in B \wedge i \in 2} \boldsymbol{S}_i. \end{cases} \tag{2.6}$$

Therefore, these operators satisfy the following relations,

$$\begin{cases} \boldsymbol{S}_A = \boldsymbol{S}_{A_1} + \boldsymbol{S}_{A_2}, \quad \boldsymbol{S}_B = \boldsymbol{S}_{B_1} + \boldsymbol{S}_{B_2}; \\ \boldsymbol{S}_1 = \boldsymbol{S}_{A_1} + \boldsymbol{S}_{B_1}, \quad \boldsymbol{S}_2 = \boldsymbol{S}_{A_2} + \boldsymbol{S}_{B_2}. \end{cases} \tag{2.7}$$

Here we note that, as discussed in the previous section, the spin state within each sublattice is ferromagnetic. This means that not only must the total spin quantum numbers of $\boldsymbol{S}_A$ and $\boldsymbol{S}_B$ take their maximum values, but the total spin quantum numbers of $\boldsymbol{S}_{A_1}$, $\boldsymbol{S}_{A_2}$, $\boldsymbol{S}_{B_1}$ and $\boldsymbol{S}_{B_2}$ must also take their maximum values. More importantly, these values are thus fixed, which enables us to treat the operators $\boldsymbol{S}_{A_1}$, $\boldsymbol{S}_{A_2}$, $\boldsymbol{S}_{B_1}$ and $\boldsymbol{S}_{B_2}$ as four single spins, and in what follows we shall denote these operators by their corresponding spin quantum numbers. The problem is then that we are given a four spin state in which the spins S_{A_1} and S_{A_2} are combined into a state with total spin S_A and the spins S_{B_1} and S_{B_2} are combined in a state with total spin S_B, and then these two states are combined into a total singlet (resulting in the ground state of our long-range AFM model), and we must express this state in a basis in which the spins S_{A_1} and S_{A_2} are combined into a state with total spin S_1 and S_{B_1} and S_{B_2} are combined into a state with total spin S_2. This change of basis involves the familiar LS-jj coupling scheme. At this point, to obtain the reduced density matrix we only have to re-express the density matrix in bases of $\langle S_1 m_1 S_2 m_2; S m|$ by means of LSjj coupling, then trace out either $\langle S_1 m_1|$ or $\langle S_2 m_2|$.

After some algebra we arrive at:

$$\rho_1 = tr_{(2)}(\rho) = \sum_{S_1 m_1} |\lambda_{S_1 m_1}|^2 |S_1 m_1\rangle\langle S_1 m_1|, \tag{2.8}$$

where λ_{S_1,m_1} is given by

$$\lambda_{S_1,m_1} = \left[\frac{(N+1)(N-N_1)!N_1!}{(N-N_1-S_1)!(N-N_1+S_1+1)!} \times \frac{(N-N_1)!N_1!}{(N_1-S_1)!(N_1+S_1+1)!}\right]^{\frac{1}{2}}. \tag{2.9}$$

The bipartite entanglement entropy between subsystems 1 and 2 is then given by,

$$S_E = S_{E1} = S_{E2} = -\sum_{S_1,m_1} \left|\lambda_{S_1 m_1}\right|^2 \ln(\left|\lambda_{S_1 m_1}\right|^2). \tag{2.10}$$

Here, in order to distinguish the entanglement entropy S from the spin number S, we use an extra subscript S_E to denote the entanglement entropy. We note that, although $\lambda_{S_1 m_1}$ is written with an explicit m_1 dependence, the actual expression is independent of m_1. As a result, we can eliminate the summation over m_1 from (2.11) by multiplying by a factor of

$2S_1 + 1$. The final expression for the entanglement entropy is then,

$$S_E = -\sum_{S_1}(2S_1 + 1)\left|\lambda_{S_1}\right|^2 \ln(\left|\lambda_{S_1}\right|^2). \tag{2.11}$$

Next we shall present the asymptotic behavior of this bipartite entanglement entropy in two limiting cases:

- $N_1 = N_2 = N$, this case gives the saturated entropy at fixed N since intuitively E should increase with the subsystem size.

- $1 \ll N_1 \ll N$, in this limit we are considering system's entanglement with its (much larger) environment, and generically we should be able to find that the entropy should be independent of the total system size as $N \to \infty$, which is indeed what we find.

By extracting the asymptotic behavior of the eigenvalues of the reduced density matrix λ_{S_1}, turning the summation into integral and forcing the normalization condition of those eigenvalues, the entanglement entropy can be analytically calculated:

$$\begin{aligned} S_E &\simeq -\int_0^\infty A(2S_1 + 1)e^{-S_1^2(\frac{1}{N-N_1}+\frac{1}{N_1})} \ln\left(Ae^{-S_1^2(\frac{1}{N-N_1}+\frac{1}{N_1})}\right) dS_1 \\ &\simeq \ln\left(N_1 - \frac{N_1^2}{N} + \frac{1}{2}\sqrt{\frac{\pi(N-N_1)N_1}{N}}\right). \end{aligned} \tag{2.12}$$

First let us consider the equal partition case, which presumably gives the upper limit of the entanglement entropy for a given total system size. For simplicity we set N to be even (note that the total system size is $2N$), thus $N_1 = \frac{N}{2}$, and $\frac{1}{A} = \frac{1}{4}(N + \sqrt{N\pi})$. So the entanglement entropy becomes,

$$S_E = \ln\left(\frac{N}{4} + \frac{1}{4}\sqrt{\pi N}\right) \simeq \ln N - \ln 4 \simeq \ln N - 1.38629. \tag{2.13}$$

For the unequal partition case, $1 \ll N_1 \ll N$, we can expand the entropy as follows,

$$\begin{aligned} S_E &\simeq \ln\left[N_1\left(1-\frac{N_1}{N}+\frac{1}{2}\sqrt{\frac{\pi(1-\frac{N_1}{N})}{N_1}}\right)\right] \\ &\simeq \ln N_1 - \frac{N_1}{N} + O\left(\left(\frac{N_1}{N}\right)^2\right). \end{aligned} \tag{2.14}$$

From this expression we see that when the assumed condition is satisfied the entropy indeed depends only on the subsystem size to leading order.

2.3 Ferromagnetic model and its entanglement entropy

In this section we consider a ferromagnetic (FM) spin-1/2 model on an arbitrary lattice with N sites,

$$H = -\sum_{i\neq j} J_{ij}\boldsymbol{S}_i \cdot \boldsymbol{S}_j, \tag{2.15}$$

with $J_{ij} > 0$. The ground state is the fully magnetized state $|S\,M\rangle$ with $S = N/2$ and $M = -S, -S+1, \cdots, S$, and is clearly long-range ordered: $\langle \boldsymbol{S}_i \cdot \boldsymbol{S}_j \rangle = 1/4$. However there is a crucial difference between the FM ground state and the AFM ground state studied earlier: the FM ground state has a finite degeneracy, and thus the system exhibits a non-zero entropy even at zero temperature, $E_0 = \log(2S+1) = \log(N+1)$, resulting from the density matrix of the entire system,

$$\rho = \frac{1}{2S+1}\sum_{M=-S}^{S} |S\,M\rangle\langle S\,M| = \frac{1}{N+1}\sum_{M=-S}^{S} |S\,M\rangle\langle S\,M| \tag{2.16}$$

In this case the entanglement entropy between two subsystems (1 and 2) is defined in the following manner. We first obtain reduced density matrices for subsystems 1 and 2 by

tracing out degrees of freedom in 2 and 1 from ρ:

$$\begin{aligned}\rho_1 = tr_{(2)}\rho = \frac{1}{N+1}\sum_{M=-S}^{S} tr_{(2)}(|S\,M\rangle\langle S\,M|) = \frac{1}{N+1}\sum_{M=-S}^{S}\rho_{1M},\\ \rho_2 = tr_{(1)}\rho = \frac{1}{N+1}\sum_{M=-S}^{S} tr_{(1)}(|S\,M\rangle\langle S\,M|) = \frac{1}{N+1}\sum_{M=-S}^{S}\rho_{2M},\end{aligned} \tag{2.17}$$

and calculate from them the entropy of the subsystems, S_{E1} and S_{E2}. The entanglement is measured by the quantum mutual information S_M as defined in Eq. (1.11)

$$S_M = (S_{E1} + S_{E2} - S_0)/2. \tag{2.18}$$

For the present case S_{E1} and S_{E2} can be easily obtained from the following observations. (i) Because the total spin is fully magnetized, so are those in the subsystems: $S_1 = N_1/2$ and $S_2 = N_2/2$. Thus this is a two-spin entanglement problem. (ii) Because the total density matrix ρ is proportional to the identity matrix in the ground state subspace, it is invariant under an arbitrary rotation in this subspace. (iii) As a result the reduced density matrix ρ_1 is also invariant under rotation in the subspace of subsystem 1 with $S_1 = N_1/2$, and is proportional to the identity matrix in this subspace. Thus

$$\rho_1 = \frac{1}{N_1+1}\sum_{M_1=-\frac{N_1}{2}}^{\frac{N_1}{2}} |\frac{N_1}{2}M_1\rangle\langle\frac{N_1}{2}M_1| \tag{2.19}$$

and $S_{E1} = \log(N_1+1)$ (in agreement with Ref. [74]). Similarly $S_{E2} = \log(N_2+1)$. Thus

$$S_M = [\log(N_1+1) + \log(N_2+1) - \log(N+1)]/2. \tag{2.20}$$

We find in both the equal partition ($N_1 = N_2 = N/2$) and unequal partition ($N_1 \ll N_2 = N - N_1$) limits, the entropy grows logarithmically with subsystem size N_1,

$$\lim_{N_1\to\infty} E \to \frac{1}{2}\log(N_1). \tag{2.21}$$

2.4 Discussion

In this chapter, we have studied magnetic systems with both long-range ferromagnetic and antiferromagnetic orders. In both cases, a logarithmic divergent term $\sim \log N_{1(A)}$ dominates the entanglement entropy, which violates the area law, despite the perfect long-range order in the ground state. This is somewhat surprising as one might think that in such Hamiltonians one can obtain certain properties of the system exactly using meanfield theory, in which the ground state is approximated by a product state with no entanglement.

Our results indicate that mean-field approximation is not appropriate for entanglement calculation, even if it is exact other purposes. This point is particularly striking for the AFM model, in which the ground state is unique. The source of the discrepancy is there still is quantum fluctuations even in such a model with super long-range interaction, which renders the ground state a singlet, even though quantum fluctuation does not reduce the size of the order parameter. The entanglement is due to the quantum fluctuation of the direction of the order parameter, which is a collective mode with zero wave vector, a zero mode this is missed by any mean-field approximation.

Second, the entropy does not obey the area law. The reasons for that are different for the two cases we studied. In the AFM model, the interaction does not depend on distance in the Hamiltonian, thus there is no notion of distance or area in this model. In the FM model, on the other hand, the ground state is independent of the Hamiltonian, as long as all interactions are FM. The fully magnetized ground states are invariant under permutation of spins, thus there is no notion of distance or area in the ground states, even though the terms in Hamiltonian can have distance dependence.

Third, the absence of an area law is special to the cases we studied, again each in their own ways. For the FM model, it is specific to zero temperature. As soon as a finite temperature is turned on, one expects the entanglement entropy or mutual information to grow with the area separating the two subsystems or blocks, as long as the interaction is not long-range. For the AFM model at zero temperature, we do expect an area-law contribution to the entropy for shortrange or even certain power-law long-range interaction due to quantum fluctuations. This is most easily seen within spinwave approximation, which is a version of mean-field theory. Within the spin-wave approximation spins are

mapped onto bosons, and the Hamiltonian is mapped onto coupled harmonic oscillators. Detailed recent studies have established the area law of entanglement for such systems. In this regard the super long-range AFM model we study here is very special in that all spin-wave degrees of freedom at finite wave vector disappear, and the only degrees of freedom contributing to the ground state are zero wave-vector modes represented by S_A and S_B; as a result there is no area-law contribution from quantum fluctuations of spin waves. We conclude by speculating that in the more general cases that do have an area-law contribution to the entanglement entropy, as long as long-range spin order is present, the logarithmic contribution due to fluctuations of the order parameter zero modes we find here will remain and show up as a subleading yet singular correction to the area law. If that is the case, then conventional long-range order contributes to the entanglement entropy in a way similar to the much subtler quantum criticality.

CHAPTER 3

LOGARITHMIC DIVERGENCE OF ENTANGLEMENT ENTROPY AND MUTUAL INFORMATION IN SYSTEMS WITH BOSE-EINSTEIN CONDENSATION

Bosonic systems are another class of systems that could exhibit long-range order. However, previous studies of entanglement entropy have mostly focused on *relativistic* free bosonic field theories [33, 37, 76], which are equivalent to coupled harmonic oscillator systems (for reviews, see Refs. [77] and [78]).

In this chapter we study the entanglement properties of free *non-relativistic* Bose gases. In previous chapter, we calculated the block entanglement entropy of some exactly soluble spin models that exhibit ferromagnetic or antiferromagnetic long-range order in the ground state, and found that such conventional orders also lead to logarithmically divergent contribution to the entropy. Bose-Einstein condensation (BEC) is perhaps the simplest example of conventional ordering. It is thus natural to study its entanglement properties. As we are going to show, a Bose-Einstein condensate (referred to as a condensate from now on) indeed makes a logarithmically divergent contribution to the entropy as well.

Besides the entanglement entropy of the ground state, the entanglement properties of system at finite temperature are also of great interest. However, the entanglement entropy is only well-defined for a pure state. For a system that is described by a mixed density matrix, the von Neumann entropy of the reduced density matrix becomes different for the two parts

of the bipartite systems. In such cases, there is a natural extension of the entanglement entropy that one can work with - the mutual information[27, 28]. We will show that a condensate, when present, makes a logarithmically divergent contribution to the mutual information.

This chapter is organized as follows. In Sec. 3.1 we study the ground state entanglement entropy of a generic free boson model that is translationally invariant [79]. In Sec. 3.2 we introduce an infinite-range hopping model for bosons which is exactly solvable, and calculate the mutual information analytically. In Sec. 3.3 we introduce a long-range hopping model for bosons in one-dimension (1D) which exhibits a finite temperature BEC for a certain parameter range, then we present a numerical study of the mutual information for this model. In the end, we summarize and discuss the results of this paper in Sec. 3.4.

3.1 Zero Temperature: Entanglement Entropy of Free Bosons

Consider a general Hamiltonian of free bosons hopping on a lattice of size L:

$$H = -\sum_{ij} t_{ij} \hat{a}_i^\dagger \hat{a}_j, \tag{3.1}$$

where $t_{ij} > 0$, $\hat{a}_i(\hat{a}_i^\dagger)$'s are the bosonic annihilation (creation) operators. If the system is translationally invariant, $t_{ij} = t_{i-j}$, then the Hamiltonian can be diagonalized by Fourier transformation:

$$H = \sum_k \varepsilon(k) \hat{b}_k^\dagger \hat{b}_k, \tag{3.2}$$

where $\hat{b}_k = \frac{1}{\sqrt{L}} \sum_j e^{-ijk} \hat{a}_j$ is the annihilation operator in k space. In most generic cases, the ground state is the $k = 0$ state. At zero temperature, all particles fall into the ground state. For a system containing N particles, the ground state is given by:

$$|\Psi_0\rangle = \frac{1}{\sqrt{N!}} (\hat{b}_0^\dagger)^N |0\rangle = \frac{1}{\sqrt{N!}} (\frac{1}{\sqrt{L}} \sum_j \hat{a}_j^\dagger)^N |0\rangle. \tag{3.3}$$

To consider its bipartite block entanglement entropy, we divide the system of size L in two parts, and label them A and B respectively. Let the sizes of each part be L_A and L_B, $L_A + L_B = L$, and define

$$\hat{a}_A^\dagger = \frac{1}{\sqrt{L_A}} \sum_{j\in A} \hat{a}_j^\dagger, \qquad \hat{a}_B^\dagger = \frac{1}{\sqrt{L_B}} \sum_{j\in B} \hat{a}_j^\dagger. \tag{3.4}$$

Then we can write $|\Psi_0\rangle$ as:

$$\begin{aligned} |\Psi_0\rangle &= \frac{L^{-N/2}}{\sqrt{N!}} (\sqrt{L_A}\hat{a}_A + \sqrt{L_B}\hat{a}_B)^N |0\rangle = \frac{L^{-N/2}}{\sqrt{N!}} \sum_{l=0}^{N} \frac{N!}{(N-l)!l!} (\sqrt{L_A}\hat{a}_A^\dagger)^l (\sqrt{L_B}\hat{a}_B^\dagger)^{N-l} |0\rangle \\ &= \sum_l \sqrt{\lambda_l} |l\rangle_A \otimes |N-l\rangle_B, \end{aligned} \tag{3.5}$$

where $\lambda_l = L^{-N} \frac{N!}{(N-l)!l!} L_A^l L_B^{N-l}$, $|l\rangle_A = \frac{1}{\sqrt{l!}} \hat{a}_A^{\dagger l} |0\rangle_A$, $|N-l\rangle_B = \frac{1}{\sqrt{(N-l)!}} \hat{a}_B^{\dagger N-l} |0\rangle_B$, and $|0\rangle = |0\rangle_A \otimes |0\rangle_B$.

This is an explicit Schmidt decomposition, and therefore the entanglement entropy is readily given by:

$$S_A = -\sum_l \lambda_l \ln \lambda_l. \tag{3.6}$$

We are interested in the asymptotic behavior in two limiting cases: (1) the equal partition case; (2) size of B is substantially larger than A, i.e., $L_B \gg L_A$.

(i) Equal partition, $L_A = L_B = \frac{L}{2}$:

$$\lambda_l = \frac{N!}{l!(N-l)!} \frac{L_A^l L_B^{N-l}}{L^N} = \frac{N!}{l!(N-l)!2^N} = \frac{N!}{(\frac{N}{2})!} \frac{(\frac{N}{2})!2^N}{(\frac{N}{2} - (\frac{N}{2} - l))!(\frac{N}{2} + (\frac{N}{2} - l))!}. \tag{3.7}$$

Let $x = \frac{N}{2} - l$, then $x \in [-\frac{N}{2}, \frac{N}{2}]$, and we can denote λ_l as $\lambda_x = \frac{2^N N!}{(\frac{N}{2})!} \frac{(\frac{N}{2})!}{(\frac{N}{2}-x)!(\frac{N}{2}+x)!}$ which can be approximated by a Gaussian distribution factor $\lambda_x \sim e^{\frac{-2x^2}{N}}$ when N is large. In the limit $N \to \infty$, the summation over n (or x) can be approximated by an integral. Also in this limit, the Gaussian factor is sharply peaked around $x = 0$, the integral region can be extended to from minus infinity to infinity. Using the fact that $\sum_x \lambda_x \simeq \int_{-\infty}^{\infty} \lambda(x)dx = 1$, we arrive at

$$\lambda(x) \simeq \sqrt{\frac{2}{N\pi}} e^{-\frac{2x^2}{N}}. \tag{3.8}$$

The entanglement entropy is then

$$S_A \simeq -\int_{-\infty}^{\infty} \lambda(x) \ln \lambda(x) dx = \frac{1}{2}\left(1 + \ln(\frac{N\pi}{2})\right) = \frac{1}{2}\ln N + O(1). \tag{3.9}$$

(ii) Unequal partition, $L_B \gg L_A$:

If $L_B \gg L_A$, $L \to \infty$, but keep $\frac{N}{L} \to \langle n \rangle$ (fixed), the distribution of λ_l approaches a Poisson distribution:

$$\lambda_l = \frac{N!}{l!(N-l)!}\frac{L_A^l L_B^{N-l}}{L^N} \xrightarrow{N\to\infty} \frac{(L_A\langle n\rangle)^l e^{-L_A\langle n\rangle}}{l!}. \tag{3.10}$$

The entropy of the Poisson distribution, which in this case is our entanglement entropy, is known to be:

$$\begin{aligned} S_A &= \frac{1}{2}[1 + \ln(2\pi L_A\langle n\rangle)] - \frac{1}{12L_A\langle n\rangle} + O(\frac{1}{(L_A\langle n\rangle)^2}) \\ &= \frac{1}{2}[1 + \ln(2\pi N_A)] - \frac{1}{12N_A} + O(\frac{1}{(N_A)^2}) = \frac{1}{2}\ln N_A + O(1), \end{aligned} \tag{3.11}$$

where $N_A = L_A\langle n\rangle$ is the average particle number in subsystem A.

Therefore, we find, in both cases, that the leading term of the mutual information goes as $\frac{1}{2}\ln N_A$ for $L_A \leq L_B$.

3.2 Mutual Information: Analytic Study of an Infinite-Range Hopping Model

In this section, we will study the natural generalization of entanglement entropy at finite temperature: the mutual information defined in Eq. 1.11

$$S_M = \frac{1}{2}(S_A + S_B - S_0). \tag{3.12}$$

Note that at finite temperature S_A and S_B are no longer the same due to the fact that the system is described by a mixed density matrix.

3.2.1 Model, spectrum and thermodynamic properties

In order to facilitate an exact solution, we consider the following infinite-range hopping model which is obtained by setting t_{ij} in Eq. (3.1) to a constant properly scaled by the system size $t_{ij} = t/L$ so that the thermodynamic limit is well-defined. The Hamiltonian is then

$$H = -\frac{t}{L}\sum_{i,j}\hat{a}_i^\dagger \hat{a}_j = -\frac{t}{L}(\sum_i \hat{a}_i^\dagger)(\sum_j \hat{a}_j). \tag{3.13}$$

By substituting the Fourier transform of $\hat{a}_j$'s defined in Sec. II, $\hat{b}_k = \frac{1}{\sqrt{L}}\sum_j e^{-ijk}\hat{a}_j$, one obtains:

$$H = -t\hat{b}_0^\dagger \hat{b}_0. \tag{3.14}$$

This model has a very simple spectrum with a ground state with energy $-t$, and all the other excited states are degenerate with zero energy. This particularly simplified spectrum makes an exact solution possible.

To study the finite temperature properties of this model, we will work with the grand canonical ensemble (GCE), in which the chemical potential μ is introduced to control the average density of the system. This model exhibits BEC at finite temperature T_C. To determine T_C, we start by considering a system of finite size L, and its occupation numbers are:

$$\langle N_{k=0}\rangle = \langle N_0\rangle = \frac{1}{e^{\beta(-t-\mu)}-1},\ \langle N_k\rangle = \frac{1}{e^{\beta(-\mu)}-1} \text{ for } k \neq 0. \tag{3.15}$$

Here $\langle N_0\rangle$ and $\langle N_k\rangle$ denote average occupation numbers for the corresponding states in k-space; $\beta = \frac{1}{T}$ is the inverse temperature. From this point on, when we write $\langle N_k\rangle$, it immediately indicates $k \neq 0$. The average total particle number of the system will be denoted as $\langle N\rangle$. To identify T_C, we know in the thermodynamic limit, when $T \to T_C + 0^+$, $\mu \to E_{k=0} = -t$, and $\frac{\langle N_0\rangle}{N} \to 0$. Therefore, $\langle N_k\rangle = \frac{1}{e^{\beta_c t}-1} \simeq \frac{\langle N\rangle}{L} = \langle n\rangle$ where $\langle n\rangle$ is the average particle density. So we obtain:

$$T_C = \frac{t}{\ln(1+1/\langle n\rangle)}. \tag{3.16}$$

Above T_C, $\langle n\rangle = \frac{L-1}{L}\frac{1}{e^{-\beta\mu}-1} + \frac{1}{L}\frac{1}{e^{\beta(-t-\mu)}-1}$, from which in the large L limit we can derive that

$$\mu = -T\ln\left(1+\frac{1}{\langle n\rangle}\right). \tag{3.17}$$

μ has a finite size correction which is negligible above T_C, but will become important below T_C.

We also know that the partition function of the system in GCE. bears the following form:

$$Z = (\frac{1}{1-e^{\beta\mu}})^{L-1}\frac{1}{1-e^{\beta(t+\mu)}}, \tag{3.18}$$

from which it is easy to show that the entropy in GCE takes the following form:

$$\begin{aligned} S_0 &= -\frac{\partial\Omega}{\partial T} = \ln Z - \frac{1}{T}\frac{\partial}{\partial\beta}\ln Z \\ &= (1+\langle N_0\rangle)\ln(1+\langle N_0\rangle) - \langle N_0\rangle\ln N_0 \\ &+ (L-1)\left[(1+\langle N_k\rangle)\ln(1+\langle N_k\rangle) - \langle N_k\rangle\ln\langle N_k\rangle\right]. \end{aligned} \tag{3.19}$$

Anticipating later relevance, we are particularly interested in the behavior of finite size systems near T_C. For a finite system, the chemical potential μ is no longer strictly equal the ground state energy below T_C, but picks up a finite size correction $\delta\mu$ determined by the following condition:

$$\frac{1}{e^{-\beta\delta\mu}-1} = \langle N_0\rangle, \tag{3.20}$$

from which we can easily derive that

$$\delta\mu = -T\ln\left(1+\frac{1}{\langle N_0\rangle}\right). \tag{3.21}$$

Consider $T = T_C = \frac{t}{\ln(1+1/\langle n\rangle)}$, and make use of the following fact

$$\langle N_0\rangle = \langle N\rangle - \sum_{k\neq 0}\langle N_k\rangle = \langle N\rangle - \frac{L-1}{e^{\beta(t-\delta\mu)}-1}, \tag{3.22}$$

we obtain

$$\langle N_0\rangle = \langle N\rangle - \frac{L-1}{e^{\beta_c(t-\delta\mu)}-1} = \langle N\rangle - \frac{L-1}{(1+L/\langle N\rangle)(1+1/\langle N_0\rangle)-1}. \tag{3.23}$$

This equation can be solved to give $\langle N_0 \rangle$ as a function of system size L at a given density $\langle n \rangle = \langle N \rangle / L$, at $T = T_C$:

$$\langle N_0 \rangle = \sqrt{L} \sqrt{\left(\frac{\langle N \rangle}{L} \right)^2 + \frac{\langle N \rangle}{L} + \frac{1}{4L}} \simeq \sqrt{L} \sqrt{\langle n \rangle^2 + \langle n \rangle}. \tag{3.24}$$

Even though this divergent N_0 does not affect the thermodynamic behavior of the system, as we will see later it makes a (leading) divergent contribution to the mutual information at $T = T_C$ depending on how the system is partitioned, or specifically how large is the subsystem size L_A compared with this $\sqrt{L}$ divergence.

3.2.2 Formalism and issues

In the following part, we will use Peschel's result [71] on the reduced density matrix of a Gaussian state:

$$\rho_A = \mathcal{K} e^{\{\ln((1+G)G^{-1})\}_{ij}^T \hat{a}_i^\dagger \hat{a}_j}, \tag{3.25}$$

where $G_{ij} = \langle \hat{a}_i^\dagger \hat{a}_j \rangle$ is the two point correlation function matrix truncated within the subsystem, and $\mathcal{K}$ is the normalization factor. The entropy is given as

$$S_A = \sum_l \left[(1 + g_l) \ln(1 + g_l) - g_l \ln g_l \right], \tag{3.26}$$

where g_l's are the complete set of eigenvalues of G's (after truncation). Actually this formula also applies to the original system.

We must note that, this formula does not lead to the correct zero temperature limit for the entropy. At zero temperature, $G_{ij} = \langle a_i^\dagger a_j \rangle = \langle n \rangle$. Its eigenvalues are all zero except for one: $g_0 = \langle n \rangle L = \langle N \rangle$, which gives us a non-zero entropy $S_{T=0} = (\langle N \rangle + 1) \ln(\langle N \rangle + 1) - \langle N \rangle \ln \langle N \rangle = \ln \langle N \rangle + \langle N \rangle \ln(1 + \frac{1}{\langle N \rangle}) \sim \ln \langle N \rangle$ at $T = 0$. This reflects the fact that we are working with GCE where the particle-number fluctuation is still permissible at $T = 0$ and the fluctuation amplitude $\delta N \sim \langle N \rangle$. However, as we show below, the mutual information still converges to the correct zero temperature limit, the entanglement entropy, at least to the leading order.

The von Neumann entropy for a subsystem A is given by

$$S_A^{(\mathrm{GCE})} = (N_A + 1)\ln(N_A + 1) - N_A \ln N_A = \ln N_A + N_A \ln(1 + \frac{1}{N_A}), \tag{3.27}$$

where $N_A = \langle n \rangle L_A$ is the average total particle number in the subsystem A. In the large N limit, the second term converges to 1. So the mutual information is given by:

$$S_M \equiv \frac{1}{2}(S_A + S_B - S_{GCE\ T=0}) = \frac{1}{2}\left(\ln \frac{N_A N_B}{N} + 1\right). \tag{3.28}$$

For $N_A \leq N_B$, we have

$$S_M \simeq \frac{1}{2}\ln N_A + O(1). \tag{3.29}$$

This agrees with Eq. (3.11) at the leading order.

3.2.3 Mutual information

According to our Eq. (3.25) and Eq. (3.26), to obtain the von Neumann entropy of the reduced density matrix, all what we have to do is to diagonalize the truncated two-point correlation function matrix. Fortunately, within this infinite-range hopping model, this is rather simple. For a finite system, we can obtain a general result for all temperatures:

$$\begin{aligned} G_{ij} &= \langle \hat{a}_i^\dagger \hat{a}_j \rangle = \langle \tfrac{1}{L} \textstyle\sum_k e^{-ik(i-j)} \hat{b}_k^\dagger \hat{b}_k \rangle \\ &= \frac{1}{L}\langle \hat{b}_0^\dagger \hat{b}_0 \rangle + \frac{1}{L}\sum_{k\neq 0} e^{-ik(i-j)} \langle \hat{b}_k^\dagger \hat{b}_k \rangle = \frac{\langle N_0 \rangle}{L} + \frac{\langle N_k \rangle}{L}\sum_{k\neq 0} e^{-ik(i-j)} \\ &= \frac{\langle N_0 \rangle}{L} + (\delta_{ij} - \frac{1}{L})\langle N_k \rangle. \end{aligned} \tag{3.30}$$

In the above calculation, we have made use of the fact that $\langle N_k \rangle$ is *k-independent*. This matrix is easily diagonalized. For a system of size L, and a G truncated to a size of $L_A \times L_A$ denoted by G_A, the eigenvalues are

$$g_1 = \frac{L_A \langle N_0 \rangle}{L} + \frac{L - L_A}{L}\langle N_k \rangle,\ g_l = \langle N_k \rangle \text{ for } l = 2, \ldots, L_A. \tag{3.31}$$

Now the von Neumann entropy of subsystem A can be calculated directly from above result:

$$\begin{aligned}
S_A &= \sum_{l=1}^{L_A} ((1+g_l)\ln(1+g_l) - g_l \ln g_l) \\
&= \left(1 + \frac{L_A\langle N_0\rangle}{L} + \frac{L-L_A}{L}\langle N_k\rangle\right)\ln\left(1 + \frac{L_A\langle N_0\rangle}{L} + \frac{L-L_A}{L}\langle N_k\rangle\right) \\
&- \left(\frac{L_A\langle N_0\rangle}{L} + \frac{L-L_A}{L}\langle N_k\rangle\right)\ln\left(\frac{L_A\langle N_0\rangle}{L} + \frac{L-L_A}{L}\langle N_k\rangle\right) \\
&+ (L_A - 1)\left[(1+\langle N_k\rangle)\ln(1+\langle N_k\rangle) - \langle N_k\rangle \ln(\langle N_k\rangle)\right].
\end{aligned} \tag{3.32}$$

Combining the above with Eq. (3.19), we can obtain the mutual information for a general bipartite system:

$$\begin{aligned}
S_M &= \frac{1}{2}(S_A + S_B - S_0) \\
&= \frac{1}{2}\Bigg[\left(1 + \frac{L_A\langle N_0\rangle}{L} + \frac{L_B}{L}\langle N_k\rangle\right)\ln\left(1 + \frac{L_A\langle N_0\rangle}{L} + \frac{L_B}{L}\langle N_k\rangle\right) \\
&- \left(\frac{L_A\langle N_0\rangle}{L} + \frac{L_B}{L}\langle N_k\rangle\right)\ln\left(\frac{L_A\langle N_0\rangle}{L} + \frac{L_B}{L}\langle N_k\rangle\right) \\
&+ \left(1 + \frac{L_B\langle N_0\rangle}{L} + \frac{L_A}{L}\langle N_k\rangle\right)\ln\left(1 + \frac{L_B\langle N_0\rangle}{L} + \frac{L_A}{L}\langle N_k\rangle\right) \\
&- \left(\frac{L_B\langle N_0\rangle}{L} + \frac{L_A}{L}\langle N_k\rangle\right)\ln\left(\frac{L_B\langle N_0\rangle}{L} + \frac{L_A}{L}\langle N_k\rangle\right) \\
&- (1+\langle N_k\rangle)\ln(1+\langle N_k\rangle) + \langle N_k\rangle \ln\langle N_k\rangle - (1+\langle N_0\rangle)\ln(1+\langle N_0\rangle) + \langle N_0\rangle \ln\langle N_0\rangle\Bigg].
\end{aligned} \tag{3.33}$$

Next, we shall discuss the asymptotic behavior of S_M in different temperature regions and with different partitions.

(1) $L_A \ll L, T > T_C$:

in this case, $\langle N_0\rangle$ and $\langle N_k\rangle \simeq \langle n\rangle$ are both of order one , so $\frac{L_A\langle N_0\rangle}{L} \to 0$, $\frac{L_A\langle N_k\rangle}{L} \to 0$, $L_B \simeq L$. Thus

$$S_M \simeq O\left(\frac{L_A}{L}\right). \tag{3.34}$$

(2) $L_A = L_B = \frac{L}{2}$, $T > T_C$: in this case, S_M is reduced to

$$\begin{aligned} S_M = \frac{1}{2}\Big(& (2 + \langle N_0\rangle + \langle N_k\rangle) \ln\left(1 + \frac{1}{2}\left(\langle N_0\rangle + \langle N_k\rangle\right)\right) \\ & - (\langle N_0\rangle + \langle N_k\rangle) \ln\left(\langle N_0\rangle/2 + \langle N_k\rangle/2\right) \\ & - (1 + \langle N_k\rangle) \ln\left(1 + \langle N_k\rangle\right) + \langle N_k\rangle \ln\langle N_k\rangle \\ & - (1 + \langle N_0\rangle) \ln(1 + \langle N_0\rangle) + \langle N_0\rangle \ln\langle N_0\rangle\Big) \end{aligned} \tag{3.35}$$

which can also be written as an explicit function of L, $\langle n\rangle$ and T using previous results.

(3) $L_A \ll L$, $T < T_C$: in this case, $\langle N_0\rangle$ becomes a macroscopic number, while $\langle N_k\rangle$ remains to be of order 1. Therefore we isolate the contribution from $\langle N_0\rangle$, and other terms are of order $O(1)$:

$$S_M = \frac{1}{2} \ln\left(1 + \frac{L_A\langle N_0\rangle}{L}\right) + O(1). \tag{3.36}$$

If we define $\langle N_{A0}\rangle = \frac{L_A\langle N_0\rangle}{L}$ to be the average particle number in the condensate of the subsystem, then

$$S_M = \frac{1}{2} \ln\langle N_{A0}\rangle + O(1). \tag{3.37}$$

(4) $L_A = L_B = \frac{L}{2}$, $T < T_C$: the leading contribution is again obtained by keeping $\langle N_0\rangle$'s contribution only:

$$S_M = \frac{1}{2} \ln\left(\frac{1}{4}\langle N_0\rangle + 1\right) + O(1) = \frac{1}{2} \ln\langle N_{A0}\rangle + O(1). \tag{3.38}$$

(5) $L_A \ll L$, $T = T_C$: as we calculated before, $\langle N_0\rangle$ diverges as $\sqrt{L}$. When $L_A \ll L$, according to Eqs. (3.36) and (3.24), we have

$$S_M = \frac{1}{2} \ln\left(1 + \frac{L_A\sqrt{(\langle n\rangle + 1)\langle n\rangle}}{\sqrt{L}}\right) + O(1) = \frac{1}{2} \ln\left(\langle n\rangle \frac{L_A}{\sqrt{L}}\right) + O(1). \tag{3.39}$$

For such partition, the scaling behavior of mutual information depends on the ratio

$\frac{L_A}{\sqrt{L}}$. If we consider L_A is a small but still finite fraction of L, the scaling behavior of the mutual information still persists: $S_M = \frac{1}{4}\ln(\langle n\rangle L_A) + O(1)$.

(6) $L_A = L/2$, $T = T_C$: by referring to Eqs. (3.38) and (3.24), we have

$$S_M = \frac{1}{2}\ln\left(\frac{1}{4}\sqrt{(\langle n\rangle + 1)\langle n\rangle L}\right) + O(1) = \frac{1}{4}\ln(\langle n\rangle L_A) + O(1). \tag{3.40}$$

To sum up, from this study, we find that the extensive part of the thermal entropy of the whole system is canceled out in the mutual information. Below T_C the mutual information is dominated by contribution from the condensate. Even above T_C, contribution from the condensate is of the same order as that from the excited states. The mutual information really characterizes the quantum feature of the system.

To visualize the behavior of mutual information, we present a numerical calculation for the mutual information of this model in Fig. (3.1). This is done by numerically diagonalizing the truncated two-point correlation function matrix then computing the von Neumann entropy of the reduced density matrix from those eigenvalues. The system is equally partitioned, $\langle n\rangle = 1$, so $T_C = \frac{1}{\ln 2}$. We see exactly what our analytic results tell us: above T_C the mutual information saturates; below T_C, $S_M \simeq \frac{1}{2}L_A$; at T_C, $S_M \simeq \frac{1}{4}L_A$. Note that in the plot, the analytic results (dash lines) deviate from the numerical calculation because we only keep terms to the subleading order; terms that goes to zero [i.e. of order $O(\frac{1}{L_A})$] in the thermodynamic limit are neglected.

3.3 Numerical Study of Mutual Information in One-dimension with Long-range Hopping

In this section, we shall present our results of numerical study of the mutual information of free bosons living on a one dimensional lattice. In this numerical study, we adopt our previous method, and calculate the von Neumann entropy of the reduced density matrix from the eigenvalues of the truncated two-point correlation function matrix. Throughout this calculation, we hold the average density fixed at $\langle n\rangle = 1$ (which means we keep adjusting the chemical potential at different temperatures) and consider equal partition only.

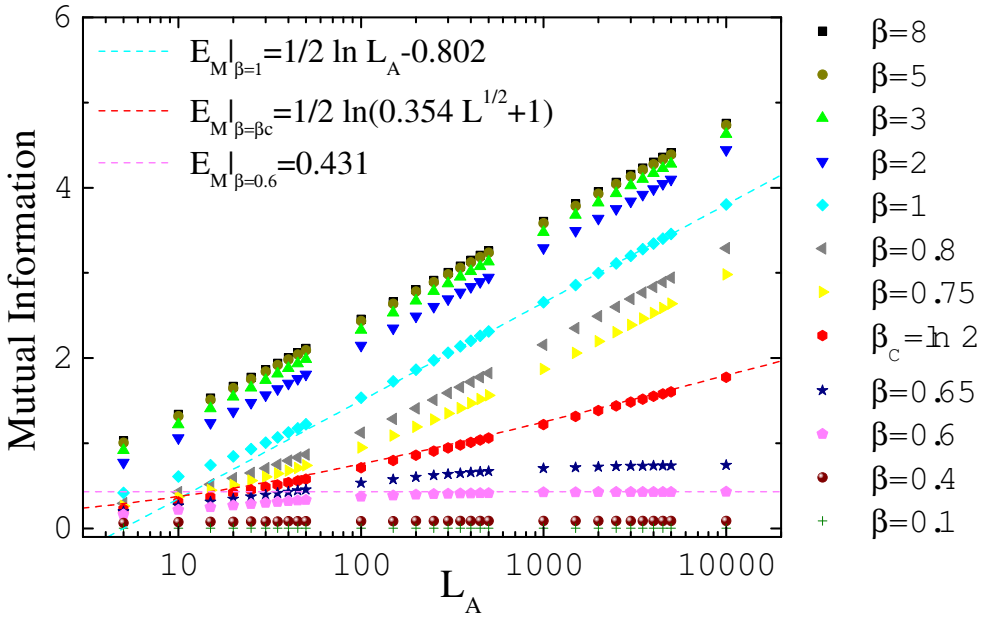

Figure 3.1: Numerical calculation of mutual information for the infinite-range hopping model for equally partitioned systems with average density $\langle n \rangle = 1$. The scatters are numerical data, while the dash lines are obtained from our analytic results corresponding to the particular temperature. We see exactly what our analytic results tell us: above $T_C = \frac{1}{\ln 2}$ the mutual information saturates; below T_C, $S_M \simeq \frac{1}{2} L_A$; at T_C, $_M \simeq \frac{1}{4} L_A$. Note that the analytic results (dash lines) deviate from the numerical calculation because we only keep terms to the subleading order; terms that goes to zero [i.e., of order $O(1/L_A)$] in the thermodynamic limit are neglected.

It is well known that for nearest-neighbor (NN) (or other short-range) hopping models whose dispersion relation at long-wave length takes the form $\epsilon(k) \sim k^2$, a finite temperature BEC can only exist in three dimensions (3D). However, 3D is in general very challenging for a numerical study that requires large system sizes. Moreover, in 3D the mutual information is dominated by area law [32], which renders the logarithmic divergence suggested by our study in Sec. III sub-leading and thus difficult to isolate. For both of these reasons, it is desirable to study a model in 1D with BEC at finite T. In 1D, the short-range hopping model does *not* support BEC at finite temperature. To stabilize a condensate in 1D, we introduce power-law long-range hopping in our free boson model to modify its long-wave length dispersion. This is similar to what was done in Ref. [75], in which the authors introduced long-range interaction between spins to stabilize magnetic order in 1D. The Hamiltonian with long-range hopping is obtained by setting t_{ij} in Eq. (3.1) to the following form, tuned by a parameter γ:

$$H = -\sum_{ij} \frac{t}{|i-j|^\gamma} a_i^\dagger a_j = -2t \sum_k (\sum_{n=1}^{L-1} \frac{\cos(nk)}{n^\gamma}) b_k^\dagger b_k = \sum_k \varepsilon_\gamma(k) b_k^\dagger b_k. \tag{3.41}$$

We will show that the long wave-length dispersion is modified to be $\varepsilon_\gamma(k) \sim k^{\gamma-1}$ for $\gamma < 3$, as a result if which a finite temperature BEC exists for $\gamma < 2$.

Consider the eigenenergy function $\varepsilon_\gamma(k) = -2t \sum_{n=1}^{L-1} \frac{\cos(nk)}{n^\gamma}$ in the thermodynamic limit:

$$\varepsilon_\gamma(k) = -2t \sum_{n=1}^{\infty} \frac{\cos(nk)}{n^\gamma} = -2t \,\mathrm{Re}\left[\sum_n \frac{e^{ink}}{n^\gamma}\right] = -2t \,\mathrm{Re}\left[F(\gamma, ik)\right], \tag{3.42}$$

where $F(\gamma, v)$ is the Bose-Einstein integral function [80] defined as:

$$F(\gamma, v) = \frac{1}{\Gamma(\gamma)} \int dx \frac{x^{\gamma-1}}{e^{x+v} - 1} = \sum_{n=1}^{\infty} \frac{e^{-nv}}{n^\gamma}. \tag{3.43}$$

The analytic properties of $F(\gamma, v)$ near $v = 0$ are known [80]:

$$F(\gamma, v) = \begin{cases} [1.5]\Gamma(1-\gamma)v^{\gamma-1} + \sum_{n=0}^{\infty} \frac{\zeta(\gamma-n)}{n!}(-v)^n, & \gamma \notin \mathbb{Z}, \\ \frac{(-v)^{\gamma-1}}{(\gamma-1)!}\left[\sum_{r=1}^{\gamma-1}\frac{1}{r} - \ln(v)\right] + \sum_{n\neq\gamma-1}^{\infty} \frac{\zeta(\gamma-n)}{n!}(-v)^n, & \gamma \in \mathbb{Z}, \end{cases} \tag{3.44}$$

where $\zeta(x)$ is the Riemann zeta function. Thus we find that $\varepsilon_\gamma(k) \to k^{\gamma-1}$ for small k when $1 < \gamma < 3$. When $\gamma > 3$, the low energy dispersion is dominated by the k^2 term. When $\gamma \leq 1$, $\varepsilon_\gamma(k)$ is not well-defined in the thermodynamic limit; in order to have a well-defined thermodynamic limit, the hopping energy t must be properly scaled by the system size in this case.

Next we will consider the thermodynamics of this model with different γ and demonstrate that for $\gamma < 2$, we indeed have a finite temperature BEC. At low temperature, only the small k part of the spectrum is important. For $1 < \gamma < 3$ we consider free bosons with a dispersion $\sigma k^{\gamma-1}$. Here $\sigma = -2t\Gamma(1-\gamma)$ is given in Eq. (3.44). The average density of such system in the thermodynamic limit is given by:

$$\frac{\langle N\rangle}{L} = \frac{1}{2\pi}\int dk\langle N_k\rangle = \frac{1}{2\pi}\frac{\sigma^{\frac{1}{1-\gamma}}}{(\gamma-1)}\int_0^\infty d\varepsilon \frac{\varepsilon^{\frac{1}{\gamma-1}-1}}{z^{-1}e^{\beta\varepsilon}-1} = \frac{(\beta\sigma)^{\frac{1}{1-\gamma}}}{2\pi(\gamma-1)}\Gamma(\frac{1}{\gamma-1})g_{\frac{1}{\gamma-1}}(z), \tag{3.45}$$

where $z = e^{\beta\mu}$, $\beta = \frac{1}{T}$ is the inverse temperature, and $g_v(z) = \frac{1}{\Gamma(v)}\int_0^\infty dx \frac{x^{v-1}}{z^{-1}e^x-1}$ is the Bose-Einstein integral function. To have a finite temperature BEC, $\langle N\rangle/L = \langle n\rangle$ must remain finite when $z \to 1$, which indicates $\frac{1}{\gamma-1} > 1$, because for $v \leq 1$, $g_v(1)$ diverges.

To have a better understanding of the thermodynamics of this model, in Fig. (3.2) we present a numerical calculation of T_C. The exact average density of the system is:

$$\frac{\langle N\rangle}{L} = \frac{1}{2\pi}\int_{-\pi}^{\pi} dk \frac{1}{e^{\beta(\varepsilon_\gamma(k)-\mu)}-1}, \tag{3.46}$$

where $\varepsilon_\gamma(k)$ is the eigenenergy function given in Eq. (3.42). T_C is computed by setting $\mu = \varepsilon_\gamma(0)$ and then solving this equation numerically. According to Fig. 3.2, T_C grows monotonically from 0 to ∞ as γ goes from 2 to 1. The divergent behavior of T_C as $\gamma \to 1$ is a consequence of the divergent bandwidth in that limit.

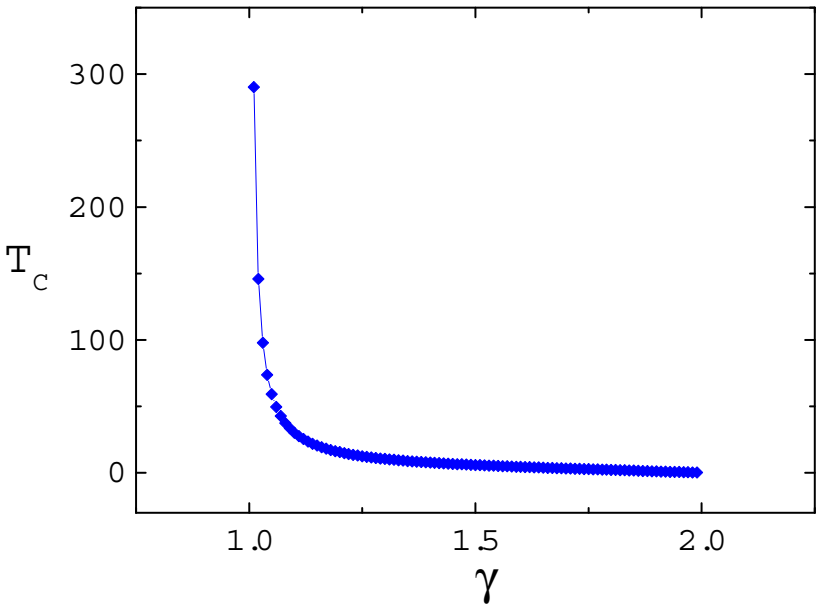

Figure 3.2: Numerical calculation of T_C (line + symbols) for the long-range hopping model in the thermodynamic limit. T_C is measured in unit of the hopping energy t which is set to 1. As one can see, T_C grows monotonically from 0 to ∞ as γ goes from 2 to 1. The divergent behavior of T_C as $\gamma \to 1$ is a consequence of the divergent bandwidth.

According to our study of the infinite range hopping model, above T_c the mutual information should saturate as the system size grows. Below T_C, the mutual information has a scaling behavior $S_M \simeq \frac{1}{2}\ln L_A$; for $T = T_C$ $S_M \simeq \frac{1}{4}\ln L_A$ for equally partitioned system in that model. We expect the $\ln L_A$ scaling behavior both below T_C and at T_C to persist in the long-range hopping model. As we shall see later, this is indeed the case. However, the details of the scaling behavior (i.e. the prefactor) can be different for different γ. To study this scaling behavior, we fix the temperature and examine the mutual information as a function of system size. This is desirable because, if our conjecture according to the study of infinite-range hopping model is correct, the mutual information will be proportional to $\ln L_A$ when $T \leq T_C$.

Before we demonstrate our results in the long-range hopping model, first let us verify our analysis in the NN hopping model in which no BEC would occur. This case actually corresponds to $\gamma \to \infty$. The Hamiltonian is given by restricting the hopping in Eq. (3.1) to the nearest neighbors only:

$$H_{n.n} = -t \sum_{\langle ij \rangle} \tilde{c}_i^\dagger \tilde{c}_j. \tag{3.47}$$

Figure 3.3 is a linear-log plot of mutual information against subsystem size at different temperatures. Throughout our study we shall consider equal partition only, i.e., $L_A = L/2$. The average density is also set to $\langle n \rangle = 1$ here, so are the other results we will show later. Clearly, at a fixed temperature, the mutual information saturates as the system size grows. At low temperatures, small systems can be considered in the zero temperature limit. This leads to the mutual information growing as $\sim \frac{1}{2}\ln L_A$, until saturation kicks in.

Next we consider $1 < \gamma < 2$. Now the finite temperature transition emerges, and the signature for the transition in mutual information - the logarithmic scaling with (sub-)system size also emerges. In Fig. 3.4, we plot the mutual information (scatters) for $\gamma = 1.7$ at different temperatures. The best fit (cyan dash line corresponding to the diamond data points) for $\beta = 0.5 > \beta_C$ gives $S_M = 0.2405 \ln L_A + 0.214$. At $\beta_C = 0.297$, the scaling behavior is fit (magenta dash line) as $S_M = 0.1226 \ln L_A + 0.1688$. Both behaviors agrees qualitatively with what has been suggested by our analytic study of the infinite-range hopping model. When the temperature is well below T_C, we have the logarithmic scaling behavior: a set of parallel linear lines on this logarithm scale plot for different

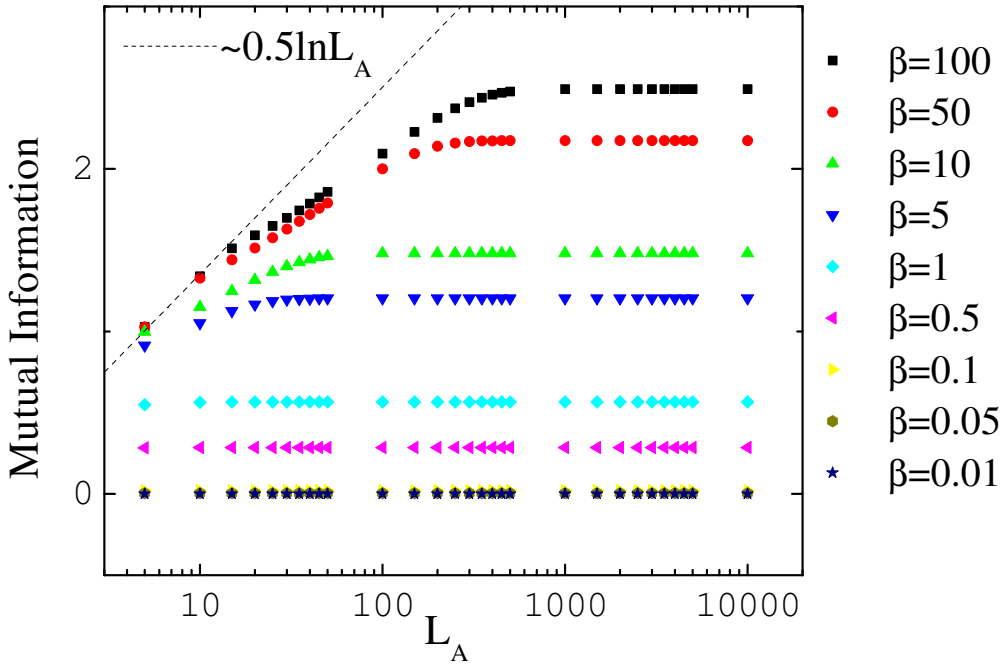

Figure 3.3: Mutual information of the nearest neighbor hopping model plotted against subsystem size on a logarithmic scale. Average density is set to $\langle n \rangle = 1$, and the system is equally partitioned, $L = 2L_A$. The black dash line is $S_M \sim \frac{1}{2} \ln L_A$. This line will be in other graphs for comparison as well. Clearly, the mutual information saturates when the system size grows large enough.

temperatures. However, the prefactor is significantly different from that of the infinite range hopping model which is $\frac{1}{2}$. In fact, by calculating mutual information of different γ's, we find that the prefactor varies as γ changes. For very low temperature, small systems again effectively fall into the zero temperature region, and the mutual information restores to the $\sim \frac{1}{2} \ln L_A$ behavior as in zero temperature. But when the system size becomes large it crosses back to the finite temperature scaling behavior again. This is evident for $\beta > 1$ in the figure. For temperature close to but still below T_C, small systems behave differently: the mutual information scales more like the line for $\beta = \beta_C$, and it bends up as the system size increases and finally crosses back to its genuine behavior below T_C. For temperature close to T_C but now above, small systems behave the other way: the mutual information bends downwards and saturates at large system size. β_c serves as a very distinctive boundary between the above two different bending behaviors. The latter two bending features are also present in Fig. 3.1, our numerical verification of the infinite-range hopping model. But the first feature at very low temperature is missing in Fig. 3.1 since in that case the mutual information scales the same way as the entanglement entropy.

Very similar behaviors were observed for the entire range $1 < \gamma < 2$. Representative results are presented in Figs. 3.5 and 3.6 for $\gamma = 1.5$ and 1.3 respectively. We thus conclude that for the entire range $1 < \gamma < 2$, mutual information saturates for $T > T_C$, while it diverges logarithmically with increasing subsystems size, for both $T < T_C$ and $T = T_C$. The coefficients in front of the logarithms are γ-dependent.

3.4 Summary and Discussion

In this chapter we have studied entanglement properties of free *non-relativistic* Bose gases. At zero temperature, all particles fall into the ground state, and we find the entanglement entropy diverges as the logarithm of the particle number in the subsystem. At finite temperatures, we studied the natural generalization of entanglement entropy - the mutual information. We find the mutual information has a similar divergence in the presence of a Bose-Einstein condensate. When the system is above T_C or does not have a condensate, the mutual information saturates for large subsystem size. It should be noted that for the special models we studied in this paper there is no area-law contribution to the mutual in-

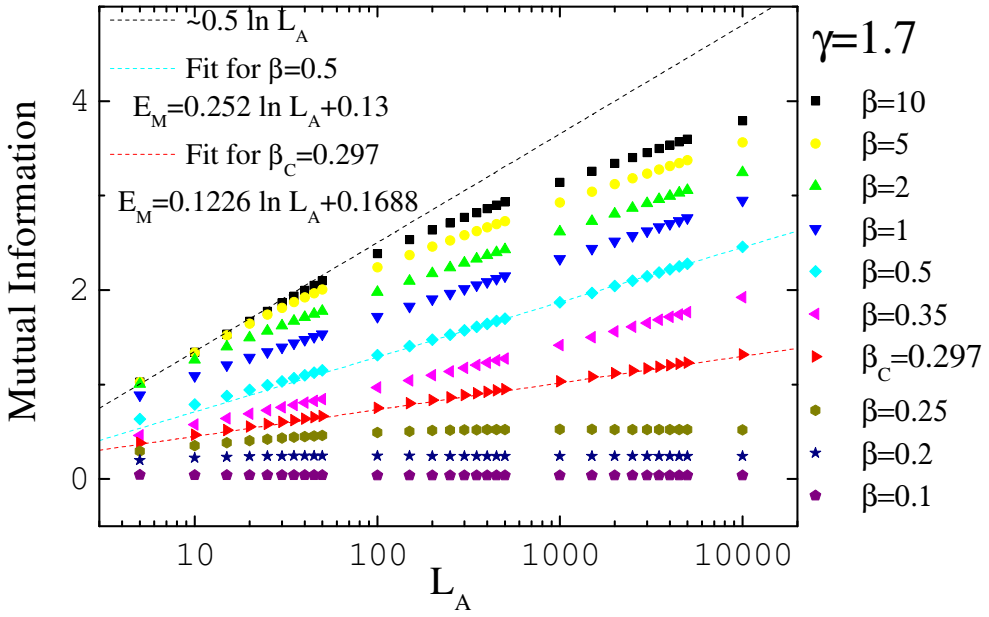

Figure 3.4: Mutual information of the long-range hopping model with the parameter $\gamma = 1.7$ as a function of subsystem size on a logarithmic scale, at various (inverse) temperatures. The average boson density $\langle n \rangle$ is set to 1, and the system is equally partitioned, $L_A = L/2$. The scaling behavior for inverse temperature $\beta = 0.5$ goes as $S_M = 0.2405 \ln L_A + 0.214$ (cyan dash line corresponding to the diamond data points). At the transition point, $\beta = \beta_C = 0.297$, the scaling law is fit to be $S_M = 0.1226 \ln L_A + 0.1688$ (red dash line corresponding to the right triangle data points).

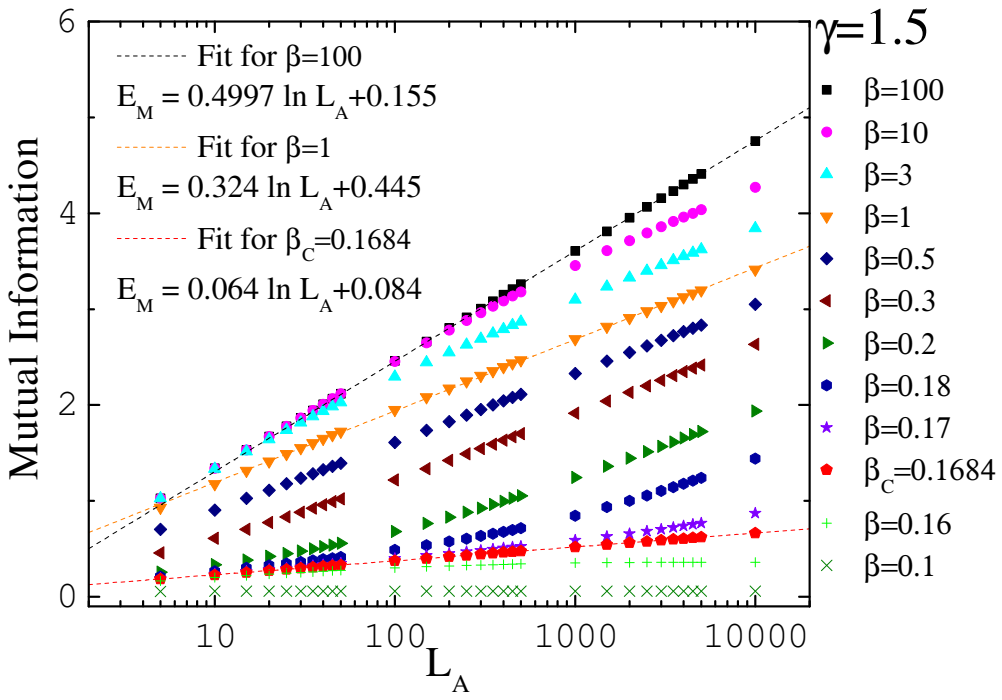

Figure 3.5: Mutual information of the long-range hopping model with the parameter $\gamma = 1.5$ as a function of subsystem size on a logarithmic scale, at various (inverse) temperatures. The average boson density $\langle n \rangle$ is set to 1, and the system is equally partitioned, $L_A = L/2$. The mutual information for $\beta = 1$ is fit to scale as $S_M \simeq 0.324 \ln L + 0.445$ (orange dash line). At $\beta_C = 0.16843$, we observer a weaker scaling behavior which is fit to be $S_M = 0.064 \ln L_A + 0.084$ (red dash line).

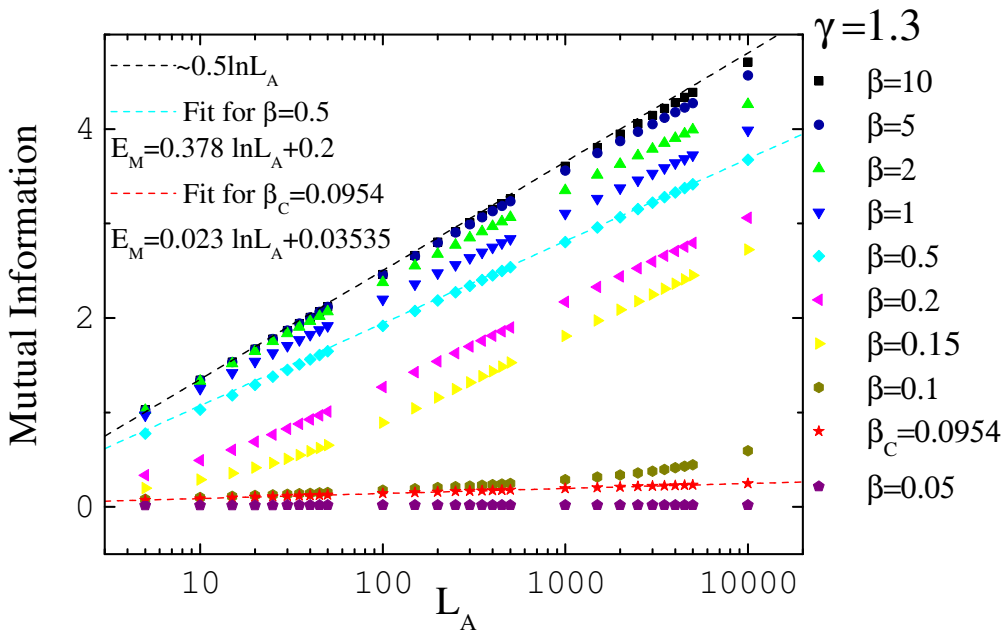

Figure 3.6: Mutual information of the long-range hopping model with the parameter $\gamma = 1.3$ as a function of subsystem size on a logarithmic scale, at various (inverse) temperatures. The average boson density $\langle n \rangle$ is set to 1, and the system is equally partitioned, $L_A = L/2$. The best fitting for $\beta = 0.5 > \beta_C$ (cyan dash line) gives $S_M = 0.378 \ln L_A + 0.2$. At $\beta_C = 0.0954$, the scaling behavior is fit (red dash line) as $S_M = 0.023 \ln L_A + 0.03535$.

formation, thus the contribution from the condensate, when present, dominates the mutual information. In more generic models in two- or three-dimensions where an area-law contribution is present, we expect such logarithmic divergent contribution from the condensate to be present as a sub-leading term in the subsystem-size dependence of the entanglement entropy and mutual information.

Physically it is easy to understand why the condensate makes such an important contribution to entanglement. First of all, BEC is intrinsically a quantum process, just like entanglement reflects the intrinsically quantum nature of the system. More specifically, when a (macroscopically) large number of particles occupy the same state (at $k = 0$), they are necessarily delocalized throughout the sample, giving rise to entanglement between blocks.

Just like in previous chapter on a very different system, our results here suggest that *conventional* ordering, like BEC, makes a logarithmic contribution to entanglement. One thus needs to take caution when using entanglement as a diagnostic for exotic phases (such as topological phases) or quantum criticality.

CHAPTER 4

ENTANGLEMENT ENTROPY OF FERMI LIQUIDS VIA HIGH-DIMENSIONAL BOSONIZATION

In this chapter, we first show that the scaling behavior of the entanglement entropy for systems with a Fermi surface is the same as that of 1D systems with Fermi points We then seek for a generalization of the latter to interacting fermions in the Fermi liquid phase. We first develop an intuitive understanding via a toy model, showing that in this model the entanglement entropy has the same form as that given in by Gioev and Klich (GK) in Ref.[56]. We then develop a more general and formal treatment using the method of high-dimensional bosonization[81, 82, 83, 84, 85]. This approach will not only lead to a reproduction of the result for free fermions obtained by GK based on Widom's conjecture[86, 87] , but will also lend itself to the inclusion and subsequent treatment of Fermi liquid type (forward scattering) interactions.

This paper is organized as follows. In Sec. 4.1, we describe the toy model for which the entanglement entropy can be written in the same form as the GK result. Then in Sec. 4.2, we briefly introduce the tool box of multi-dimensional bosonization, and apply it to free fermions to reproduce the GK formula. The main results of this work are presented in Sec. 4.3 in which we calculate the entanglement entropy of a Fermi liquid for a special geometry using a combination of multi-dimensional bosonization and the replica trick. We subsequently summarize and discuss our results. Some technical details are discussed in two appendices.

4.1 The Intuitive picture - a toy model

Consider a set of decoupled parallel 1D chains of non-interacting spinless fermions with spacing a as shown in Fig. 4.1(a). Here we only consider $d = 2$ for simplicity, but this toy model is viable in general d dimensions. The asymptotic behavior of entanglement entropy in large L limit of a convex subsystem A of this model can be obtained by simply counting the number of chains that intersect A, and each segment contributes a $(1/3)\log L$ where L is the linear dimension of the subsystem[32, 88]. Due to the logarithm, different shapes only lead to differences at the area law level. Since each segment must have two intersections, we can count the intersections instead, which also automatically takes care of non-convex geometries. Although there is an additional correction for multiple intervals on a single chain[89, 90, 91], as long as only the $\log L$ behavior is concerned, that contribution is negligible. For L large enough, we can write the number of these intersections as an integral over the surface of A projected onto the direction perpendicular to the chains times one half of the chain density, $1/a$. To make contact with the GK result, we note this model also has Fermi surfaces as shown in Fig. 4.1(b) with a total "area" of $4\pi/a$. This enables us to replace the density of chains by an integral over the Fermi surfaces of the system

$$\frac{1}{a} = \frac{1}{4\pi}\oint_{\partial\Gamma} dS_k,$$

where Γ indicates the occupied area in momentum space so its boundary $\partial\Gamma$ is the Fermi surface(s). Therefore we can write the entanglement entropy as

$$\begin{aligned} S(\rho_A) &= \frac{1}{2}\times\frac{1}{3}\log L\times\frac{1}{a}\oint_{\partial A}|\hat{\boldsymbol{n}}\cdot dS_x| \\ &= \frac{1}{12(2\pi)^{2-1}}\log L\times\oint_{\partial A}\oint_{\partial\Gamma}|dS_x\cdot dS_k|, \end{aligned} \tag{4.1}$$

where $\hat{\boldsymbol{n}}$ is the direction along the chains which is also normal to the Fermi surface, and an overall factor of $\frac{1}{2}$ accounts for the double counting of chain segments. In Eq. (4.1) we recover the GK formula in this special case but written in a slightly different way. In Ref.

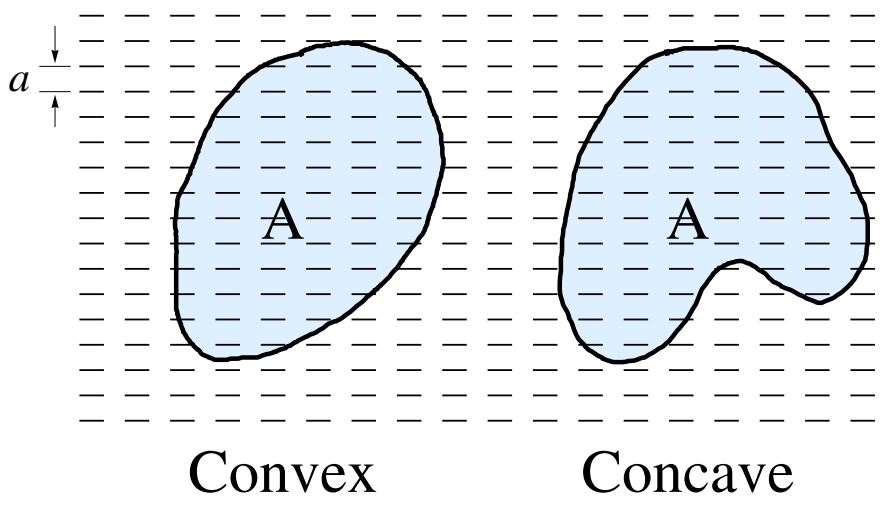

(a)

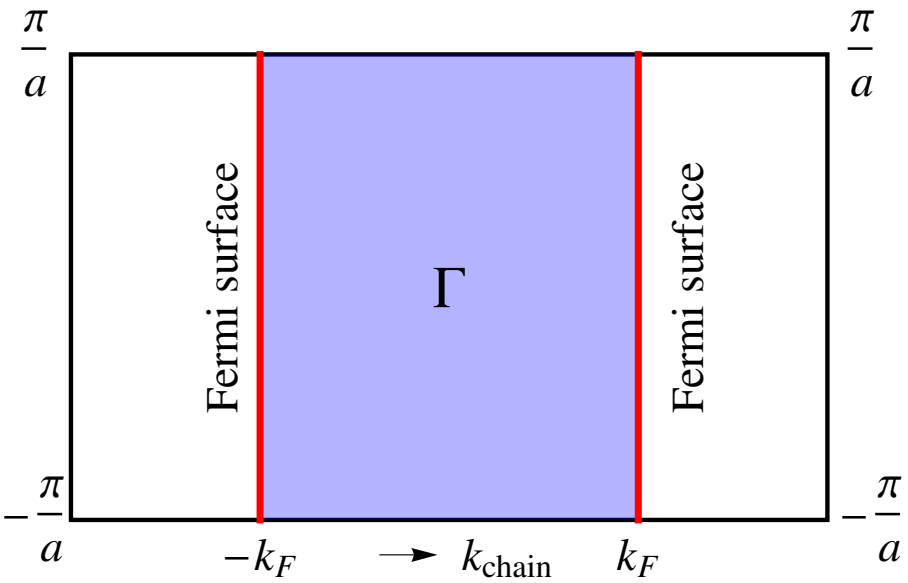

(b)

Figure 4.1: The toy model both in real space and in momentum space. (a) A set of parallel decoupled $1d$ chains of spinless free fermions (dash lines); the subsystem division is represented by the solid lines, both convex and concave geometries. (b) Fermi surfaces of the toy model.

[56] the entanglement entropy is given as:

$$S = \frac{1}{12}\frac{L^{d-1}\log L}{(2\pi)^{d-1}}\oint_{\partial A}\oint_{\partial \Gamma}\left|\hat{\boldsymbol{n}}_{\boldsymbol{x}}\cdot\hat{\boldsymbol{n}}_{\boldsymbol{p}}\right| dS_{\boldsymbol{x}} dS_{\boldsymbol{p}}, \tag{4.2}$$

where the real space surface integral is carried out over the subsystem whose volume is normalized to 1. The surface area is factored out as L^{d-1}. However, in our formula the surface area $\sim L^{d-1}$ is implicitly included in the integral over the surface of the subsystem.

We note that the model discussed in Ref.[92] is equivalent with our toy model, but motivated from a different perspective. In Ref.[92], models are constructed from the momentum space, either with Fermi surfaces as our toy model, or a square Fermi surface, and a boxlike and a spherical geometry are discussed. In contrast, our toy model is constructed from a real space perspective, and general single connected geometries are discussed.

Motivated by the toy model, in this work we extend this intuitive understanding of GK's result to generic free Fermi systems and generalize it to include Fermi liquid interactions in two dimensions (2D) via high dimensional bosonization. Using the method of multi-dimensional bosonization, the Fermi liquid theory can be written as a tensor product of low-energy effective theories of quasi-1D systems similar to this toy model, along all directions. This provides us with a tool to treat the entanglement entropy of fermions in high dimensions, even in the presence of *interactions*.

At this point, we could also include forward scattering for each chain, and from 1D bosonization we know that for spinless fermions this only leads to renormalization of the Fermi velocity, thus does not change the logarithmic scaling of the entanglement entropy for this toy model. This hints that the same conclusion might hold for Fermi liquids, as we can include Fermi liquid interactions in a similar way via high dimensional bosonization. Although as we show later, this is indeed true at the leading order, the situation is more delicate than it seems to be. The Fermi liquid interactions couple a family of "toy models" aligned along different directions in the language of high dimensional bosonization, and lead to a correction to the entanglement entropy $\sim O(1)\times\log L$.

4.2 Multi-dimensional bosonization

The scheme of multi-dimensional bosonization was first introduced by Haldane[82], followed by others[81, 83, 84, 85]. The basic idea is to start with a low energy effective Hamiltonian (obtained through a renormalization group (RG) approach) restricted to within a thin shell of thickness λ around the Fermi surface, $k_F - \lambda/2 < |k| < k_F + \lambda/2$. Then one divides this thin shell into N patches with dimensionality $\sim \Lambda^{d-1} \times \lambda$ as shown in Fig.(2) in such a way that $\lambda \ll \Lambda \ll k_F$ and $\Lambda^2/k_F \ll \lambda$, where $d = 2, 3$ is the space dimension, Λ is the linear dimension of the tangential extent of each patch. The condition $\lambda \ll \Lambda$ minimizes inter-patch scattering; $\Lambda \ll k_F$ and $\Lambda^2/k_F \ll \lambda$ together makes the curvature of the Fermi surface negligible. In the end we shall take the limit $\Lambda/k_F \to 0$, so that the sum over all patches can be converted to an integral over the Fermi surface. In this work, we treat the free theory in general d dimensions, but shall restrict ourselves to $d = 2$ when interactions are included. For an arbitrary patch $\boldsymbol{S}$, labeled by the Fermi momentum $\boldsymbol{k}_S$ at the center of the patch, we introduce the patch fermion field operator

$$\psi(\boldsymbol{S}; \boldsymbol{x}) = e^{i\boldsymbol{k}_S \cdot \boldsymbol{x}} \sum_{\boldsymbol{p}} \theta(\boldsymbol{S}; \boldsymbol{p}) e^{i(\boldsymbol{p}-\boldsymbol{k}_S)\cdot \boldsymbol{x}} \psi_{\boldsymbol{p}}, \tag{4.3}$$

where $\psi_{\boldsymbol{p}}$ is the usual fermion field in momentum space,

$$\theta(\boldsymbol{S}; \boldsymbol{p}) = \begin{cases} 1 & \text{if } \boldsymbol{p} \text{ lies in the patch } \boldsymbol{S}, \\ 0 & \text{if } \boldsymbol{p} \text{ lies outside patch } \boldsymbol{S}. \end{cases}$$

The effective Fermi liquid Hamiltonian can be written as

$$\begin{aligned} H[\psi^\dagger, \psi] = & \int d^d x \sum_{S} \psi^\dagger(\boldsymbol{S}; \boldsymbol{x}) (\frac{\boldsymbol{k}_S}{m^*} \cdot \nabla) \psi(\boldsymbol{S}; \boldsymbol{x}) \\ + & \int d^d x d^d y \sum_{\boldsymbol{S},\boldsymbol{T}} V(\boldsymbol{S}, \boldsymbol{T}; \boldsymbol{x} - \boldsymbol{y}) \psi^\dagger(\boldsymbol{S}; \boldsymbol{x}) \psi(\boldsymbol{S}; \boldsymbol{x}) \psi^\dagger(\boldsymbol{T}; \boldsymbol{y}) \psi(\boldsymbol{T}; \boldsymbol{y}), \end{aligned} \tag{4.4}$$

with m^* being the effective mass, $V(\boldsymbol{S}, \boldsymbol{T}; \boldsymbol{x} - \boldsymbol{y})$ the effective interaction in the forward scattering channels. Even though this model is restricted to special interactions of this form, forward scattering is known to be the only marginal interaction in RG analysis[93].

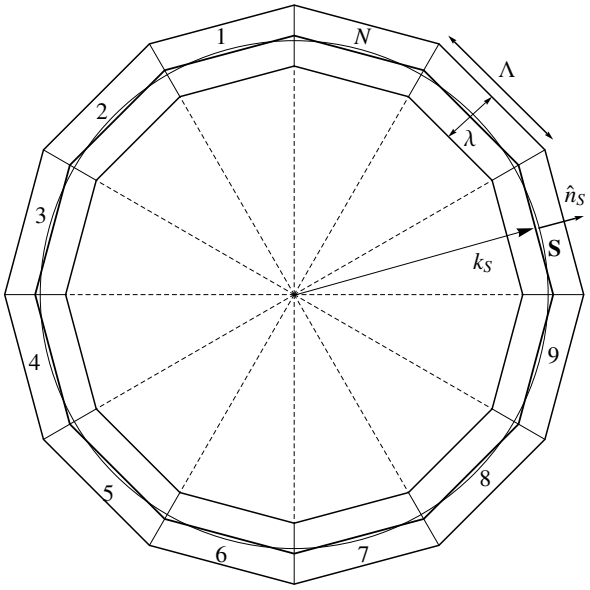

(a)

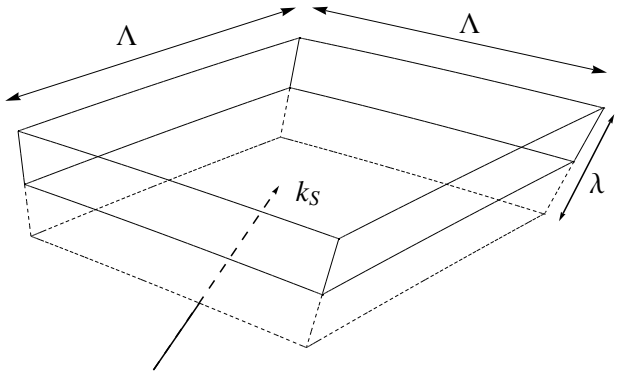

(b)

Figure 4.2: Patching of the Fermi surface. The low energy theory is restricted to within a thin shell about the Fermi surface with a thickness $\lambda \ll k_F$, in the sense of renormalization. The thin shell is further divided into N different patches; each has a transverse dimension Λ^{d-1} where $d = 2,\ 3$ is the space dimensions. The dimensions of the patch satisfy three conditions: (1) $\lambda \ll \Lambda$ minimizes inter-patch scattering; (2) $\Lambda \ll k_F$ and $\Lambda^2/k_F \ll \lambda$ together makes the curvature of the Fermi surface negligible. (a): Division of a 2D Fermi surface into N patches. Patch $\boldsymbol{S}$ is characterized by the Fermi momentum $\boldsymbol{k_S}$. (b): A patch for $d = 3$. The patch has a thickness λ along the normal direction and a width Λ along the transverse direction(s).

As the leading order contribution of the entanglement entropy is dominated by the low energy modes around the Fermi surface, it is sufficient to consider this model. Similar to the 1D case, the bosonic degrees of freedom are the density modes of the system, in this case defined within each patch of the Fermi surface:

$$J(\boldsymbol{S};\boldsymbol{q}) = \sum_{\boldsymbol{k}} \theta(\boldsymbol{S};\boldsymbol{k}-\boldsymbol{q})\theta(\boldsymbol{S};\boldsymbol{k})\{\psi^\dagger_{\boldsymbol{k}-\boldsymbol{q}}\psi_{\boldsymbol{k}} - \delta^d_{\boldsymbol{q},0}\langle\psi^\dagger_{\boldsymbol{k}}\psi_{\boldsymbol{k}}\rangle\}. \tag{4.5}$$

Though $\boldsymbol{q}$ is not explicitly bounded in the above definition of the patch density operator, its transverse components $\boldsymbol{q}_{\boldsymbol{S}\perp} = (q^{(1)}_{\boldsymbol{S}\perp},\ldots,q^{(\alpha)}_{\boldsymbol{S}\perp},\ldots,q^{(d-1)}_{\boldsymbol{S}\perp})$ (those parallel to the Fermi surface) are limited $q^{(\alpha)}_{\boldsymbol{S}\perp} \in (-\Lambda,\Lambda)$ due to the patch confinement. Their commutation relation is

$$[J(\boldsymbol{S};\boldsymbol{q}), J(\boldsymbol{T};\boldsymbol{p})] \simeq \delta_{\boldsymbol{S},\boldsymbol{T}}\delta^d_{\boldsymbol{q}+\boldsymbol{p},0}\sum_{k}\theta(\boldsymbol{S};\boldsymbol{k})[\theta(\boldsymbol{S};\boldsymbol{k}-\boldsymbol{q}) - \theta(\boldsymbol{S};\boldsymbol{k}+\boldsymbol{q})]n_{\boldsymbol{k}} \tag{4.6}$$

$$= \delta_{\boldsymbol{S},\boldsymbol{T}}\delta^d_{\boldsymbol{q}+\boldsymbol{p},0}\Omega\,(\hat{\boldsymbol{n}}_{\boldsymbol{S}}\cdot\boldsymbol{q})\theta_2(\boldsymbol{q}_{\boldsymbol{S}\perp}) + \mathcal{O}(\lambda/\Lambda), \tag{4.7}$$

where

$$\theta_2(\boldsymbol{q}_{\boldsymbol{S}\perp}) = \prod_{\alpha}(1 - q^{(\alpha)}_{\boldsymbol{S}\perp}/\Lambda), \tag{4.8}$$

$\Omega = \Lambda^{d-1}\,[L_0/(2\pi)]^d$, $n_{\boldsymbol{k}} = \langle\psi^\dagger_{\boldsymbol{k}}\psi_{\boldsymbol{k}}\rangle$ is the occupation number of state with momentum $\boldsymbol{k}$, $\hat{\boldsymbol{n}}_{\boldsymbol{S}}$ is the outward normal direction of patch $\boldsymbol{S}$, $\boldsymbol{q}_{\boldsymbol{S}\perp}$ represents all other component(s) of $\boldsymbol{q}$ that are perpendicular to $\hat{\boldsymbol{n}}_{\boldsymbol{S}}$, and L_0 is the linear dimension of the entire system. The appearance of $\delta_{\boldsymbol{q}+\boldsymbol{p},0}$ is a result of momentum conservation. The calculation of the commutator is reduced to computing the difference of occupied states, i.e. the area difference below the Fermi surface, between the two θ functions ($\theta(\boldsymbol{S};\boldsymbol{k}-\boldsymbol{q}) - \theta(\boldsymbol{S};\boldsymbol{k}-\boldsymbol{p})$) as indicated by Eq. (4.6). This is similar to 1D bosonization. If we consider both $\boldsymbol{k}$ and $\boldsymbol{q}$ to be 1D momenta, Eq. (4.6) would give us the 1D bosonization commutator. The 2D result Eq. (4.7) is similar, because the Fermi surface confined within the patch is essentially flat thus the dispersion is 1D. That leads to the $\hat{\boldsymbol{n}}_{\boldsymbol{S}}\cdot\boldsymbol{q}$ dependence of the commutator as that of the 1D case, even for $\boldsymbol{q}_{\boldsymbol{S}\perp} \neq 0$. The difference is that, as illustrated in Fig. (3), due to the patch confinement on the transverse direction(s), when $\boldsymbol{q}_{\boldsymbol{S}\perp}$ increases $\boldsymbol{k}\pm\boldsymbol{q}$ would increasingly find itself outside the patch thus not contributing to the commutator. According to Fig. (3), one can see that this gives rise to the factor $\theta_2(\boldsymbol{q}_{\boldsymbol{S}\perp})$, which diminishes the commutator at large $\boldsymbol{q}_{\boldsymbol{S}\perp}$. It is

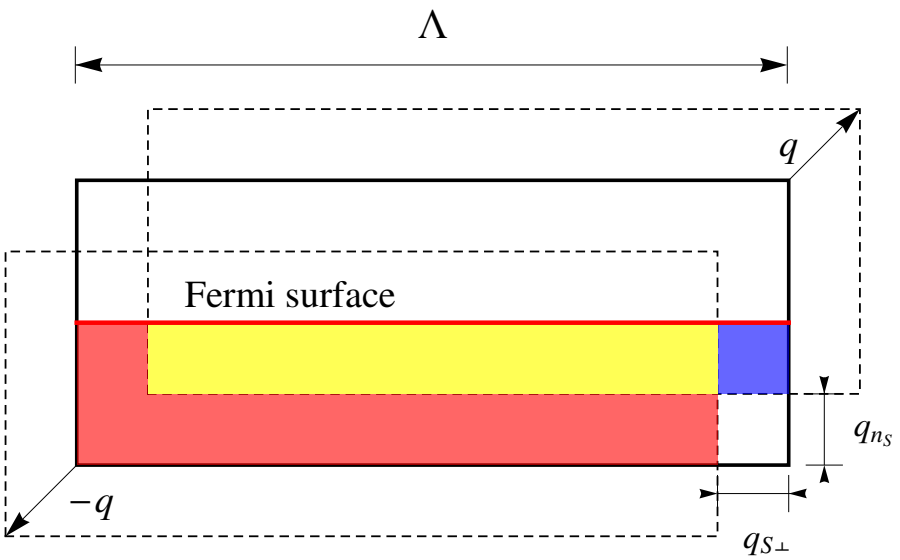

Figure 4.3: Origin of the bosonic commutator of patch density operators illustrated for $d = 2$. As shown in Eq. (4.7), the commutator is reduced to computing the difference of occupied states , i.e. the area difference below the Fermi surface, between the two θ functions $(\theta(\boldsymbol{S};\boldsymbol{k}-\boldsymbol{q})-\theta(\boldsymbol{S};\boldsymbol{k}+\boldsymbol{p}))$. The solid box indicates the original patch, or $\theta(\boldsymbol{S};k)$. The red line shows the Fermi surface. Both $\theta(\boldsymbol{S};\boldsymbol{k}-\boldsymbol{q})$ and $\theta(\boldsymbol{S};\boldsymbol{k}+\boldsymbol{p})$ are denoted by dashed boxes. The occupied part in $\theta(\boldsymbol{S};\boldsymbol{k}+\boldsymbol{q})$ is denoted by blue, that of $\theta(\boldsymbol{S};\boldsymbol{k}-\boldsymbol{q})$ is denoted by red, and the overlapping region is denoted by yellow. Subtracting the remaining blue area from the red, we obtain that $\theta(\boldsymbol{S};\boldsymbol{k}-\boldsymbol{q})$ occupies $(\Lambda-q_{S\perp})q_{\hat{\boldsymbol{n}}_S}$ more states, which gives us the commutator.

usually neglected in literature because the long wavelength limit is taken[81, 83, 84, 85]. However, as it is important in the present context to correctly count the number of total degrees of freedom, this $\theta_2(\boldsymbol{q}_{S\perp})$ factor cannot be neglected because it comes from counting the transverse degrees of freedom. To simplify things, we replace $\theta_2(\boldsymbol{q}_{S\perp})$ by

$$\theta_2(\boldsymbol{q}_{S\perp}) = 1 \quad \text{for } -\Lambda/2 < q_{S\perp}^{(\alpha)} < \Lambda/2, \tag{4.9}$$

and we also limit $\boldsymbol{q}_{S\perp}$ to this range. This approximation makes it easier to do Fourier transform while keeping the total degrees of freedom intact. To see that, it is sufficient to consider one direction, comparing the area enclosed by the two different functions: $\theta_2(q_\perp) = 1 - q_\perp/\Lambda$ over the range $(-\Lambda, \Lambda)$ and $\theta_2(q_\perp) = 1$ over the range $(-\Lambda/2, \Lambda/2)$. Both functions enclose the same area thus the same number of states. This approximation can also be interpreted as relaxation of the hard wall cutoff in Eq. (4.5), softening of the step function $\theta(\boldsymbol{S}; \boldsymbol{k})$. In Eq. (4.5), $\boldsymbol{q}$ is not bounded while $\boldsymbol{k}$ is bounded by $\theta(\boldsymbol{S}; \boldsymbol{k})$. If we relax the restriction on $\boldsymbol{k}$ on the transverse direction, allowing $\boldsymbol{k}$ with $\left|k_{S\perp}^{(\alpha)}\right| > \Lambda/2$ in the summation, but require $q_{S\perp}^{\alpha}$ to be bounded within the patch, we would obtain the alternative $\theta_2(q_\perp)$.

Using from now on the above approximation, we construct the local bosonic degrees of freedom $\phi(\boldsymbol{S}; \boldsymbol{x}) = \phi(\boldsymbol{S}; x_S, \boldsymbol{x}_{S\perp})$ as

$$J(\boldsymbol{S}; \boldsymbol{x}) = \sqrt{\Omega}\partial_{x_S}\phi(\boldsymbol{S}; x_S, \boldsymbol{x}_{S\perp}), \tag{4.10}$$

where $J(\boldsymbol{S}; \boldsymbol{x}) = \sum_{\boldsymbol{q}} e^{i\boldsymbol{q}\cdot\boldsymbol{x}} J(\boldsymbol{S}; \boldsymbol{q})$, $x_S = \boldsymbol{x} \cdot \hat{\boldsymbol{n}}_S$, and $\boldsymbol{x}_{S\perp} = \boldsymbol{x} - (\boldsymbol{x} \cdot \hat{\boldsymbol{n}}_S)\hat{\boldsymbol{n}}_S$. The commutation relations for the ϕ's are then

$$[\partial_{x_S}\phi(\boldsymbol{S}; \boldsymbol{x}), \phi(\boldsymbol{T}; \boldsymbol{y})] = i2\pi\Omega\delta_{S,T}\delta(x_S - y_S)\prod_{\alpha=1}^{d-1}\left(\frac{\sin(\Lambda(x_{S\perp}^{(\alpha)} - y_{S\perp}^{(\alpha)}))}{2\pi(x_{S\perp}^{(\alpha)} - y_{S\perp}^{(\alpha)})}\right) \tag{4.11}$$

which is the bosonic commutation relation we are looking for. The factor $\prod_\alpha \left(\frac{\sin(\Lambda(x_{S\perp}^{(\alpha)} - y_{S\perp}^{(\alpha)}))}{2\pi(x_{S\perp}^{(\alpha)} - y_{S\perp}^{(\alpha)})}\right)$ arising from transverse directions must be treated with care in different circumstances. In most literature, the focus is the physics at large length scale $l \gg 1/\Lambda$; therefore, this factor is usually approximated by $\delta^{d-1}(\boldsymbol{x}_{S\perp} - \boldsymbol{y}_{S\perp})$ which is good in that limit without further

discussion. This is also what we shall do for most of the time unless noted otherwise:

$$[\partial_{x_S}\phi(\boldsymbol{S};\boldsymbol{x}),\phi(\boldsymbol{T};\boldsymbol{y})]\xrightarrow{\left|x_{S\perp}^{(\alpha)}-y_{S\perp}^{(\alpha)}\right|\gg 1/\Lambda}\simeq i2\pi\Omega\delta_{S,T}^{d-1}\delta(x_S-y_S)\delta^{d-1}(\boldsymbol{x}_{S\perp}-\boldsymbol{y}_{S\perp}). \tag{4.12}$$

However, the more accurate expression (4.11) is useful for us to understand how to count the transverse degrees of freedom correctly. It tells us that the transverse degrees are not independent on the short length scale $l < 1/\Lambda$. More importantly, later on we need to consider the limit $\delta^{d-1}(\boldsymbol{x}_{S\perp}-\boldsymbol{y}_{S\perp})|_{\boldsymbol{y}_{S\perp}\to\boldsymbol{x}_{S\perp}}$; without Eq. (4.11), this limit would be ill-defined.

With the above, the Hamiltonian $H[\psi^\dagger,\psi]$ is found to be quadratic in terms of these $J(\boldsymbol{S};\boldsymbol{q})$'s:

$$H[\psi^\dagger,\psi]=\frac{1}{2}\sum_{\boldsymbol{S},\boldsymbol{T};\boldsymbol{q}}\frac{v_F^*\delta_{\boldsymbol{S},\boldsymbol{T}}}{\Omega}J(\boldsymbol{S};-\boldsymbol{q})J(\boldsymbol{T};\boldsymbol{q})+V(\boldsymbol{S},\boldsymbol{T};q)J(\boldsymbol{S};-\boldsymbol{q})J(\boldsymbol{T};\boldsymbol{q}), \tag{4.13}$$

where $V(\boldsymbol{S},\boldsymbol{T};\boldsymbol{q})$ is the Fourier transform of $V(\boldsymbol{S},\boldsymbol{T};\boldsymbol{x}-\boldsymbol{y})$. So it is also quadratic in the bosonic fields associated with the $J(\boldsymbol{S};\boldsymbol{q})$'s.

4.2.1 Entanglement Entropy of Free Fermions

The kinetic energy part of Eq. (4.4) or its bosonized version Eq. (4.13) can be written in terms of the boson fields constructed above as:

$$\begin{aligned}H_0&=\frac{1}{2}\sum_{\boldsymbol{S};\boldsymbol{q}}\frac{v_F^*}{\Omega}J(\boldsymbol{S};-\boldsymbol{q})J(\boldsymbol{S};\boldsymbol{q})\\&=\frac{2\pi v_F^*}{\Omega V}\sum_{\boldsymbol{S}}\int d^2x\left(\partial_{x_S}\phi(\boldsymbol{S};\boldsymbol{x})\right)^2.\end{aligned} \tag{4.14}$$

We see that there is no coupling between different patches. The theory is thus formally a tensor product of many independent theories, one for each patch. We can therefore calculate the entanglement entropy patch by patch and sum up contributions from each patch in the end. Within a single patch there is no dynamics in the perpendicular direction as dictated by the Hamiltonian, and the problem is reduced to a *one dimensional* problem! Note that transverse degrees of freedom are not completely independent. According to Eq. (4.11), the commutator is non-vanishing for $x_{S\perp}\neq y_{S\perp}$ up to a length scale $\sim 2\pi/\Lambda$. This is

a consequence of restricting $\boldsymbol{q}_{\boldsymbol{S}\perp}$ to within the range $[-\Lambda/2, \Lambda/2]$. Physically one can view this as *discretization* along the transverse direction due to a restricted momentum range, similar to the relation between a lattice and its Brillouin zone. In this view the single patch problem is reduced to a 1D problem with a chain density of $(\Lambda/(2\pi))^{d-1}$. Therefore, the Hamiltonian (4.14) becomes

$$H_0 = \frac{2\pi v_F^*}{\Omega V} \sum_{\boldsymbol{S};\boldsymbol{x}_{\boldsymbol{S}\perp}} \int dx_{\boldsymbol{S}} \left(\partial_{x_{\boldsymbol{S}}} \phi(\boldsymbol{S};\boldsymbol{x})\right)^2 . \tag{4.15}$$

Note that the bosonized theory of a single patch is chiral. To directly make use of our toy model, we need to consider two patches having opposite $\hat{\boldsymbol{n}}_{\boldsymbol{S}}$ simultaneously. This is because for a 1D fermion model at non-zero filling, there are two Fermi points. Both need to be considered to construct well-defined local degrees of freedom. Once we consider such two patches together, it is more convenient to combine the two chiral theories into a non-chiral theories. This is also what we will do for the rest of this work. Introduce the non-chiral fields

$$\begin{cases} \varphi(\boldsymbol{S};\boldsymbol{x}) = \frac{1}{\sqrt{2}} \left(\phi(\boldsymbol{S};\boldsymbol{x}) - \phi(-\boldsymbol{S};\boldsymbol{x})\right), \\ \chi(\boldsymbol{S};\boldsymbol{x}) = \frac{1}{\sqrt{2}} \left(\phi(\boldsymbol{S};\boldsymbol{x}) + \phi(-\boldsymbol{S};\boldsymbol{x})\right), \end{cases} \tag{4.16}$$

where $-\boldsymbol{S}$ indicates the patch with normal direction opposite to that of patch $\boldsymbol{S}$: $\hat{\boldsymbol{n}}_{-\boldsymbol{S}} = -\hat{\boldsymbol{n}}_{\boldsymbol{S}}$. One finds that χ and φ are mutually dual fields with $\boldsymbol{S}$ restricted to one hemisphere, but $\partial_{x_{\boldsymbol{S}}}\varphi$ and φ now commute while χ and φ have a non-trivial commutator:

$$\begin{aligned} &[\varphi(\boldsymbol{S};\boldsymbol{x}), \partial_{y_{\boldsymbol{S}}}\varphi(\boldsymbol{S};\boldsymbol{y})] = [\chi(\boldsymbol{S};\boldsymbol{x}), \partial_{y_{\boldsymbol{S}}}\chi(\boldsymbol{S};\boldsymbol{y})] = 0, \\ &[\partial_{x_{\boldsymbol{S}}}\varphi(\boldsymbol{S};\boldsymbol{x}), \chi(\boldsymbol{T};\boldsymbol{y})] = [\partial_{x_{\boldsymbol{S}}}\chi(\boldsymbol{S};\boldsymbol{x}), \varphi(\boldsymbol{T};\boldsymbol{y})] \\ &= 2i\pi\Omega\delta_{\boldsymbol{S},\boldsymbol{T}}\delta(x_{\boldsymbol{S}} - y_{\boldsymbol{S}})\delta^{d-1}(\boldsymbol{x}_{\boldsymbol{S}\perp} - \boldsymbol{y}_{\boldsymbol{S}\perp}). \end{aligned} \tag{4.17}$$

Therefore, two patches with opposite $\hat{\boldsymbol{n}}_{\boldsymbol{S}}$ are equivalent to a set of ordinary 1D boson fields. Throughout the rest of this work, we shall assume this chiral-to-nonchiral transformation is done, and when we refer to patches we always refer to the two companion patches that form a non-chiral patch together. For the non-chiral boson theory, it is known that the entanglement entropy of a single interval (with two end points) is $(1/3)\log L$.

Before we proceed further, we note that the relation between boson fields and the original fermion fields is not completely local. However, the underlying physical quantity that matters is not the fields, but the fermion density, or in other words, the fermion number basis one chooses to expand the Hilbert space of the problem. This physical basis is also what one uses to do the partial trace. It is known that the fermion density operator obeys a locally one-to-one corresponding relation to the boson fields. Thus we argue that in 1D the nonlocal relation between the fermion and boson fields does not affect the partial trace operation, so as the calculation of entanglement entropy.

By referring to our result for the toy model, the contribution from a single patch is readily given

$$S(\boldsymbol{S}) = \frac{1}{12}\log L \oint_{\partial A} \left|\hat{\boldsymbol{n}}_{\boldsymbol{S}} \cdot d\vec{S}_x\right| \times \left(\frac{\Lambda}{2\pi}\right)^{d-1}, \tag{4.18}$$

where an additional factor of $1/2$ has been introduced in order to count only once each pair of patches forming a non-chiral theory. Identifying $\hat{\boldsymbol{n}}_{\boldsymbol{S}}\Lambda^{d-1}$ as the surface element at the Fermi surface $d\vec{S}_k$ and taking the $N \to \infty$ limit, the total entanglement entropy is

$$S = \frac{1}{12(2\pi)^{d-1}}\log L \oint_{\partial A}\oint_{\partial \Gamma} \left|d\vec{S}_k \cdot d\vec{S}_x\right|. \tag{4.19}$$

So we recover the GK result for generic free fermions.

4.2.2 Solution for the Fermi liquid case and non-locality of the Bogoliubov fields

When Fermi liquid interactions (forward scattering) are included, the full Hamiltonian will no longer be diagonal in the patch index $\boldsymbol{S}$. But it is still quadratic in terms of the patch density operators, i.e. the bosonic degrees of freedom, and can be diagonalized by a Bogoliubov transformation. According to Eq. (4.7) and ignoring terms of $O(\lambda/\Lambda)$, one can define a set of boson creation/annihilation operators $\hat{a}^\dagger(\boldsymbol{q})/\hat{a}(\boldsymbol{q})$ as follows:

$$\phi(\boldsymbol{S};\boldsymbol{x}) = i\sum_{\boldsymbol{q},\hat{\boldsymbol{n}}_{\boldsymbol{S}}\cdot\boldsymbol{q}>0} \frac{a^\dagger(\boldsymbol{S};\boldsymbol{q})e^{-i\boldsymbol{q}\cdot\boldsymbol{x}} - a(\boldsymbol{S};\boldsymbol{q})e^{i\boldsymbol{q}\cdot\boldsymbol{x}}}{\sqrt{|\hat{\boldsymbol{n}}_{\boldsymbol{S}}\cdot\boldsymbol{q}|}}. \tag{4.20}$$

It can be shown that the full Hamiltonian is diagonal in $\boldsymbol{q}$, and it can be diagonalized

by a Bogoliubov transformation[85] independently for each $\boldsymbol{q}$ sector. In Ref. [85], only a Hubbard-U like interaction is considered for practical reasons. But in principle, such a Bogoliubov transformation also applies to general interactions:

$$\begin{aligned}\hat{a}_i(\boldsymbol{q}) &= \sum_j u_{ij}\alpha_j(\boldsymbol{q}) + v_{ij}\beta_j^\dagger(\boldsymbol{q}),\\ \hat{b}_i(\boldsymbol{q}) &= \sum_j u_{ij}\beta_j(\boldsymbol{q}) + v_{ij}\alpha_j^\dagger(\boldsymbol{q}),\end{aligned} \tag{4.21}$$

where both i and j refer to the patch index, α_j and β_j are the Bogoliubov bosonic annihilation operators that diagonalize the Hamiltonian. With proper choice of u's and v's, the Hamiltonian is readily diagonalized. Ref. [85] solves the Hubbard-U like interaction and provides a successful description of Fermi liquids, even in the strong U limit.

However, even for this simple case in which U has no $\boldsymbol{q}$-dependence, the Bogoliubov transformation still depends on $\boldsymbol{q}$. To be more precise, u_{ij} and v_{ij} will depend only on the angle between the patch normal direction $\hat{\boldsymbol{n}}_S$ and $\boldsymbol{q}$, leading to discontinuities in the derivatives at $q = 0$. Consequently, the real space fields constructed from the Bogoliubov operators α_j and β_j are *no longer* local with respect to the original boson fields. The real space Bogoliubov fields are constructed in a manner similar to Eq. (4.20):

$$\tilde{\phi}(\boldsymbol{S};\boldsymbol{x}) = i\sum_{\boldsymbol{q},\hat{\boldsymbol{n}}_S\cdot\boldsymbol{q}>0} \frac{\alpha^\dagger(\boldsymbol{S};\boldsymbol{q})e^{-i\boldsymbol{q}\cdot\boldsymbol{x}} - \alpha(\boldsymbol{S};\boldsymbol{q})e^{i\boldsymbol{q}\cdot\boldsymbol{x}}}{\sqrt{\hat{\boldsymbol{n}}_S\cdot\boldsymbol{q}}}. \tag{4.22}$$

Then one can show that the original local degrees of freedom $\phi(\boldsymbol{S};\boldsymbol{x})$ can be expressed in terms of above Bogoliubov fields as

$$\phi(\boldsymbol{S};\boldsymbol{x}) = \tilde{\phi}(\boldsymbol{S};\boldsymbol{x}) + \int d\boldsymbol{y}\sum_l f(\boldsymbol{S},l;\boldsymbol{x}-\boldsymbol{y})\tilde{\phi}(l;\boldsymbol{y}), \tag{4.23}$$

where $f(\boldsymbol{S},l;\boldsymbol{x}-\boldsymbol{y})$ is typically long-range, even for the short-range Hubbard-U interaction. For more general cases, with further $\boldsymbol{q}$-dependence in the interaction, the non-locality would only be enhanced. The loss of locality prevents us from calculating the entanglement entropy directly using those eigen modes, since it is difficult to implement the partial trace using those non-local degrees of freedoms. Therefore, although the Bogoliubov fields

have a local core as we would expect for Fermi liquids from adiabaticity, they *do* acquire a nonlocal dressing due to interaction. Though in principle the partial trace can be done with those Bogoliubov fields, such nonlocality makes it difficult and we have not been able to do it, which further renders calculating the entanglement entropy impossible. This is very different from the 1D theory, where for local interactions the eigen fields remain local, since there are only two Fermi points. There the transformation can never involve such angular $\boldsymbol{q}$-dependence due to limited dimensionality. Despite these technical difficulties, the non-locality may suggest possible corrections to the entanglement entropy. This is indeed the case as revealed by our later calculation for Fermi liquid interactions, although in this case such extra contributions are only of $O(1) \times \log L$ which is of $O(1/L)$ comparing to the leading term. This shows that the mode-counting argument in Ref.[92], though correctly suggesting the $\log L$ violation to the area law for Fermi liquids, does not always fully account for all sources of entanglement entropy.

4.3 Entanglement entropy from the Green's function

In order to preserve locality, we need to work with the original local degrees of freedom. To do that, we adopt the approach used by Calabrese and Cardy[**?**] (CC) on calculating the entanglement entropy of a free massive $1D$ bosonic field theory. The calculation is done in terms of the Green's function by applying the replica trick. In our case, we find that the CC approach can be generalized in a special geometry for solving the interacting theory which is quadratic after bosonization. In this way, we avoid diagonalizing the Hamiltonian and thus the nonlocality issue. However, we do have to regularize the theory by adding a mass term by hand. In the end we shall take the small mass limit, and replace the divergent correlation length $\xi \sim 1/m$ by the subsystem size L. The regularization procedure facilitates the calculation, but also strictly restricts us to computing the entanglement entropy only at the $\log L$ level.

In this section, by using the replica trick we convey the calculation of entanglement entropy into computing the Green's function on an n-sheeted replica manifold. We first demonstrate the method by applying it to free fermion theory in d-dimensional space; then

based on it we compute the entanglement entropy perturbatively for a simple Fermi liquid theory in powers of the interaction strength up to the second order.

4.3.1 The Replica Trick and Application to 1D Free Bosonic Theory

In this part, we briefly describe the replica trick in (1 + 1) space-time dimensions ((1 + 1)d) so that later on we can straightforwardly generalize it to (2 + 1) space-time dimensions ((2 + 1)d) accordingly for our problem.

The replica trick makes use of the following identity:

$$S_A = -\mathrm{Tr}(\rho_A \ln \rho_A) = -\lim_{n\to 1} \frac{\partial}{\partial n} \mathrm{Tr}\rho_A^n. \tag{4.24}$$

To compute $\mathrm{Tr}\rho_A^n$, CC use path integral to express the density matrix ρ in terms of the boson fields

$$\rho(\{\phi(x)\}|\{\phi(x')'\}) = Z^{-1}\langle\{\phi(x)\}|e^{-H}|\{\phi(x')'\}\rangle, \tag{4.25}$$

where $Z = \mathrm{Tr}e^{-\beta H}$ is the partition function, β is the inverse temperature, and $\{\phi(x)\}$ are the corresponding eigenstates of $\hat{\phi}(x)$: $\hat{\phi}(x)|\{\phi(x')\}\rangle = \phi(x')|\{\phi(x')\}\rangle$. ρ can be expressed as a (Euclidean) path integral:

$$\rho = Z^{-1}\int [d\phi(x,\tau)] \prod_x \delta(\phi(x,0) - \phi(x)') \prod_x \delta(\phi(x,\beta) - \phi(x)'')e^{-S_E}, \tag{4.26}$$

where $S_E = \int_0^\beta L_E d\tau$, with L_E being the Euclidean Lagrangian. The normalization factor Z, i.e. the partition function is found by setting $\{\phi(x)''\} = \{\phi(x)'\}$ and integrating over these variables. This has the effect of sewing together the edges along $\tau = 0$ and $\tau = \beta$ to form a cylinder of circumference β as illustrated in Fig. (4.4) (left panel).

The reduced density matrix of an interval $A = (x_i, x_f)$ can be obtained by sewing together only those points which are not in the interval A. This has the effect of leaving an open cut along the line $\tau = 0$ which is shown in Fig. 4.4 (right panel). To compute ρ_A^n, we make n copies of above set-up labeled by an integer k with $1 \le k \le n$, and sew them together cyclically along the open cut so that $\phi(x)'_k = \phi(x)''_{k+1}$[and $\phi(x)'_n = \phi(x)''_1$] for all $x \in A$. In Fig. 4.5(a) we show the case $n = 2$. Let us denote the path integral on this

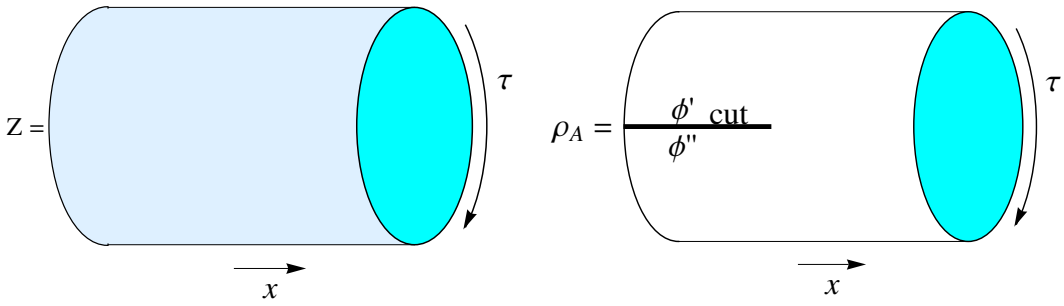

Figure 4.4: Path integral representation of the reduced density matrix. Left: When we sew $\phi(x)' = \phi(x)''$ together for all x's, we get the partition function Z. Right: When only sew $x \notin A$ together, we get ρ_A.

n-sheeted structure (known as n-sheeted Riemann surface) by $Z_n(A)$. Then

$$\mathrm{Tr}\rho_A^n = \frac{Z_n(A)}{Z^n}, \tag{4.27}$$

so that

$$S_A = -\lim_{n\to 1}\frac{\partial}{\partial n}\frac{Z_n(A)}{Z^n}. \tag{4.28}$$

If we consider the theory as that of one field living on this complex $n-$sheeted Riemann surface instead of a theory of n copies, it is possible to remove the replica index n from the fields, and instead consider a problem defined on such an n-sheeted Riemann surface which can be realized by imposing proper boundary conditions.

In Ref.[**?**], CC consider the entanglement entropy between the two semi-infinite 1D system (i.e. cutting an infinite chain into two halves at $x = 0$) for free massive boson fields. For such geometry, as illustrated in Fig. 4.5(b), the $n-$sheeted Riemann surface constraint is realized by imposing a $2n\pi$ periodicity on the angular variable of the polar coordinates of the $(1+1)d$ plane instead of the usual 2π one. In this way, the $(1+1)d$ variable $\boldsymbol{x} = (x, \tau)$ acquires n branches $\boldsymbol{x}_n$, and each branch corresponds to one copy of ϕ. Notation-wise this corresponds to

$$\phi(x,\tau)_k \Rightarrow \phi(\boldsymbol{x}_k) \Rightarrow \phi(\boldsymbol{x}), \tag{4.29}$$

and the sewing conditions $\phi(x)'_k = \phi(x)''_{k+1}$ simply becomes the continuity condition for $\phi(\boldsymbol{x})$

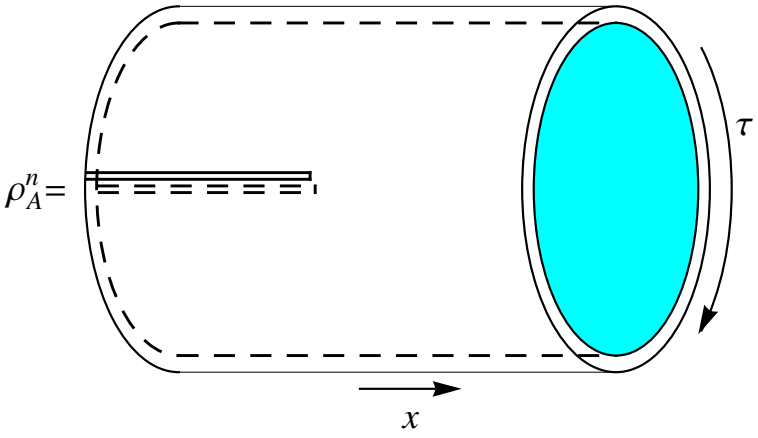

(a)

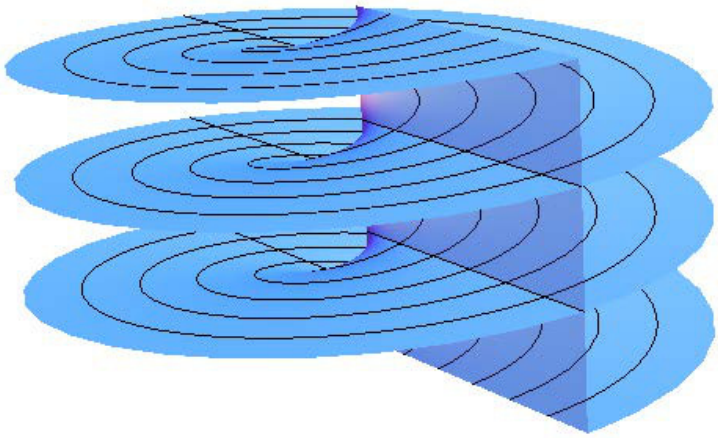

(b)

Figure 4.5: Formation of the $n-$sheeted Riemann surface in the replica trick. By sewing n copies of the reduced density matrices together, one obtains the replica partition function Z_n. In the zero temperature limit, $\beta \to \infty$, each cylinder representing one copy of ρ_A becomes an infinite plane. Those $n-$planes sewed together form a $n-$sheeted Riemann surface in Fig. 4.5(b) which can be simply realized by enforcing a $2n\pi$ periodicity on the angular variable of the polar coordinates of the $(1+1)d$ plane instead of the usual 2π one. (a): n copies of the reduced density matrices. For clarity only $n = 2$ is shown. (b): Visualization of a $n-$sheeted Riemann surface.

across its consecutive branches. Here we use a generalized polar coordinate: $\boldsymbol{x} = (r, \theta)$ with $0 < r < \infty$, and $0 \leq \theta < 2n\pi$.

The massive free boson theory considered by CC is defined by the following action

$$\mathcal{S} = \int \frac{1}{2}((\partial_\mu \phi)^2 - m^2\phi^2) d^2 r.$$

The $(1+1)d$ bosonic Green's function $G^{(n)}_{0,b}(\boldsymbol{r}, \boldsymbol{r}') = \langle \phi(\boldsymbol{r})\phi(\boldsymbol{r}')\rangle$ on the $n-$sheeted Riemann surface satisfies the differential equation

$$(-\nabla^2_{\boldsymbol{r}} + m^2) G^{(n)}_{0,b} = \delta(\boldsymbol{r} - \boldsymbol{r}').$$

To compute the partition function, one can make use of the identity

$$\frac{\partial}{\partial m^2} \log Z_n = -\frac{1}{2} \int d^{d+1} x G^{(n)}(\boldsymbol{x}, \boldsymbol{x}). \tag{4.30}$$

Note that here the integration is over the entire $n-$sheeted space. The above is applicable to general quadratic theories of bosons, and will be applied by us later to bosonized theories of interacting fermions. Here we use $G^{(n)}(\boldsymbol{x}, \boldsymbol{x}')$, a general two point correlation function on the $n-$sheeted Riemann surface in d-dimensional space for later use, instead of the specific $G^{(n)}_{0,b}$ defined above. Accordingly, S_A is then given as

$$S_A = -\lim_{n\to 1} \frac{\partial}{\partial n} e^{-\frac{1}{2}\int dm^2 \int d^{D+1} x (G^{(n)}(\boldsymbol{x},\boldsymbol{x}) - nG^{(1)}(\boldsymbol{x},\boldsymbol{x}))}. \tag{4.31}$$

Here and in the following, we will leave it understood that the first term in the integrand is integrated over the n-sheeted geometry, whereas the second is integrated over a one-sheeted geometry. There should be no confusion as the superscript of G generally indicates the geometry.

The benefit of the above approach is that the two point correlation function or Green's function, defined in terms of certain differential equation obtained from the equation of motion, can be solved for on the $n-$sheeted Riemann surface thus enabling us to compute the entanglement entropy. Although CC's work only considers massive $(1+1)d$ boson fields, it is also applicable to our case. The price one has to pay is to introduce a mass term

for regularization. At the end of the calculation the inverse mass, which is the correlation length of the system, shall be considered to be on the same scale as L: $1/m \sim L$, where L is the characteristic length scale of the subsystem. The validity of such consideration is well-established in other cases,[88, 94] where the correlation length is either set by finite temperature or mass. The only modification necessary to apply the above to a bosonized Fermi surface in higher dimensions is to introduce a sum over the patch index.

4.3.2 Geometry and Replica Boundary Conditions

Through the remainder of this work, instead of the general geometry considered before, we work with a special half-cylinder geometry as shown in Fig. 4.6(a): the system is infinite in the $\hat{x}$ direction while obeying periodic boundary condition along the $\hat{y}$ direction with length L. The system is cut along the $\hat{y}$ axis so that we are computing the entanglement entropy between the two half planes. We require L to be large so that it can be considered $\sim \infty$ unless otherwise noted.

We choose such this simple geometry for the following reasons. Cutting the system straight along the $\hat{y}$ direction, yielding a two half-plane geometry, is a straightforward $(2+1)d$ generalization of the semi-infinite chain geometry considered in CC. It makes any straight line intersect the boundary only once, dividing it into two semi-infinite segments, for all patch directions as in the 1D case, except for lines parallel to the $\hat{\boldsymbol{n}}_S = \hat{y}$ patch direction. The degrees of freedom associated with this special patch do not contribute to the entanglement entropy, since they are not coupled (have no dynamics) along $\hat{x}$, and are of measure zero in the large patch number limit anyway.

For this simple geometry, the $(2+1)d$ n-sheeted geometry is constructed from n identical copies

$$S^n = \{(x, y, \tau) \in \mathbb{R} \times \mathbb{R} \times \mathbb{R}\}, \tag{4.32}$$

sliced along "branch cuts"

$$C^n = \{(x, y, \tau) \in \mathbb{R}^- \times \mathbb{R} \times \{0\}\}, \tag{4.33}$$

and then appropriately glued together along these cuts. This happens exactly as in 1D, and

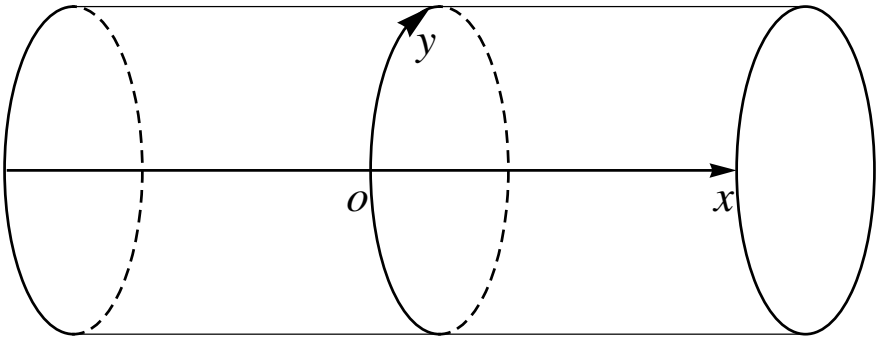

(a)

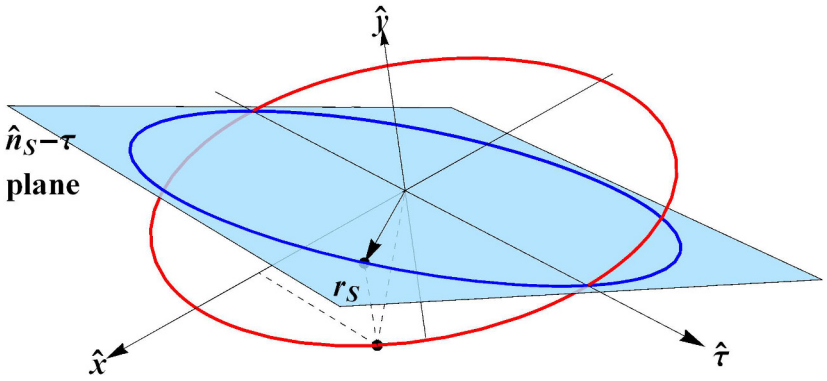

(b)

Figure 4.6: The half-cylinder geometry and equivalence of boundary conditions in $\hat{x} - \hat{\tau}$ and $\hat{\boldsymbol{n}}_S - \hat{\tau}$ planes. The system is infinite in the $\hat{x}$ direction while obeys periodic boundary condition along the $\hat{y}$ direction with length L. The system is cut along the $\hat{y}$ axis so that we are computing the entanglement entropy between the two half planes. (a): The half-cylinder geometry. (b): The projection of $\boldsymbol{r}_S$ onto the $\hat{x} - \hat{\tau}$ plane. Consider polar coordinates of an arbitrary $\hat{\boldsymbol{n}}_S - \hat{\tau}$ plane (the blue plane). Since the polar coordinates in the $\hat{x} - \hat{\tau}$ plane satisfies the $2n\pi$ periodic boundary condition, consider the one-to-one projection of the vector $\boldsymbol{r}_S$ onto the $\hat{x} - \hat{\tau}$ plane. Consider, if we move the vector in the $\hat{x} - \hat{\tau}$ plane around the origin n times (the red circle). Due to the one-to one mapping, $\boldsymbol{r}_S$ should also move around the origin n times (the blue "circle", it is actually a eclipse), thus obeys the $2n\pi$ periodicity as well.

the y coordinate is so far a mere spectator. This defines an $n-$sheeted, or in this case more appropriately the $n-$layered, replica manifold which is a simple enough generalization of the $(1+1)d$ case. The n-sheeted Riemann surface, as discussed in Sec. 4.3.1 and shown in Fig. 4.5(b), now acquires an extra direction $\hat{y}$ perpendicular to the $\hat{x}-\hat{\tau}$ plane. It can still be implemented by imposing the same $2n\pi$ periodicity boundary conditions on θ, the angular variable of the polar coordinates $(x,\tau) = (r\cos\theta, r\sin\theta)$ in the $\hat{x}-\hat{\tau}$ plane. Therefore, we can safely make use of the CC result, i.e. the solution to the Green's function on a $n-$sheeted Riemann surface, to the free fermion theory, and can further use it as a starting point for treating the interacting theory. This is obviously true for the patch with $\hat{\boldsymbol{n}}_S = \hat{x}$, but it also holds for general $\hat{\boldsymbol{n}}_S$ as we shall validate as the following.

For a general patch direction $\hat{\boldsymbol{n}}_S$, the noninteracting Green's function associated with this patch embodies correlations in the affine $\hat{\boldsymbol{n}}_S - \hat{\tau}$ "planes". The geometry of each such "plane" is that of the n-sheeted Riemann surface of the $(1+1)d$ problem, as we will now argue. With each patch direction we thus associate a different foliation of the n-sheeted $(2+1)d$ geometry into $(1+1)d$ counterparts.

To be more precise, for given patch S, instead of the Cartesian coordinates (x, y, τ), we consider a parallel/perpendicular decomposition $(x_S, x_{S\perp}, \tau)$ for each sheet via

$$(x, y) = x_S \hat{\mathbf{n}}_S + x_{S\perp} \hat{\mathbf{n}}_{S\perp}\,, \tag{4.34}$$

where the $\hat{\boldsymbol{n}}_{S\perp}$ are the perpendicular unit vectors aligned with the patch S. The natural choice of coordinates for a given patch is to choose polar coordinates within the $\hat{\boldsymbol{n}}_S - \hat{\tau}$ plane:

$$\boldsymbol{r}_S = (x_S + x_{S\perp}\frac{\hat{n}^x_{S\perp}}{\hat{n}^x_S}, \tau) = (r_S\cos\theta_S, r_S\sin\theta_S)\,, \tag{4.35}$$

because these are the coordinates in which the $\hat{\boldsymbol{n}}_S - \hat{\tau}$ planes restricted to each sheet are naturally glued together by extending the range of θ_S to $2\pi n$, as we will now show. The shift $x_{S\perp}\hat{n}^x_{S\perp}/\hat{n}^x_S$ of x_S is necessary as to ensure that $x = 0$, the location of the onset of the branch cut, corresponds to $\boldsymbol{r}_S = 0$ which is what makes these coordinates convenient. The $\hat{\boldsymbol{n}}_S - \hat{\tau}$ planes are now defined by fixed $x_{S\perp}$.

If we can establish that the $2\pi n$ periodicity of θ is equivalent to a $2\pi n$ periodicity of

θ_S, then CC's solution would be justified in the above set-up so that the non-interacting Green's function $G_0(\boldsymbol{S}, \boldsymbol{S};, r_S, \theta_S, r'_S, \theta'_S)$ can be expressed through CC's result. This can be achieved by establishing a one-to-one correspondence (mapping) between θ and θ_S. The mapping is intuitively constructed, as shown in Fig. 4.6(b), as the vertical projection from the $\hat{\boldsymbol{n}}_S - \hat{\tau}$ plane (the blue plane in Fig. 4.6(b)) onto the $\hat{x} - \hat{\tau}$ plane along the $\hat{y}$ direction. Consider moving the projection of $\boldsymbol{r}_S$ in the $\hat{x} - \hat{\tau}$ plane around the origin n times (the red circle). It is clear that $\boldsymbol{r}_S$ (on the blue ellipse) follows its projection while also moving around the origin n times, always being on the same sheet. In particular, the branch cut is always traversed simultaneously for $\theta = \theta_S = \pi \bmod 2\pi$. The $\hat{\boldsymbol{n}}_S - \hat{\tau}$ planes, the leaves of our foliation, thus have the familiar 1+1d n-sheeted geometry, and θ_S obeys the same $2n\pi$ periodicity as θ.

Finally, the periodicity condition of the $\hat{y}$ direction is necessary for the total entanglement entropy to be finite; it also provides the only length scale for the subsystem which is needed for extracting the scaling behavior of entanglement entropy. However, if we are only concerned with the integral form of the entanglement entropy as in Eq. (4.19), not requiring it to be finite as a whole, but rather requiring only the entanglement entropy per unit length to be finite, we may take the y direction to be infinite. This point of view will be taken here and in the following in order to simplify our calculation.

4.3.3 Entanglement entropy of free fermions revisited

In order to treat the interacting theory, in this section we re-derive the free fermion result for the half cylinder geometry via the replica trick. Later we shall generalize the method to include interactions. Rewriting the Hamiltonian Eq. (4.14) in terms of the non-chiral fields, and adding the mass term by hand, we have

$$H[\phi(\boldsymbol{S};\boldsymbol{x})] = \sum_S \int d^2x \frac{2\pi v_F^*}{\Omega V}\Big((\partial_{x_S}\varphi(\boldsymbol{S};\boldsymbol{x}))^2 + (\partial_{x_S}\chi(\boldsymbol{S};\boldsymbol{x}))^2\Big) + \frac{m^2}{2}\varphi(\boldsymbol{S};\boldsymbol{x})^2. \tag{4.36}$$

For convenience, we use the Lagrangian formalism and work with the $\varphi(\boldsymbol{S};\boldsymbol{x})$ representation through the rest of this work.

Switching to imaginary time $t \to i\tau$, and rescaling the coordinates in the following manner:

$$\tau \to \sqrt{\frac{V}{16\pi^3 v_F^* \Omega}}\frac{\tau}{m}, \quad \boldsymbol{x} \to \sqrt{\frac{\Omega V}{4\pi^2 v_F^*}}\frac{\boldsymbol{x}}{m}, \tag{4.37}$$

we obtain the following Lagrangian density in the φ representation :

$$\mathcal{L} = -\frac{m^2}{2}[(\partial_\tau \varphi(\boldsymbol{S};\boldsymbol{x}))^2 + (\partial_S \varphi(\boldsymbol{S};\boldsymbol{x}))^2 + (\varphi(\boldsymbol{S};\boldsymbol{x}))^2]. \tag{4.38}$$

Then we can work out the Euler-Lagrangian (E-L) equation of motion. Making use of the E-L equation of motion, we find the Green's function $G_0^{(n)}(\boldsymbol{S},\boldsymbol{T};\boldsymbol{x},\boldsymbol{x}') = \langle T\varphi(\boldsymbol{S};\boldsymbol{x})\varphi(\boldsymbol{T};\boldsymbol{y})\rangle_0$ satisfies the following differential equation:

$$\begin{aligned} &-\left(\partial_\tau^2 + \partial_{x_S}^2 - 1\right) G_0^{(n)}(\boldsymbol{S},\boldsymbol{T};\boldsymbol{x},\boldsymbol{y}) \\ &= C\delta_{\boldsymbol{S},\boldsymbol{T}}\delta(\tau-\tau_y)\delta(x_S - y_S)\delta^{d-1}(\boldsymbol{x}_{S\perp} - \boldsymbol{y}_{S\perp}), \end{aligned} \tag{4.39}$$

where $C = 2\pi\Omega m^{d-1}\left(\sqrt{\frac{\Omega V}{4\pi^2 v_F^*}}\right)^{d-2}$. The rescaling makes the Green's function dimensionless, thus easier to handle when it comes to computing $\int d^{d+1}x G^{(n)}(\boldsymbol{x},\boldsymbol{x})$. The extra factor C generated on the right hand side (*rhs*) will be canceled by the Jacobian of the integral over the Green's function, leaving only a factor of $1/m^2$. All that needs to be computed is then an integral over the dimensionless G. Therefore, it is legitimate to ignore this factor from now on. The δ-functions originate from the commutator Eq. (4.11), and are *coarse-grained*. After we include the patch index, perform the integral over m^2, and take the n derivative, Eq. (4.31) becomes

$$S_A = \frac{1}{2}\log(m^2 a_0^2)\lim_{n\to 1}\frac{\partial}{\partial n}\sum_{\boldsymbol{S}}(C_G(\boldsymbol{S};n) - nC_G(\boldsymbol{S};1)), \tag{4.40}$$

where a_0 is an ultraviolet cutoff, and

$$C_G(\boldsymbol{S};n) = \int d^{d+1}x G_0^{(n)}(\boldsymbol{S},\boldsymbol{S};\boldsymbol{x},\boldsymbol{x}). \tag{4.41}$$

The exponential factor in Eq. (4.31) becomes one after the $n \to 1$ limit is applied. Note that $\frac{1}{2}\log(m^2a^2) \sim -\log L$. Our major task is now computing $C_G(\boldsymbol{S};n)$.

Observing that there is no $x_{S\perp}$ dependence on the left hand side (lhs) of Eq. (4.39), we can write

$$G_0^{(n)}(\boldsymbol{S},\boldsymbol{T};\boldsymbol{x},\boldsymbol{y}) = \delta_{\boldsymbol{S},\boldsymbol{T}}\delta^{d-1}(\boldsymbol{x}_{S\perp}-\boldsymbol{y}_{S\perp})G_{0,b}^{(n)}(\boldsymbol{S};\boldsymbol{r}_{\boldsymbol{x}},\boldsymbol{r}_{\boldsymbol{y}}),$$

and we obtain a $(1+1)d$ equation

$$-(\partial_\tau^2+\partial_{x_S}^2+1)G_{0,b}^{(n)}(\boldsymbol{S};\boldsymbol{r}_{\boldsymbol{S},\boldsymbol{x}},\boldsymbol{r}_{\boldsymbol{S},\boldsymbol{y}}) = \delta(\tau-\tau_y)\delta(x_{\boldsymbol{S}}-y_{\boldsymbol{S}}) \tag{4.42}$$

in which $\boldsymbol{r}_{\boldsymbol{S},\boldsymbol{x}(\boldsymbol{y})}$ is as defined in Eq. (4.35). The same equation appears in CC. We shall also suppress the subscript $\boldsymbol{S}$ unless necessary, as it is normally already specified in the notation for $G_{0,b}$.

The transverse part of the integral in $C_G(\boldsymbol{S};n)$ can be factored out as

$$\int d^{d-1}x_{\boldsymbol{S}\perp}\delta^{d-1}(\boldsymbol{x}_{\boldsymbol{S}\perp}-\boldsymbol{y}_{\boldsymbol{S}\perp})\Big|_{\boldsymbol{y}\to\boldsymbol{x}}.$$

Recalling our discussion about Eq. (4.11), this is a coarse-grained δ-function. At short distances, instead of a divergence, we should use

$$\delta^{d-1}(x_{\boldsymbol{S}\perp}-y_{\boldsymbol{S}\perp})\Big|_{\boldsymbol{y}\to\boldsymbol{x}} = (\Lambda/(2\pi))^{d-1}. \tag{4.43}$$

Therefore, the transverse direction integral becomes

$$(\Lambda/(2\pi))^{d-1}\int d^{d-1}\boldsymbol{x}_{\boldsymbol{S}\perp} = (\Lambda/(2\pi))^{d-1}\oint_{\partial A} d\boldsymbol{S}_{\boldsymbol{x}}\cdot\hat{\boldsymbol{n}}_{\boldsymbol{S}}.$$

Identifying $\Lambda^{d-1}\hat{\boldsymbol{n}}_{\boldsymbol{S}}$ as the surface element $d\boldsymbol{S}_{\boldsymbol{k}}$, for a given patch the integration can be rewritten as $(2\pi)^{-d+1}\oint_{\partial_A}|d\boldsymbol{S}_{\boldsymbol{x}}\cdot d\boldsymbol{S}_{\boldsymbol{k}}|$. This leaves us with only an integral over $(G_{0,b}^{(n)}(\boldsymbol{S};\boldsymbol{r}_x,\boldsymbol{r}_x)-nG_{0,b}^{(1)}(\boldsymbol{S};\boldsymbol{r}_x,\boldsymbol{r}_x))$.

The solution for the $(1+1)d$ Green's function on the $n-$sheeted replica manifold is given in CC:

$$G_{0,b}^{(n)}(\boldsymbol{S};\boldsymbol{r}_x,\boldsymbol{r}_y) = \frac{1}{2\pi n}\sum_{k=0}^{\infty} d_k C_{k/n}(\theta_x-\theta_y)g_{k/n}(r_x,r_y), \tag{4.44}$$

where $d_0 = 1, d_k = 2$ for $k > 0$, $C_\nu(\theta) = \cos(\nu\theta)$, $g_\nu(r, r') = \theta(r - r')I_\nu(r')K_\nu(r) + \theta(r' - r)I_\nu(r)K_\nu(r')$, and $I_\nu(r)$ and $K_\nu(r)$ are the modified Bessel functions of the first and second kind respectively. r and θ are again the polar coordinates of the $\hat{\boldsymbol{n}}_{\boldsymbol{S}} - \hat{\tau}$ plane, and we have suppress the index $\boldsymbol{S}$ of r as only one patch direction is involved.

The integral over $G^{(n)}_{0,b}$ is

$$\int d^2 r_x G^{(n)}_{0,b}(\boldsymbol{S}; \boldsymbol{r}_x, \boldsymbol{r}_x) = \int dr_x r_x \sum_k d_k g_{k/n}(r_x, r_x). \tag{4.45}$$

The integral is divergent since the integrand $r_x g_{k/n}(r_x, r_x)|_{r_x\to\infty} = 1/4$, a consequence of the fact that we are calculating the partition function of an infinite system. But this divergence should be canceled in $C_G(\boldsymbol{S}; n) - nC_G(\boldsymbol{S}; 1)$. To regularize the divergence, we use the Euler-MacLaurin (E-M) summation formula following CC, and sum over k first:

$$\frac{1}{2}\sum_{k=0}^{\infty} d_k f(k) = \int_0^\infty f(k)dk - \frac{1}{12}f'(0) - \sum_{j=2}^{\infty}\frac{B_{2j}}{(2j)!}f^{(2j-1)}(0), \tag{4.46}$$

where B_{2n} are the Bernoulli numbers, $f^{(2j-1)}(0) = \partial_k^{2j-1} f(k)|_{k=0}$. Note that the first term, the integral over k, is always canceled by rescaling $k/n \to k$ in $g_{k/n}$. For the remaining terms, which contain derivatives with respect to k, we may add a constant, in this case $-1/4$, under the derivative, which allows us to pull the derivative outside the integral. The integrand now is well-behaved at infinity. To be more precise, according to Eq. (4.46), we need to compute

$$\begin{aligned}\int dr_x r_x \partial_k^j g_{k/n}(r_x, r_x)\Big|_{k\to 0} &= \partial_k^j \int dr_x (r_x g_{k/n}(r_x, r_x) - 1/4)\Big|_{k\to 0} \\ &= \partial_k^j(-\frac{k}{2n}).\end{aligned} \tag{4.47}$$

So we have

$$C_G(\boldsymbol{S}; n) - nC_G(\boldsymbol{S}; 1) = \frac{1 - n^2}{24n}. \tag{4.48}$$

Combining the above results into Eq. (4.40) and converting the sum over $\boldsymbol{S}$ into an integral around the Fermi surface, we obtain Eq. (4.19) for this geometry.

4.3.4 Differential Equations of the Green's Functions and an Iterative Solution

In this part, we derive the differential equations of the Green's functions for the quadratic boson theory with inter-patch coupling, and provide an iterative solution. Including the Fermi liquid interaction $V(\boldsymbol{S},\boldsymbol{T};\boldsymbol{x}-\boldsymbol{y}) = U_{\boldsymbol{S},\boldsymbol{T}}$, the Hamiltonian becomes

$$H[\phi(\boldsymbol{S};\boldsymbol{x})] = \frac{2\pi v_F^*}{\Omega V}\int d^2x\Big[\sum_{\boldsymbol{S}}(\partial_{\boldsymbol{S}}\phi(\boldsymbol{S};\boldsymbol{x}))^2 + \sum_{\boldsymbol{S},\boldsymbol{T}} g_{\boldsymbol{S},\boldsymbol{T}}\partial_{\boldsymbol{S}}\phi(\boldsymbol{S};\boldsymbol{x})\partial_{\boldsymbol{T}}\phi(\boldsymbol{T};\boldsymbol{x})\Big] \tag{4.49}$$

where $g_{\boldsymbol{S},\boldsymbol{T}} = \frac{U_{\boldsymbol{S},\boldsymbol{T}}\Omega}{2\pi v_F^*}$ is order $1/N$. This Hamiltonian can be written in terms of the non-chiral fields as

$$\begin{aligned} H = \frac{2\pi v_F^*}{\Omega V}\int d^2x\Big(&\sum_{\boldsymbol{S}}\left((\partial_{x_{\boldsymbol{S}}}\varphi(\boldsymbol{S};\boldsymbol{x}))^2 + (\partial_{x_{\boldsymbol{S}}}\chi(\boldsymbol{S};\boldsymbol{x}))^2\right) \\ &+ \sum_{\boldsymbol{S},\boldsymbol{T}} g_{\boldsymbol{S},\boldsymbol{T}}(\partial_{x_{\boldsymbol{S}}}\chi(\boldsymbol{S};\boldsymbol{x})\partial_{x_{\boldsymbol{T}}}\chi(\boldsymbol{T};\boldsymbol{x}) + \partial_{x_{\boldsymbol{S}}}\varphi(\boldsymbol{S};\boldsymbol{x})\partial_{x_{\boldsymbol{T}}}\varphi(\boldsymbol{T};\boldsymbol{x}))\Big), \end{aligned} \tag{4.50}$$

where we have made use of the fact that $g_{\boldsymbol{S},\boldsymbol{T}} = g_{-\boldsymbol{S},-\boldsymbol{T}}$, which is required by time-reversal symmetry. Here the summation over $\boldsymbol{S}$ is restricted to a semicircle. This Hamiltonian contains generalized type kinetic terms (inter-patch coupling due to interaction) which are not diagonal. To obtain the corresponding Lagrangian, one needs to invoke the general Legendre transformation[95], and obtains the following Lagrangian densities, respectively, in terms of φ or χ:

$$\begin{aligned} \mathcal{L}_\varphi = \frac{1}{2}\Big[&\sum_{\boldsymbol{S}}\left((\partial_t\varphi(\boldsymbol{S};\boldsymbol{x}))^2 - (\partial_{\boldsymbol{S}}\varphi(\boldsymbol{S};\boldsymbol{x}))^2\right) \\ &+ \sum_{\boldsymbol{S},\boldsymbol{T}}\left(h_2(\boldsymbol{S},\boldsymbol{T})\partial_t\varphi(\boldsymbol{S};\boldsymbol{x})\partial_t\varphi(\boldsymbol{T};\boldsymbol{x}) - f_1(\boldsymbol{S},\boldsymbol{T})\partial_{\boldsymbol{S}}\varphi(\boldsymbol{S};\boldsymbol{x})\partial_{\boldsymbol{T}}\varphi(\boldsymbol{T};\boldsymbol{x})\right)\Big] \\ \mathcal{L}_\chi = \frac{1}{2}\Big[&\sum_{\boldsymbol{S}}\left((\partial_t\chi(\boldsymbol{S};\boldsymbol{x}))^2 - (\partial_{\boldsymbol{S}}\chi(\boldsymbol{S};\boldsymbol{x}))^2\right) \\ &+ \sum_{\boldsymbol{S},\boldsymbol{T}}\left(h_1(\boldsymbol{S},\boldsymbol{T})\partial_t\chi(\boldsymbol{S};\boldsymbol{x})\partial_t\chi(\boldsymbol{T};\boldsymbol{x}) - f_2(\boldsymbol{S},\boldsymbol{T})\partial_{\boldsymbol{S}}\chi(\boldsymbol{S};\boldsymbol{x})\partial_{\boldsymbol{T}}\chi(\boldsymbol{T};\boldsymbol{x})\right)\Big], \end{aligned} \tag{4.51}$$

where

$$f_1(\boldsymbol{S},\boldsymbol{T}) = g_{\boldsymbol{S},\boldsymbol{T}} + g_{-\boldsymbol{S},-\boldsymbol{T}} - g_{\boldsymbol{S},-\boldsymbol{T}} - g_{-\boldsymbol{S},\boldsymbol{T}},$$
$$f_2(\boldsymbol{S},\boldsymbol{T}) = g_{\boldsymbol{S},\boldsymbol{T}} + g_{-\boldsymbol{S},-\boldsymbol{T}} + g_{-\boldsymbol{S},\boldsymbol{T}} + g_{\boldsymbol{S},-\boldsymbol{T}},$$

and $h_{1(2)}(\boldsymbol{S},\boldsymbol{T})$ is defined through

$$\{I + [f_{1(2)}(\boldsymbol{S},\boldsymbol{T})]\}^{-1} = I + [h_{1(2)}(\boldsymbol{S},\boldsymbol{T})]. \tag{4.52}$$

Here, I is the identity matrix, and $[f(h)_i(\boldsymbol{S},\boldsymbol{T})]$ is the matrix formed by $f(h)_i(\boldsymbol{S},\boldsymbol{T})$, $i = 1, 2$. Applying this result and making use equations of motion obtained from the Hamiltonian, we obtain the Lagrangians $\mathcal{L}_\varphi$ or $\mathcal{L}_\chi$. Here we arbitrarily choose to work with $\mathcal{L}\varphi$. Then, by making use of the E-L equation of motion, applying the same rescaling Eq. (4.37), and letting $t = i\tau$, we obtain the differential equations that the interacting Green's function $G^{(n)} = \langle\varphi(\boldsymbol{S};\boldsymbol{x})\varphi(\boldsymbol{T};\boldsymbol{x}')\rangle$'s satisfies:

$$\begin{aligned} &-(\partial_\tau^2 + \partial_{\boldsymbol{S}}^2 - 1)G^{(n)}(\boldsymbol{S},\boldsymbol{T};\boldsymbol{x},\boldsymbol{x}') + \sum_l (h_2(l,\boldsymbol{T})\partial_\tau^2 + f_1(l,\boldsymbol{T})\partial_l\partial_{\boldsymbol{T}})G^{(n)}(l,\boldsymbol{T};\boldsymbol{x},\boldsymbol{x}') \\ &= C\delta_{\boldsymbol{S},\boldsymbol{T}}\delta(\tau-\tau')\delta(x_{\boldsymbol{S}} - x'_{\boldsymbol{S}}))\delta(x_{\boldsymbol{S}\perp} - x'_{\boldsymbol{S}\perp}). \end{aligned} \tag{4.53}$$

Here the Jacobian due to change of variables is the same as in the free fermion case. The entanglement entropy is still given by Eq. (4.40), but replacing $G_0^{(n)}$ with $G^{(n)}$ in $C_G(\boldsymbol{S};n)$. In the following, we omit the replica index n in the Green's function unless different values of n are involved in a single equation.

As is well known, differential equations such as the above can be converted to an integral form[96] relating the full Green's function to the noninteracting one. This leads to an iterative (perturbative) definition of the former in terms of the latter. In the present case, this integral equation reads

$$\begin{aligned} &G(\boldsymbol{S},\boldsymbol{T};\boldsymbol{x},\boldsymbol{y}) \\ &= G_0(\boldsymbol{S},\boldsymbol{T};\boldsymbol{x},\boldsymbol{y}) + \int d^3z G_0(\boldsymbol{S},\boldsymbol{S};\boldsymbol{x},\boldsymbol{z})\Big(\sum_l (h_2(l,\boldsymbol{T})\partial_\tau^2 + f_1(l,\boldsymbol{T})\partial_l\partial_{\boldsymbol{T}})G(l,\boldsymbol{T};\boldsymbol{z},\boldsymbol{y})\Big) \\ &= G_0(\boldsymbol{S},\boldsymbol{T};\boldsymbol{x},\boldsymbol{y}) + \delta G(\boldsymbol{S},\boldsymbol{T};\boldsymbol{x},\boldsymbol{y}). \end{aligned} \tag{4.54}$$

Given this equation, we can now compute the Green's function and thus the entanglement entropy perturbatively in powers of U.

4.3.5 Entanglement Entropy from the Iterative Solution

In Eq. (4.54), the G_0 term is the same as that of the free fermions, thus yields the same contribution to entanglement entropy. To study how the correction term $\delta G(\boldsymbol{S}, \boldsymbol{T}; \boldsymbol{x}, \boldsymbol{y})$ affects the entanglement entropy, we need to study

$$\int d^3x \delta G(\boldsymbol{S}, \boldsymbol{S}; \boldsymbol{x}, \boldsymbol{x}) = \sum_{M=1}^{\infty} \int d^3x \delta^{(M)} G(\boldsymbol{S}, \boldsymbol{S}; \boldsymbol{x}, \boldsymbol{x}), \tag{4.55}$$

where $\delta^{(M)}G$ denotes the Mth order correction. There are two distinctive types of terms in the perturbative expansion of δG. In general, at order M , we have in total $3(M+1)$ integrals. Let us examine one of the many terms contributing to the M-th order correction, to be summed over patch indices:

$$\begin{aligned}
&\int d^3x \delta^{(M)} G(\boldsymbol{S}, \boldsymbol{S}; \boldsymbol{x}, \boldsymbol{x}) \\
&\sim \int d^3x \prod_{i=0}^{M-1} (d^3 z_i) G_0(\boldsymbol{S}, \boldsymbol{S}; \boldsymbol{x}, z_0) \times \partial^2_{\tau_0} G_0(l_0, l_0; z_0, z_1) \cdots \times \partial^2_{\tau_i} G_0(l_i, l_i; z_i, z_{i+1}) \\
&\times \cdots \times \partial^2_{\tau_{M-1}} G_0(\boldsymbol{S}, \boldsymbol{S}; z_{M-1}, \boldsymbol{x}).
\end{aligned} \tag{4.56}$$

Here we only include the $\tau-$derivatives. In general we would also have spatial ($\hat{\boldsymbol{n}}_{l_i}$) derivative terms, as well as terms with mixed derivatives. But $\hat{\tau}$ and $\hat{\boldsymbol{n}}_{\boldsymbol{S}}$ directions are equivalent. Using rotational symmetry, and the fact that the two different derivatives in each term are with respect to independent variable that are each integrated over, one can see that all terms are identical except for S-dependent pre-factors. The two categories of terms are defined by the set $\{l_i\}$: 1) $l_i = \boldsymbol{S}\ \forall\ i$, i.e. with intra-patch coupling only; and 2) $\exists\ l_i \neq \boldsymbol{S}$ containing inter-patch coupling. We shall label the two categories as

$$\delta^{(M)} G(\boldsymbol{S}, \boldsymbol{S}; \boldsymbol{x}, \boldsymbol{x}) = \delta^{(M)}_{\text{intra}} G(\boldsymbol{S}, \boldsymbol{S}; \boldsymbol{x}, \boldsymbol{x}) + \delta^{(M)}_{\text{inter}} G(\boldsymbol{S}, \boldsymbol{S}; \boldsymbol{x}, \boldsymbol{x}) \tag{4.57}$$

Intra-patch coupling and comparison with 1D. Setting $l_i = \boldsymbol{S}$ for all i's in Eq. (4.56), first we consider the transverse direction

$$G_0(\boldsymbol{S}, \boldsymbol{S}; \boldsymbol{z}_i, \boldsymbol{z}_{i+1}) \sim \delta(z^{(\boldsymbol{S})}_{\perp,i} - z^{(\boldsymbol{S})}_{\perp,i+1}).$$

We can immediately integrate out the transverse component of all $\boldsymbol{z}_i$'s and obtain

$$\begin{aligned}
&\int d^3x \delta^{(M)}_{\text{intra}} G(\boldsymbol{S}, \boldsymbol{S}; \boldsymbol{x}, \boldsymbol{x}) \sim \\
&\int dx_{\boldsymbol{S}\perp} \delta(x_{\boldsymbol{S}\perp} - z_{\boldsymbol{S}\perp,0}) \delta(z_{\boldsymbol{S}\perp,M-1} - y_{\boldsymbol{S}\perp})|_{y\to\boldsymbol{x}} \times \int \prod_i dz_{\boldsymbol{S}\perp,i} \prod_i \delta(z_{\boldsymbol{S}\perp,i} - z_{\boldsymbol{S}\perp,i+1}) \qquad (4.58) \\
&= \int dx_{\boldsymbol{S}\perp} \delta(0) = \; L^{d-1}(\Lambda/(2\pi))^{d-1}.
\end{aligned}$$

In the last line we use again the fact that the transverse δ-function is a coarse-grained one (Eq.(4.43)).

The rest of $\delta^{(M)}_{\text{intra}} G$ is obtained by substituting $G_0(\boldsymbol{S}, \boldsymbol{S}; \boldsymbol{z}_i, \boldsymbol{z}_{i+1})$ with the $(1+1)d$ Green's function $G_{0,b}(\boldsymbol{S}; z_{\boldsymbol{S},i}, z_{\boldsymbol{S},i+1})$. Although a direct computation is possible, we first give a general argument that for any M the contribution to entanglement entropy from $\delta^M_{\text{intra}} G$ vanishes. We do so by making a comparison with the 1D case where a rigorous solution is available.

For the 1D Luttinger liquid with only forward scattering, the entanglement entropy can be calculated directly via bosonization and the result remains at $1/3 \log L$ in the presence of interactions. The calculation is possible because, in our language, there are only two patches, so the transformation which diagonalizes the Hamiltonian is not plagued by the nonlocality issue we encounter in the 2D theory. However, we can also treat the 1D case with our perturbative approach. The resulting series of integrals turns out to be *identical* to the one obtained from the intra-patch contributions in the higher dimensional case except for the transverse $\delta-$function. Therefore, we argue that at all orders, the intra-patch coupling terms have vanishing contribution to the entanglement entropy. We shall demonstrate such behavior explicitly up to second order in U later on.

Scaling analysis of inter-patch coupling. For terms with inter-patch coupling, we find that they are of order $O(1/L)$ comparing to the leading term according a scaling argument. The crucial observation here is that, as long as $\exists\, l_i \neq \boldsymbol{S}$, we do not encounter the

factor $\delta^{D-1}(0) = L^{D-1}(\Lambda)^{D-1}$, Eq. (4.43) because for $l \neq \boldsymbol{S}$

$$\delta(z_{1\perp}^{(\boldsymbol{S})} - z_{\perp}^{(\boldsymbol{S})})\delta(z_{\perp}^{(l)} - z_{1\perp}^{(l)}) = \frac{\delta^2(\boldsymbol{z}_1 - \boldsymbol{z})}{|\sin(\theta_l - \theta_{\boldsymbol{S}})|}, \tag{4.59}$$

where $\theta_{\boldsymbol{S}}$ (θ_l) is the angle between $\hat{\boldsymbol{n}}_{\boldsymbol{S}}$ ($\hat{\boldsymbol{n}}_l$) and the $\hat{x}$-axis in the $x-y$ plane. Therefore, when we integrate out the $(M+1)$ transverse δ-functions, the factor $\delta^{D-1}(0) = L^{D-1}(\Lambda)^{D-1}$ would be suppressed by even a single $l_i \neq \boldsymbol{S}$.

To examine the remaining integral, we can ignore the angular part as it cannot affect the scaling behavior. The asymptotic expansion of $K_\nu(r)$ and $I_\nu(r)$ for real r at large value is[97]

$$K_\nu(r) \simeq \sqrt{\tfrac{\pi}{2r}} e^{-r}\Big[1 + \sum_{n=1}^{\infty} \tfrac{(\nu,n)}{(2r)^n}\Big],$$
$$I_\nu(r) \simeq \tfrac{e^r}{\sqrt{2\pi r}}\Big[1 + \sum_{n=1}^{\infty} \tfrac{(-1)^n(\nu,n)}{(2r)^n}\Big],$$

where $(\nu, n) = \frac{\Gamma(1/2+\nu+n)}{n!\Gamma(1/2+\nu-n)}$. By using the above asymptotic expansion of Bessel functions, the leading term for $\partial_{\tau_0}^2 G_0(l_i, l_; \boldsymbol{z}_i, \boldsymbol{z}_{i+1})$ behaves as $\sim \theta(z_i - z_{i+1}) e^{-(z_i - z_{i+1})}/(z_i - z_{i+1}) + \theta(z_{i+1} - z_i) e^{-(z_{i+1} - z_i)}/(z_{i+1} - z_i)$. All of these terms peak around $z_{i+1} = z_i$ and are otherwise exponentially suppressed. We may therefore again estimate this integral by letting $\boldsymbol{x} = \boldsymbol{z}_0 = \boldsymbol{z}_1 = \cdots = \boldsymbol{z}_{M-1}$ and removing $(M+1)$ of the integrals. The remaining integrals yield, at the leading order, $\int d^{M+1}z\, 1/z^M \sim \int dz z^M z^{-M}$. However, at the leading order, there is no ν dependence. According to the formalism in Sec. 4.3.3, such terms have no contribution to the entanglement entropy. Therefore, the term that contributes to the entanglement entropy is the next order which behaves as $\int dz \frac{1}{z}$ and is of order $O(\log L)$, leading only to a correction $\sim O(\log L) \times \log L$ to the entanglement entropy.

Next, we shall demonstrate in detail our above analysis, for both inter-patch and intra-patch coupling terms by explicit calculation up to the second order.

First Order Correction. The first order term correction to $\int dx G(\boldsymbol{S}, \boldsymbol{S}; \boldsymbol{x}, \boldsymbol{x})$ is

$$\delta^{(1)} C_G(\boldsymbol{S}; n) = \int d^3x d^3z G_0(\boldsymbol{S}, \boldsymbol{S}; \boldsymbol{x}, \boldsymbol{z})(h_2(\boldsymbol{S}, \boldsymbol{S})\partial_{\tau_z}^2 + f_1(\boldsymbol{S}, \boldsymbol{S})\partial_{z_{\boldsymbol{S}}}^2) G_0(\boldsymbol{S}, \boldsymbol{S}; \boldsymbol{z}, \boldsymbol{x}). \tag{4.60}$$

As we have pointed, it is sufficient to calculate either piece of the two terms due to the equivalence of the imaginary time direction and the real space direction. The other piece should be just the same except for the coefficient. Here we choose to compute the first term.

The transverse degrees of freedom provide an overall factor counting the total degrees of freedom as discussed in the general case. Then we can also integrate out the angular degrees of freedom in the $\hat{x}_S - \hat{\tau}$ plane, both θ_x and θ_z as defined in Eq. (4.44), after which one obtains

$$\delta^{(1)} C_G(\boldsymbol{S}; n) \sim \sum_k \frac{d_k}{2} \delta^{(1)} G_{k/n} \oint_{\partial A} |d\boldsymbol{S}_x \cdot d\boldsymbol{S}_k|, \tag{4.61}$$

where

$$\delta^{(1)} G_{k/n} = \int dr_x dr_z r_x r_z g_{k/n}(r_x, r_z)(\partial^2_{r_z} - \frac{k^2}{r_z^2 n^2}) g_{k/n}(r_x, r_z). \tag{4.62}$$

The two k summation is reduced to one due to orthogonality of the angular function $C_{k/n}(\theta)$. By employing the E-M formula and properties of the Bessel functions, we show in Appendix A.1 that sum over k-values in Eq. (4.61) can be converted into an integral, which cancels in Eq. (4.40) for the same scaling reasons discussed above, following Eq. (4.46). Therefore, we find that the contribution of Eq. (4.60) to the entanglement entropy vanishes.

Second Order Correction. The second order correction is

$$\begin{aligned} \delta^{(2)} C_G(\boldsymbol{S}; n) = & \int d^3x d^3z d^3z_1 G_0(\boldsymbol{S}, \boldsymbol{S}; \boldsymbol{x}, z) \\ & \times \sum_l \Big(h_2(l, \boldsymbol{S}) \partial^2_{\tau_z} + f_1(l, \boldsymbol{S}) \partial_{z_l} \partial_{z_S} \Big) G_0(l, l; z, z_1) \\ & \times (h_2(\boldsymbol{S}, \boldsymbol{S}) \partial^2_{\tau_{z_1}} + f_1(\boldsymbol{S}, \boldsymbol{S}) \partial^2_{z_{1S}}) G_0(\boldsymbol{S}, \boldsymbol{S}; z_1, \boldsymbol{x}). \end{aligned} \tag{4.63}$$

- for $l = \boldsymbol{S}$:

$$\begin{aligned} & \int d^3x d^3z d^3z_1 G_0(\boldsymbol{S}, \boldsymbol{S}; \boldsymbol{x}, z) \\ & \times (h_2(\boldsymbol{S}, \boldsymbol{S}) \partial^2_{\tau_z} + f_1(\boldsymbol{S}, \boldsymbol{S}) \partial^2_{z_S}) G_0(\boldsymbol{S}, \boldsymbol{S}; z, z_1) \\ & \times (h_2(\boldsymbol{S}, \boldsymbol{S}) \partial^2_{\tau_{z_1}} + f_1(\boldsymbol{S}, \boldsymbol{S}) \partial^2_{z_{1S}}) G_0(\boldsymbol{S}, \boldsymbol{S}; z_1, \boldsymbol{x}). \end{aligned} \tag{4.64}$$

According to our general discussion, we only need to consider the following piece:

$$\begin{aligned}&\int d^3x d^3z d^3z_1 G_0(\boldsymbol{S},\boldsymbol{S};\boldsymbol{x},z)\partial^2_{\tau_z} G_0(\boldsymbol{S},\boldsymbol{S};z,z_1)\times\partial^2_{\tau_{z_1}} G_0(\boldsymbol{S},\boldsymbol{S};z_1,\boldsymbol{x})\\&=(2\pi)^{-1}\oint_{\partial A}|d\boldsymbol{S}_x\cdot d\boldsymbol{S}_k|\sum_k\frac{d_k}{4}\delta^{(2)}G_{k/n},\end{aligned}\tag{4.65}$$

where

$$\begin{aligned}\delta^{(2)}G_{k/n}=&\int dr_x dr_z dr_1 r_x r_z r_1 g_{k/n}(r_x,r_z)\\&\times(\partial^2_{r_z}-k^2/(r_z n)^2)g_{k/n}(r_z,r_1)\\&\times(\partial^2_{r_1}-k^2/(r_1 n)^2)g_{k/n}(r_1,r_x).\end{aligned}\tag{4.66}$$

In the above, we have proceeded as in the first order calculation, integrating out the angular part first to obtain the expression for $\delta^{(2)}G_{k/n}$.

After a lengthy but similar calculation as for the first order (see Appendix B), we find, using the E-M formula:

$$\begin{aligned}\frac{1}{2}\sum d_k\delta^{(2)}G_{k/n}=&\int dr_x dr_z dr_1 r_x r_z r_1\int_0^\infty dk\, p_{k/n}(r_x,r_z,r_1)\\&+\left[\frac{1}{12}\partial_k+\sum_{j=2}^\infty\frac{B_{2j}}{(2j)!}\partial_k^{(2j-1)}\right]\frac{n}{16k},\end{aligned}\tag{4.67}$$

where $p_{k/n}(r_x,r_z,r_1)$ is the product of $g_{k/n}$ dependent terms in Eq. (4.66). The usual scaling argument for the integral shows that the entire expression is proportional to n, and thus cancels the second ($n=1$) term in Eq. (4.40):

$$S(\boldsymbol{S})\sim-\frac{\partial}{\partial n}\int d^2x(G_n-nG_1))\Big|_{n=1}.$$

Therefore, at the second order level for the $l=\boldsymbol{S}$ piece we still have no correction to the scaling law of entanglement entropy.

- for $l\neq\boldsymbol{S}$:

The integrand we need to consider is

$$
\begin{aligned}
&G_0(\boldsymbol{S},\boldsymbol{S};\boldsymbol{x},\boldsymbol{z}) \times \Big(h_2(l,\boldsymbol{S})\partial^2_{\tau_z} + f_1(l,\boldsymbol{S})\partial_{z_l}\partial_{z_S}\Big) G_0(l,l;\boldsymbol{z},\boldsymbol{z}_1) \\
&\times (h_2(\boldsymbol{S},\boldsymbol{S})\partial^2_{\tau_{z_1}} + f_1(\boldsymbol{S},\boldsymbol{S})\partial^2_{z_{1S}}) G_0(\boldsymbol{S},\boldsymbol{S};\boldsymbol{z}_1,\boldsymbol{x}).
\end{aligned}
\tag{4.68}
$$

The first thing to notice in Eq. (4.68) is that we have derivatives along directions different from the patch normal direction $\hat{\boldsymbol{n}}_S$ acting on the non-interacting Green's function. We expand this term as

$$
\begin{aligned}
&\partial_{z_l}\partial_{z_S} G_0(l,l;\boldsymbol{z},\boldsymbol{z}_1) = \delta(z^{(l)}_\perp - z^{(l)}_{1\perp})\partial_{z_l}\partial_{z_S} G_{0,b}(l;\boldsymbol{z},\boldsymbol{z}_1) \\
&+ \partial_{z_S}\delta(z^{(l)}_\perp - z^{(l)}_{1\perp})\partial_{z_l} G_{0,b}(l;\boldsymbol{z},\boldsymbol{z}_1).
\end{aligned}
\tag{4.69}
$$

For the first term, we can decompose the derivative ∂_{z_S} into terms that act along $\hat{\boldsymbol{n}}_l$ and along its transverse direction, respectively. The non-interacting Green's function only depends on the transverse coordinates via $G_0(l,l;\boldsymbol{x},\boldsymbol{y}) \sim \delta(x^{(l)}_\perp - y^{(l)}_\perp)$, which indicates that those derivative terms vanish. Thus it is $\sim \delta(z^{(l)}_\perp - z^{(l)}_{1\perp})\partial^2_{z_l} G_{0,b}(l;\boldsymbol{z},\boldsymbol{z}_1)$. For the second term, we integrate by parts with respect to z_S, which leads to (including now the first G_0 factor, which depends on $\boldsymbol{z}$)

$$
-\delta(x^{(\boldsymbol{S})}_\perp - z^{(\boldsymbol{S})}_{1\perp})\delta(z^{(l)}_\perp - z^{(l)}_{1\perp})\partial_{z_S} G_{0,b}(\boldsymbol{S};\boldsymbol{x},\boldsymbol{z})\partial_{z_l} G_{0,b}(l;\boldsymbol{z},\boldsymbol{z}_1).
$$

Therefore, the overall integrand is proportional to $\delta(x^{(\boldsymbol{S})}_\perp - z^{(\boldsymbol{S})}_\perp)\delta(z^{(\boldsymbol{S})}_{1\perp} - x^{(\boldsymbol{S})}_\perp)\delta(z^{(l)}_\perp - z^{(l)}_{1\perp})$. Note that the $x^{(\boldsymbol{S})}_\perp$ dependence only appears in these δ-functions, we can integrate it out, leaving only $\delta(z^{(\boldsymbol{S})}_\perp - z^{(\boldsymbol{S})}_{1\perp})\delta(z^{(l)}_\perp - z^{(l)}_{1\perp}) \sim \delta(\boldsymbol{z}_1 - \boldsymbol{z})$.

Secondly, it is sufficient to focus on the following terms in the integrand

$$
\begin{aligned}
&\Big(G_{0,b}(\boldsymbol{S};\boldsymbol{x},\boldsymbol{z})\partial^2_{\tau_z} G_{0,b}(l;\boldsymbol{z},\boldsymbol{z}_1) + \partial_{z_S} G_{0,b}(\boldsymbol{S};\boldsymbol{x},\boldsymbol{z}) \\
&\times \partial_{z_l} G_{0,b}(l;\boldsymbol{z},\boldsymbol{z}_1)\Big)\partial^2_{\tau_{z_1}} G_{0,b}(\boldsymbol{S};\boldsymbol{z}_1,\boldsymbol{x}),
\end{aligned}
$$

to ease the presentation. For other combinations, the rest of this section is equally applicable with minor modifications that only leads to different coefficients and do not affects the

scaling analysis. We first perform the intra-patch integration

$$\int d^3x G_{0,b}(\boldsymbol{S};\boldsymbol{x},z)G_{0,b}(\boldsymbol{S};z_1,\boldsymbol{x}) = H(\boldsymbol{S};z,z_1), \tag{4.70}$$

where

$$\begin{aligned} H(\boldsymbol{S};z,z_1) &= \sum_k \frac{d_k}{2\pi n} C_{k/n}(\theta_z,\theta_{z_1})(\theta(r_z-r_1) \\ &\times (r_z K_{z+} I_1 - r_1 I_{1-} K_z) + \theta(r_1-r_z) \\ &\times (r_1 K_{1+} I_z - r_z I_{z-} K_1)). \end{aligned}$$

So for a given $\boldsymbol{S}$ the contribution to entanglement entropy due to coupling with patch l can be written as

$$\begin{aligned} &\Big|\frac{1}{\sin(\theta_l-\theta_S)}\Big| \int d^3z d^3z_1 \delta^2(z_1-z)\Big(\partial^2_{\tau_{z_1}} H(\boldsymbol{S};z,z_1) \\ &\times \partial^2_\tau G_{0,b}(l;z_1,z) + \partial_{z_S}\partial^2_{\tau_{z_1}} H(\boldsymbol{S};z,z_1)\partial_{z_l} G_{0,b}(l;z_1,z)\Big) \\ &= \Big|\frac{1}{\sin(\theta_l-\theta_S)}\Big| \int d^3z d\tau_1 \Big(\partial^2_{\tau_{z_1}} H(\boldsymbol{S};z,z_1)\partial^2_\tau G_{0,b}(l;z_1,z) \\ &+ \partial_{z_S}\partial^2_{\tau_{z_1}} H(\boldsymbol{S};z,z_1)\partial_{z_l} G_{0,b}(l;z_1,z)\Big)\Big|_{\substack{z_{1,x}=z_{,x} \\ z_{1,y}=z_{,y}}}, \end{aligned} \tag{4.71}$$

where $z_{,x}, z_{,y}$ indicate the two spatial components of z.

As we argued in previous section, for extracting the order of magnitude of the result it is sufficient to set $\tau_1 = \tau$ in the final line of Eq. (4.71) and remove the integral over τ_1. We also note that the derivatives do not alter the leading power of r, owing to the presence of the exponential function. Therefore, it is sufficient to examine

$$\int d^3z \left(H(\boldsymbol{S};z,z_1)G_{0,b}(l;z_1,z)\right)\Big|_{z_1=z}. \tag{4.72}$$

At the lowest order in $1/r$, we have

$$G_{0,b}(\boldsymbol{S};r,r) \sim I_\nu(r)K_\nu(r) \sim 1/r, \tag{4.73}$$

$$
\begin{aligned}
&H(\boldsymbol{S};r,r)\sim rI_{\nu}(r)K_{\nu+}(r)-rK_{\nu}(r)I_{\nu-}(r)\\
=&(1+\frac{(\nu+1,1)}{2r}+\dots)(1-\frac{(\nu,1)}{2r}+\dots)\\
&-(1-\frac{(\nu-1,1)}{2r}+\dots)(1+\frac{(\nu,1)}{2r}+\dots)\\
=&\frac{1}{r}+O(\frac{1}{r^2}).
\end{aligned}
\tag{4.74}
$$

Since the τ derivative does not alter the leading powers, we extract the leading term to be

$$
\Big(H(\boldsymbol{S};z,z_1)\partial_\tau^2 G_{0,b}(\boldsymbol{S};z_1,z)\Big)\Big|_{z_1=z}\sim\frac{1}{z^2}. \tag{4.75}
$$

For a triple integral over $1/z^2$, one would get a linear divergence, i.e. the result would be $\sim L$. This is indeed the case as we have already seen in previous calculation. However, at the lowest order, everything is independent on $\nu = k/n$. Actually what finally appears in the entanglement entropy are the $k-$derivatives of these terms appearing in the E-L summation formula. This means the leading term has vanishing contribution to the entanglement entropy. The first term contributing to entanglement entropy is then $\sim \int d^3z\frac{1}{z^3}$ the upper limit of which is order $O(\log L)$ and only leads a correction up to $\sim O(\log L)\times\log L$ to the free fermion entanglement entropy.

4.4 Summary and Concluding Remarks

In this paper, we developed an intuitive understanding of the logarithmic correction to the area law for the entanglement entropy of free fermions in one and higher dimensions on equal footing – the criticality associated with the Fermi surface (or points). Then we used the tool of high dimensional bosonization to compute the entanglement entropy, and generalized this procedure to include Fermi liquid interactions. In the presence of such interactions we calculated the entanglement entropy for a special geometry perturbatively in powers of the interaction strength up to the second order, and find no correction to the leading scaling behavior. We also point out that the situation is the same at higher orders. Our results thus strongly suggest that the leading scaling behavior of the block entanglement entropy of a Fermi liquid is the *same* as that of a free Fermi gas with the same Fermi surface, not only for the special block geometry studied in this paper, but for

arbitrary geometries. Explicit demonstration of the latter is an obvious direction for future work.

In the special geometry in which we performed explicit calculations using the replica trick, a mass-like term is introduced to regularize the theory at long distance, as is done in closely related contexts[88, 94]. For a Fermi liquid (which is quantum-critical) the corresponding length scale $\xi \sim v_F/m$ must be identified with the block size L, and is thus *not* an independent length scale. On the other hand, such a mass-like term can also describe a superconducting gap due to pairing. In particular, for a weak-coupling superconductor, ξ, the superconducting coherence length, is much longer than all microscopic length scales, but finite nevertheless. In this case it is *independent* of L, and the interplay between the two is interesting. For $L < \xi$, the Fermi liquid result (4.1) still holds. But for $L > \xi$, the logarithmic factor in the entanglement entropy *saturates* at $\log \xi$, and we expect:

$$S(\rho_A) = \frac{1}{12(2\pi)^{2-1}} \log \xi \times \oint_{\partial A} \oint_{\partial \Gamma} |dS_x \cdot dS_k|, \tag{4.76}$$

which agrees with the conjecture made in Ref.[92].

More generally, Fermi liquids are (perhaps the best understood) examples of quantum critical phases (or points) in high dimensions. Unlike in 1D where conformal symmetry powerfully constrains the behavior of entanglement entropy, our understanding of entanglement properties of such high-dimensional quantum critical phases or points (many of them have Fermi surfaces but are *not* Fermi liquids) is very limited. Our work can be viewed as a step in that general direction. Furthermore, the formalism developed in this work has potential applicability to systems with composite or emergent fermions with Fermi surfaces as well, or more generally, *non-Fermi liquid* phases with Fermi surfaces. The system studied in Ref.[69], where there is an emergent spinon Fermi surface, is a potential example.

CHAPTER 5

CONCLUSION AND OPEN QUESTIONS

In this dissertation, we studied entanglement entropy of different systems that all exhibit logarithmic divergences. However, apparently not all logarithms are equal. They are of drastically different origins, and bear different implications to more generic or higher dimensional systems.

5.1 Logarithmic Entanglement Entropy and Spontaneous (Continuous) Symmetry Breaking

In Chapters 2 and 3, we studied the entanglement entropy (mutual information if a mixed state) of systems that are long-range ordered. But in both cases the models we studied are simplified for practical reasons. The system is either taken to be finite or restricted to one dimension or taken to be mean-field like. In the following, we further discuss the more generic systems, i.e. either taking the thermodynamic limit, to the higher dimensions, or doing both.

For the ferromagnetic case, the ground state is hardly affected by the dimensions nor the range of the interactions. For the antiferromagnetic case, the systems is not even ordered in one dimension with short-range coupling. But we can considers systems in two dimensions or above which restores the long-range Neel order, things are immediately very different. As in higher dimensions, for the Heisenberg antiferromagnet we expect the ground state to break the $SU(2)$ spin rotational symmetry spontaneously. As we speculated in Chapter 2 and confirmed by Ref. [25, 98], the logarithmic term does persist. In this case, we no

longer have the zero modes that we argue to give rise to the logarithmic divergence. It turns out that the Goldstone modes are responsible for the logarithmic term in the entanglement entropy as shown by Ref. [98].

In the Bose-Einstein condensation case, as we have mentioned, the more generic way to deplete the condensate is to add repulsive interactions. For a weakly interacting Bose gas, at the mean field level, we interpret the system as that it is composed of the underlying condensate, and its low energy excitations which are described by a quadratic bosonic theory. If we simply interpret the overall state as a tensor product of the two, then we would expect the total entanglement entropy to be the summation of contribution from each part. Then the logarithm due to the condensate must persist. But the quadratic theory presumably would contribute at least at the order of area law. In $d-$dimensional space that would be $\sim L_A^{d-1}$, which makes the $(1/2)\log L_A$ subleading. We also note that quadratic bosonic theory is actually gapless with a dispersion $\epsilon(\boldsymbol{k}) \sim |\boldsymbol{k}|$. This is actually the Goldstone modes for spontaneously breaking the global $U(1)$ symmetry, similar to the spin model case, thus should also give rise to an additional logarithmic term. However, the true ground state certainly is no simple tensor product state, and it is an open question that whether the intertwining of the fluctuations and the underlying condensate increase the entanglement significantly.

5.2 Universal Subleading Correction to the Coefficient of the Logarithm?

For systems that follow the area law, we know cases where the area law receives a universal constant correction, which could be due to either topological order (for gapped systems in 2D) or quantum criticality. In the Fermi liquids case, our calculation also points to a subleading correction of $O(1)$. One is immediately tempted to ask, could it be universal? First of all, we have a natural candidate for this correction: the quasi-particle weight Z which is dimensionless and universal. When we solve the Fermi liquid properties using bosonization, it shows up in the interacting Green's function. Therefore, we should also expect it in the replica Green's function. Then the next question is doest it survive the replica

limit? To answer this question, we need to work out how to compute the contribution of inter-patch processes at the second order. *If* the correction is indeed universal, does it have a topological interpretation? Another interesting question is, can we extract it using some setup similar to the Levine-Wen or the Kitaev-Preskill set-up which are used to extract the topological entanglement entropy?

5.3 Experimental Prospect of Entanglement Entropy Measurement in Extended Quantum Systems

In the end of this dissertation, let us conclude with remarks on experimental prospect of entanglement entropy measurement in extended quantum systems. Although in recent years preparing and measuring (a few) entangled photons[**?**] has become a routine for quantum information science, a direct experimental measurement of entanglement entropy in many-body systems is considered unfeasible by most people due to numerous difficulties. First of all, entanglement entropy is a zero-temperature property. Measuring the entropy at low temperature is already a difficult task, and is usually measured indirectly via quantities like specific heat or thermopower. Therefore, measuring entropy of part of a system, if we simply assume that does measure the von Neumann entropy, is certainly much more difficult. Second, it is even more difficult to realize or define the sharp (virtual) partition boundaries in such experiments. And the study of entanglement entropy of more realistic partitions with indistinct boundaries remains totally unexplored.

Despite the seemingly hopeless situation, progress have been made by dedicated efforts[99, 100, 101, 102, 103]. Although these works take very different perspectives, the philosophy is the same - to find an experimentally well-defined partition method and measurement-friendly observables. While the solutions to the partition issue are versatile, the solution to the measurement issue appears to point to the same direction — noise signals due to quantum fluctuations. For example, in Ref. [104] the authors utilize space-time duality, and partition the system in the time instead of in real space by a switch, for example a quantum point contact (QPC). As the QPC is turned on, entanglement is generated as time flows. It is shown that, for two noninteracting Fermi seas connected by a QPC, there is a universal

relation between entanglement entropy generated during a period of time and the fluctuations of current flowing the QPC. Later similar relations between entanglement and full counting statistics[101] and bipartite fluctuations[102, 103] are also established. Another promising tool for measuring entanglement comes from a new experimental technique — the spin noise spectroscopy (SNS)[105, 100]. The technique measures signals originated from fluctuations, thermal or quantum, of spins in the subsystems which are defined by the path of a laser traveling through the media. Although no direct relation between the SNS signals and entanglement entropy has been established yet, it is not completely hopeless, as the works by Klich el at. and the subsequent works have already shown us the deep connection between noises/fluctuations and entanglement.

APPENDIX A

CALCULATION OF $\delta G_{k/n}$

A.1 $\delta^{(1)} G_{k/n}$

Throughout the Appendix, we shall denote the modified Bessel functions $K_\nu(r_i)$, $I_\nu(r_i)$ as K_i, I_i for simplicity with $\nu = k/n$. We also have $K(I)_{\nu\pm1}(r_i)$ which shall be shortened as $K(I)_{i,\pm}$.

$$\delta^{(1)} G_{k/n} = \int dr_x dr_z r_x r_z g_{k/n}(r_x, r_z) \times (\partial^2_{r_z} - \frac{k^2}{r_z^2 n^2}) g_{k/n}(r_z, r_x). \tag{A.1}$$

Expanding $(\partial^2_{r_z} - \frac{k^2}{r_z^2 n^2}) g_{k/n}(r_z, r_x)$, and noting the identities $I'K - K'I = 1/x$, $X'' - (\nu^2/x^2)X = X - (1/x)X'$ where $X = K, I$, we get

$$\begin{aligned} &(\partial^2_{r_z} - \frac{k^2}{r_z^2 n^2}) g_{k/n}(r_z, r_x) \\ =& -\frac{\delta(r_x - r_z)}{r_x} + \theta(r_x - r_z)(1 - \frac{1}{r_z}\partial_{r_z}) I_z K_x + \theta(r_z - r_x)(1 - \frac{1}{r_z}\partial_{r_z}) I_x K_z. \end{aligned} \tag{A.2}$$

Then integrating over r_x first, and making use of the following formula

$$\int dx x X_\nu^2(x) = \frac{1}{2} x^2 (X_\nu^2(x) - X_{\nu-1}(x) X_{\nu+1}(x)), \tag{A.3}$$

where $X_\nu(x)$ can be the first or second kind of modified Bessel function, I_ν or K_ν, and the identities $I_- K + I K_- = I_+ K + I K_+ = 1/x$ in addition to those given above, $\delta^{(1)} G_{k/n}$ is reduced

to

$$\delta^{(1)}G_{k/n} = \int drr\Big(- IK + r^2(I^2 - I_+I_-)K^2\Big). \tag{A.4}$$

We apply the same strategy as in Sec. 4.3.3, making use of the E-M formula to do the sum over the k-index in Eq. (4.61). This converts the sum into a divergent integral over k which cancels in Eq. (4.40) as before, and a sum over terms of the form $\partial_k^j \delta^{(1)}G_{k/n}\big|_{k\to 0}$ that turn out to vanish, as we will now show. Again, we can include proper constants under the derivative into the integrand. These derivatives then act on well defined integrals. The first term has been discussed in Sec. 4.3.3:

$$\int dr\partial_k^j(-rI_{k/n}K_{k/n}) = \partial_k^j \int dr(-rIK + \frac{1}{4}) = \partial_k^j\Big(\frac{k}{2n}\Big). \tag{A.5}$$

The second term can be shown to be

$$\begin{aligned} &\int dr\partial_k^j(r^3(I^2 - I_+I_-)K^2) \\ &= \partial_k^j \int dr(r^3(I^2 - I_+I_-)K^2 - \frac{1}{4}) \\ &= \partial_k^j\Big(- \frac{1}{16} - \frac{k}{2n}\Big). \end{aligned} \tag{A.6}$$

Summing the two terms together, we find

$$\Big(\partial_k^j \delta^{(1)}G_{k/n}\Big)\Big|_{k\to 0} = \partial_k^j(-\frac{1}{16}) = 0, \tag{A.7}$$

for all $j > 0$.

A.2 $\delta^{(2)}G_{k/n}$

Let us first compute the integral:

$$\begin{aligned} &\int dr_2 r_2 g_\nu(r, r_2)\Big(\partial_{r_2}^2 g_\nu(r_2, r_1) - \left(\frac{\nu}{r_2}\right)^2 g_{k/n}(r_2, r_1)\Big) \\ &= \theta(r - r_1)h(r, r_1) + \theta(r_1 - r)h(r_1, r) \end{aligned} \tag{A.8}$$

with

$$
\begin{aligned}
&h(r,r_1) = -I_1K + \frac{1}{2}(f_1(r,r_1) + KI_1 \ln\frac{r}{r_1}),\\
&f_1(r,r_1) = KK_1(r_1^2(I_1^2 - I_{1,+}I_{1,-}) - I_1^2) - II_1\\
&\times(r^2(K^2 - K_+K_-) - K^2) + KI_1(F(r) - F(r_1) - IK + I_1K_1),\\
&F(r) = 2\int drrIK = r^2IK + r^2I_+K_-.
\end{aligned}
$$

The IK_1 term in $h(r,r_1)$ results from δ-functions (derivatives of δ-functions) coming from the derivative applied on the step function ($\theta(r)$). The remaining part comes from terms involving a product of two θ-functions. Here one needs to distinguish between $r > r_1$ and $r < r_1$, which gives rise to the terms in $\theta(r - r_1)$ and $\theta(r_1 - r)$, respectively. The remaining integral

$$
\begin{aligned}
&\int drdr_1rr_1(\theta(r - r_1)h(r,r_1) + \theta(r_1 - r)h(r_1,r))\\
&\Big(-\frac{\delta(r_1 - r)}{r} + \theta(r_1 - r)(1 - \frac{1}{r_1}\partial_{r_1})K_1I + \theta(r - r_1)(1 - \frac{1}{r_1}\partial_{r_1})KI_1\Big)
\end{aligned}
\tag{A.9}
$$

can be carried out by applying the identities of Bessel functions I and K used in Appx. A. In applying the E-M formula to the sum over k in (4.65), we again arrive at a divergent k-integral that can be rescaled and subsequently canceled (see (4.67) and below), and a sum over derivative terms that are well-behaved. In the latter terms, we always add proper constants under the derivatives to regularize the integrand at infinity, as before. We divide (A.9) into two terms. The first is the one containing the δ-function. After integrating out r_1, this term becomes

$$
\begin{aligned}
&\partial_k^j(-\int drrh(r,r)) = \partial_k^j(-\int dr(rh(r,r) + \frac{1}{4}))\\
&= \partial_k^j(-\int dr(r(-IK + \frac{r^2}{2}(-K^2I_+I_- + I^2K_+K_-)) + \frac{1}{4}))\\
&= \partial_k^j(0).
\end{aligned}
\tag{A.10}
$$

The second term is expanded to

$$\int drdr_1 rr_1\Big(\theta(r-r_1)h(r,r_1)K(I_1 - I_1'/r_1) + \theta(r_1-r)h(r_1,r)I(K_1 - K_1'/r_1)\Big). \tag{A.11}$$

Due to the complexity of $h(r, r_1)$, we examine each of the three terms of $h(r, r_1)$ separately. The first term is simple. Applying those identities of K's and I's and including the proper constant, we get

$$\begin{aligned}
&\partial_k^j\Big(\int drdr_1(rr_1(\theta(r-r_1)(-I_1K)K(I_1 - I_1'/r_1) \\
&+ \theta(r_1-r)(-IK_1)I(K_1 - K_1'/r_1)) - \frac{1}{4})\Big) \\
&= \partial_k^j\big(\frac{k}{2n}\big).
\end{aligned} \tag{A.12}$$

The second term of $h(r, r_1)$ contributes

$$\begin{aligned}
&\partial_k^j\big(\frac{1}{2}\int drdr_1 rr_1\theta(r-r_1)f1(r,r_1)K(I_1 - \frac{1}{r_1}I_1') \\
&+ \frac{1}{2}\int drdr_1 rr_1\theta(r_1-r)f1(r_1,r)(K_1 - \frac{1}{r_1}K_1')I\big).
\end{aligned} \tag{A.13}$$

By interchanging the dummy variables r and r_1, employing the properties of the modified Bessel functions with care, and including the regularization constant, we arrive at

$$\partial_k^j\Big(\frac{1}{2}\int drdr_1(rr_1\theta(r-r_1)f_1(r,r_1)(2KI_1 - KI_1'/r_1 - K'I_1/r) - \frac{1}{8})\Big) = \partial_k^j(-\frac{k}{2n}). \tag{A.14}$$

The last part of $h(r, r_1)$ contributes as

$$\begin{aligned}
&\int drdr_1\frac{rr_1}{2}\theta(r-r_1)KI_1\ln\frac{r}{r_1}(K'I_1/r \\
&- KI_1'/r_1) = -\frac{1}{16\nu}.
\end{aligned} \tag{A.15}$$

Summing all the above terms together we get

$$\partial_k^j(\delta^{(2)}G_{k/n}) = \partial_k^j(-\frac{n}{16k}). \tag{A.16}$$

BIBLIOGRAPHY

[1] E. Schrödinger and M. Born, Mathematical Proceedings of the Cambridge Philosophical Society **31**, 555 (1935).

[2] A. Einstein, B. Podolsky, and N. Rosen, Physical Review **47**, 777 (1935).

[3] J. S. Bell, Physics **1**, 195 (1964).

[4] S. J. Freedman and J. F. Clauser, Physical Review Letters **28**, 938 (1972).

[5] A. Aspect, P. Grangier, and G. Roger, Physical Review Letters **47**, 460 (1981).

[6] A. Aspect, P. Grangier, and G. Roger, Physical Review Letters **49**, 91 (1982).

[7] A. Aspect, J. Dalibard, and G. Roger, Physical Review Letters **49**, 1804 (1982).

[8] J.-W. Pan *et al.*, Review of Modern Physics **84**, 777 (2012).

[9] P. W. Shor, in *Proc. 35nd Annual Symposium on Foundations of Computer Science*, edited by S. Goldwasser (IEEE Computer Society Press, 1994), pp. 124–134.

[10] C. H. Bennett *et al.*, Physical Review Letters **70**, 1895 (1993).

[11] M. A. Nielsen and I. Chuang, *Quantum Computation and Quantum Information* (Cambridge University Press, Cambridge, 2000).

[12] L. Amico and R. Fazio, Journal of Physics A: Mathematical and Theoretical **42**, 504001 (2009).

[13] J. I. I. Latorre and A. Riera, Journal of Physics A: Mathematical and Theoretical **42**, 504002 (2009).

[14] J. Eisert, M. Cramer, and M. B. B. Plenio, Reviews of Modern Physics **82**, 277 (2010).

[15] S. R. White, Physical Review Letters **69**, 2863 (1992).

[16] F. Verstraete, D. Porras, and J. Cirac, Physical Review Letters **93**, 4 (2004).

[17] D. Perez-Garcia, F. Verstraete, M. M. Wolf, and J. I. Cirac, Quantum Inf. Comput. 1 (2006).

[18] M. Levin and X. Wen, Physical Review Letters **96**, 110405 (2006).

[19] A. Kitaev and J. Preskill, Physical Review Letters **96**, 110404 (2006).

[20] H. Li and F. D. M. Haldane, Physical Review Letters **101**, 010504 (2008).

[21] R. Horodecki, M. Horodecki, and K. Horodecki, Reviews of Modern Physics **81**, 865 (2009).

[22] M. B. Plenio and S. Virmani, Quant.Inf.Comput. **7**, 1 (2007).

[23] X. Wen, *Quantum Field Theory of Many-body Systems: From the Origin of Sound to an Origin of Light and Electrons*, illustrate ed. (Oxford University Press, USA, 2004), Chap. 6, pp. 252–255.

[24] A. Renyi, in *Proceedings of the Fourth Berkeley Symposium on Mathematics, Statistics and Probability* (PUBLISHER, 1960), pp. 547–561.

[25] M. B. Hastings, I. González, A. B. Kallin, and R. G. Melko, Physical Review Letters **104**, 157201 (2010).

[26] S. T. Flammia, A. Hamma, T. L. Hughes, and X. Wen, Physical Review Letters **103**, 261601 (2009).

[27] M. Cramer, J. Eisert, M. B. Plenio, and J. Dreiß ig, Physical Review A (Atomic, Molecular, and Optical Physics) **73**, 12309 (2006).

[28] M. M. Wolf, F. Verstraete, M. B. Hastings, and J. I. Cirac, Physical Review Letters **100**, 70502 (2008).

[29] N. Regnault, B. Bernevig, and F. Haldane, Physical Review Letters **103**, 016801 (2009).

[30] P. Calabrese and A. Lefevre, Physical Review A **78**, 032329 (2008).

[31] L. Bombelli, R. Koul, J. Lee, and R. Sorkin, Physical Review D **34**, 373 (1986).

[32] M. Srednicki, Physical Review Letters **71**, 666 (1993).

[33] C. Holzhey, F. Larsen, and F. Wilczek, Nuclear Physics B **424**, 443 (1994).

[34] C. Callan and F. Wilczek, Physics Letters B **333**, 55 (1994).

[35] T. Fiola, J. Preskill, A. Strominger, and S. Trivedi, Physical Review D **50**, 3987 (1994).

[36] S. Hawking, J. Maldacena, and A. Strominger, Journal of High Energy Physics **0105**, 001 (2001).

[37] P. Calabrese and J. Cardy, Journal of Statistical Mechanics: Theory and Experiment **2004**, P06002 (2004).

[38] J. Bekenstein, Physical Review D **7**, 2333 (1973).

[39] S. Hawking, Nature **248**, 30 (1974).

[40] K. Audenaert, J. Eisert, M. Plenio, and R. Werner, Physical Review A **66**, 042327 (2002).

[41] T. Osborne and M. Nielsen, Physical Review A **66**, 032110 (2002).

[42] A. Osterloh, L. Amico, G. Falci, and R. Fazio, Nature **416**, 608 (2002).

[43] G. Vidal, J. I. I. Latorre, E. Rico, and A. Kitaev, Physical Review Letters **90**, 227902 (2003).

[44] X. Chen, Z.-x. Liu, and X. Wen, Physical Review B **84**, 235141 (2011).

[45] U. Schollwöck, Reviews of Modern Physics **77**, 259 (2005).

[46] M. Fannes, B. Nachtergaele, and R. F. Werner, Letters in Mathematical Physics **25**, 249 (1992).

[47] M. B. Hastings, Journal of Statistical Mechanics: Theory and Experiment **2007**, P08024 (2007).

[48] I. Peschel, Journal of Statistical Mechanics: Theory and Experiment **2004**, P12005 (2004).

[49] N. Schuch, M. Wolf, F. Verstraete, and J. Cirac, Physical Review Letters **100**, 030504 (2008).

[50] F. Verstraete and J. Cirac, Physical Review B **73**, 094423 (2006).

[51] E. H. Fradkin and J. E. Moore, Physical Review Letters **97**, 50404 (2006).

[52] R. B. Laughlin, Physical Review Letters **50**, 1395 (1983).

[53] B. Hsu and E. H. Fradkin, Journal of Statistical Mechanics: Theory and Experiment **2010**, P09004 (2010).

[54] L. Amico, R. Fazio, A. Osterloh, and V. Vedral, Reviews of Modern Physics **80**, 517 (2008).

[55] M. M. Wolf, Physical Review Letters **96**, 10404 (2006).

[56] D. Gioev and I. Klich, Physical Review Letters **96**, 100503 (2006).

[57] T. Barthel, M.-C. Chung, and U. Schollwöck, Physical Review A **74**, 022329 (2006).

[58] W. Li *et al.*, Physical Review B **74**, 073103 (2006).

[59] G. Refael and J. Moore, Physical Review Letters **93**, 260602 (2004).

[60] R. Santachiara, J.STAT.MECH. L06002 (2006).

[61] A. Feiguin *et al.*, Physical Review Letters **98**, 160409 (2007).

[62] N. E. Bonesteel and K. Yang, Physical Review Letters **99**, 140405 (2007).

[63] R. Santachiara, F. Stauffer, and D. Cabra, J. Stat. Mech.: Theory Exp. L06002 (2006).

[64] J. I. Latorre, R. Orús, E. Rico, and J. Vidal, Physical Review A **71**, 64101 (2005).

[65] T. Barthel, S. Dusuel, and J. Vidal, Physical Review Letters **97**, 220402 (2006).

[66] J. Vidal, S. Dusuel, and T. Barthel, Journal of Statistical Mechanics: Theory and Experiment **2007**, P01015 (2007).

[67] M. Cramer, J. Eisert, and M. Plenio, Physical Review Letters **98**, 220603 (2007).

[68] G. Levine and D. Miller, Physical Review B **77**, 205119 (2008).

[69] Y. Zhang, T. Grover, and A. Vishwanath, Physical Review Letters **107**, 067202 (2011).

[70] R. Helling, H. Leschke, and W. Spitzer, International Mathematics Research Notices **1482**, 20 (2010).

[71] I. Peschel, Journal of Physics A: Mathematical and General **36**, L205 (2003).

[72] B.-Q. Jin and V. E. Korepin, Journal of Statistical Physics **116**, 79 (2004).

[73] W. Ding, N. E. Bonesteel, and K. Yang, Physical Review A **77**, 052109 (2008).

[74] V. Popkov and M. Salerno, Physical Review A **71**, 12301 (2005).

[75] E. Yusuf, A. Joshi, and K. Yang, Physical Review B **69**, 144412 (2004).

[76] H. Casini, C. D. Fosco, and M. Huerta, Journal of Statistical Mechanics: Theory and Experiment **2005**, P07007 (2005).

[77] G. Adesso and F. Illuminati, J.PHYS.A **40**, 7821 (2007).

[78] S. L. Braunstein and P. van Loock, Rev. Mod. Phys. **77**, 513 (2005).

[79] I. Klich, Journal of Physics A: Mathematical and General **39**, L85 (2006).

[80] J. Robinson, Physical Review **83**, 678 (1951).

[81] A. Houghton and J. B. Marston, Physical Review B **48**, 7790 (1993).

[82] F. D. M. Haldane, in *Proceedings of the International School of Physics "Enrico Fermi", Course CXXI "Perspectives in Many-Particle Physics"* (PUBLISHER, 1993), pp. 5–29.

[83] A. H. Castro Neto and E. H. Fradkin, Physical Review Letters **72**, 1393 (1994).

[84] A. H. Castro Neto and E. H. Fradkin, Physical Review B **49**, 10877 (1994).

[85] A. H. Castro Neto and E. H. Fradkin, Physical Review B **51**, 4084 (1995).

[86] H. Widom, Oper. Th.: Adv. Appl **4**, 477 (1982).

[87] A. Sobolev, Funkts. Anal. Prilozh. **44**, 86 (2010).

[88] V. E. Korepin, Physical Review Letters **92**, 096402 (2004).

[89] P. Calabrese, J. Cardy, and E. Tonni, Journal of Statistical Mechanics: Theory and Experiment **2009**, P11001 (2009).

[90] V. Alba, L. Tagliacozzo, and P. Calabrese, Journal of Statistical Mechanics: Theory and Experiment **2011**, P06012 (2011).

[91] S. Furukawa, V. Pasquier, and J. Shiraishi, Physical Review Letters **102**, 170602 (2009).

[92] B. Swingle, Physical Review Letters **105**, 050502 (2010).

[93] R. Shankar, Reviews of Modern Physics **66**, 129 (1994).

[94] M. P. Hertzberg and F. Wilczek, Physical Review Letters **106**, 050404 (2010).

[95] H. Goldstein and C. P. Poole, *Classical Mechanics* (Addison Wesley, 2001).

[96] S. Doniach and E. H. Sondheimer, *Green's Functions for Solid State Physicists* (World Scientific Publishing Company, 1998), p. 317.

[97] Z. Wang and D. Guo, *An Introduction to Special Function* (Peking University Press, 2000).

[98] M. A. Metlitski and T. Grover, arXiv: 1112.5166 (2011).

[99] I. Klich, G. Refael, and A. Silva, Physical Review A **74**, 32306 (2006).

[100] B. Mihaila *et al.*, Physical Review A **74**, 063608 (2006).

[101] I. Klich, L. Levitov, V. Lebedev, and M. Feigelman, in *AIP Conference Proceedings* (AIP, 2009), No. 2, pp. 36–45.

[102] H. Song *et al.*, Physical Review B **83**, 161408 (2011).

[103] H. F. Song *et al.*, Physical Review B **85**, 035409 (2011).

[104] I. Klich and L. Levitov, Physical Review Letters **102**, 100502 (2009).

[105] S. A. Crooker, D. G. Rickel, A. V. Balatsky, and D. L. Smith, Nature **431**, 49 (2004).

BIOGRAPHICAL SKETCH

Ding, Wenxin

Education

- Ph.D. Candidate in Physics, Florida State University, 2006-present.
  Current GPA: 3.9 / 4
- B.S. in Physics, Zhejiang University, 2002-2006.
  GPA: Overall 3.74 / 4, Major 3.63 / 4

Research experience

- March 15 - 19, 2010, Portland, Oregon: March Meeting of America Physics Society (APS).
  - Presentation 1: W33.00007: Entanglement Entropy and Mutual Information in Bose-Einstein Condensates, by Wenxin Ding, Kun Yang.
  - Presentation 2: L21.00012: Edge states and transmission coefficients of monolayer-bilayer graphene zigzag interfaces, by Wenxin Ding, Zi-Xiang Hu, Oskar Vafek, Kun Yang.
- January 20 - June 12, 2009, Kavli Institute of Theoretical Physics (KITP) Program: Low Dimensional Electron Systems.
- June 30 - July 18, 2008, Boulder School for Condensed Matter and Material Physics: Strongly Correlated Materials.
- March 10 - 14, 2008, New Orleans, Louisiana: March Meeting of America Physics Society (APS). Presentation: W15.00008: Entanglement Entropy of States with Long-Range Magnetic Order, by Wenxin Ding, Nicholas Bonesteel, Kun Yang.
- August 13th-August 16th, 2007, Princeton Center for Complex Materials (PCCM) Summer School on Condensed Matter Physics
- March 5th -9th, 2007, APS March Meeting (no presentation), Denver, CO.

- Sept. 2006-present, Graduate Research Assistant Science, Condensed Matter / Theory, NHMFL.
- September 2005-June 2006, Member of team on strong correlation systems, Supervisor: Prof. Xin Wan, Zhejiang Institute of Modern Physics, Physics Department, Zhejiang University.
- May 2004 - May 2005, Participation in the Student Research Training Program (SRTP) under the supervision of Prof. Zhengmao Sheng, on Analytical Study of Nonlinear Integrable Systems.
- August 1st - August 19th, 2005 Particle Physics, Astronomy, and Cosmology Summer School, held by Zhejiang Institute of Modern Physics, Zhejiang University.

Publication

- **Wenxin Ding**, Alexander Seidel, and Kun Yang, Phys. Rev. X **2**, 011012 (2012), *Entanglement entropy of Fermi liquids via multi-dimensional bosonization*.
- Zi-Xiang Hu and **Wenxin Ding**, Phys. Lett. A **376**, 610 (2012), *Edge States at the Interface between Monolayer and Bilayer Graphene*.
- **Wenxin Ding** and Kun Yang, Phys. Rev. A **80**, 012329 (2009), *Entanglement entropy and mutual information in Bose-Einstein condensates*.
- **Wenxin Ding**, Nicholas E. Bonesteel, and Kun Yang, Phys. Rev. A **77**, 052109 (2008), *Block entanglement entropy of ground states with long-range magnetic order*.

Honors and Awards

- May 2012, Dirac-Hellman Award, the Department of Physics, Florida State University.
- October 2004, Excellent Student for 2003-2004 academic year.
- October 2004, Third-Class Academic Scholarship for 2003-2004 academic year.

Social Experiences & Services

- Performing Chinese calligraphy at Tallahassee's annual Asian festival 2010.
- Fall 2006, Voluntary Work in Football Sale for Chinese Student & Scholar Associate (CSSA), FSU.
- March-May, 2004, participation in the OpenCourseWare (OCW) Translation Project of Massachusetts Institute of Technology (MIT), course 8.01, 8.022 (translating), under the supervision of Prof. Zhengmao Sheng.

Language

- TOEFL: 62/65/66 TWE 4.5 total 643, Test date: May 2005
- GRE General: Verbal 700, 96%, Quantitative 800, 92%, AW 4.0, 32%, Test date: October 2004

Activities

- Chinese calligraphy, basketball, hiking, rock climbing, swimming and Fishing.